University of Illinois at Urbana-Champaign

Air Conditioning and Refrigeration Center A National Science Foundation/University Cooperative Research Center

Refrigerator/Freezer System Modeling

M. P. Goodson and C. W. Bullard

ACRC TR-61 August 1994

For additional information:

Air Conditioning and Refrigeration Center
University of Illinois
Mechanical & Industrial Engineering Dept.
1206 West Green Street
Urbana, IL 61801

(217) 333-3115

Prepared as part of ACRC Project 30
Cycling Performance of Refrigerator-Freezers
C. W. Bullard, Principal Investigator

The Air Conditioning and Refrigeration Center was founded in 1988 with a grant from the estate of Richard W. Kritzer, the founder of Peerless of America Inc. A State of Illinois Technology Challenge Grant helped build the laboratory facilities. The ACRC receives continuing support from the Richard W. Kritzer Endowment and the National Science Foundation. The following organizations have also become sponsors of the Center.

Acustar Division of Chrysler
Allied Signal, Inc.
Amana Refrigeration, Inc.
Brazeway, Inc.
Carrier Corporation
Caterpillar, Inc.
E. I. duPont Nemours & Co.
Electric Power Research Institute
Ford Motor Company
Frigidaire Company
General Electric Company
Harrison Division of GM
ICI Americas, Inc.
Modine Manufacturing Company
Peerless of America, Inc.
Environmental Protection Agency
U.S. Army CERL
Whirlpool Corporation

For additional information:

Air Conditioning & Refrigeration Center
Mechanical & Industrial Engineering Dept.
University of Illinois
1206 West Green Street
Urbana, IL 61801

217 333 3115

Abstract

This report describes the development of a refrigerator/freezer model (RFSIM) that is capable of running in either design mode (user-specified superheat and subcooling) or full simulation mode. The primary purpose was to build on the foundation of an earlier version of the model, to make it refrigerant-independent, and to compare it to experimental data. First, a capillary tube-suction line heat exchanger (ct-sl hx) model, based on first principles, replaced a curve fit of experimental data that had previously calculated the mass flow rate through the capillary tube, in such a way that the speed and robustness of the model were not sacrificed. Second, a study of several void fraction correlations was also conducted to determine which one would most accurately calculate the refrigerant in the two-phase zones of the condenser and evaporator, and refrigerant inventory equations for the single-phase components and the lubrication oil were also included in the model. Lastly, several heat transfer and pressure drop correlations were added to allowed the calculation of the overall heat transfer coefficients and pressure drops in each zone of the evaporator and condenser. The predictions of the model in both design and simulation mode were then compared to experimental data. The results of the design mode analysis showed that the model predicted several system variables, including efficiency and evaporator capacity, very accurately. The accuracy of the design model could only be improved by using more accurate maps. The simulation model results reflected the errors in the ct-sl hx component model, which significantly underpredicts the mass flow rate. Simulation results using propane are consistent with these findings, but reflect additional errors associated with the lack of compressor map data obtained with propane.

Table of Contents

List of Figures

Page

List of Tables

Chapter 1: Introduction

The Air Conditioning and Refrigeration Center (ACRC) refrigerator/freezer model (RFSIM) has been developed in response to government demands on manufacturers to produce more energy efficient refrigerator/freezer systems by 1998. By utilizing the model's ability to operate as a flexible design and simulation tool, a wider range of design options could be considered, and product lead-times shortened.

RFSIM was developed from the ACRC2 simulation model written by Porter and Bullard (1992). Porter's model had two basic advantages over other existing refrigerator/freezer models. First it was capable of running in simulation mode, in addition to design mode, which most other public domain models are limited to (Arthur D. Little, 1982; Merriam et. al., 1993). Thus ACRC2 was able to predict the performance of a system operating over a wide range of conditions. Second, it employed a Newton-Raphson solution technique to solve the nonlinear set of equations, while most other models used successive substitution methods. The Newton-Raphson method has several advantages: it is reliable and rapidly convergent; the order of the equations is not important; and it is easier to modify the equations because they are not entangled with the solution algorithm.

The ability of the ACRC2 model to simulate the system using other refrigerants, however, was limited by the many user specified parameters which were experimentally determined for a system using R-12. For example, the overall heat transfer coefficients in each zone of the condenser and evaporator had to be user-specified, making the model refrigerant-specific. New parameters for a different refrigerant could be obtained but extensive experimentation would have been required. Furthermore, an empirically obtained curve fit equation for mass flow rate through the capillary tube was used because there was no physically-based component model for the capillary tube-suction line heat exchanger (ct-sl hx).

The purpose of this report was to build on the foundation of the ACRC2 model to develop a more generalized (i.e. refrigerant-independent) model. This was accomplished by making the following modifications.

First, the curve-fit used for mass flow rate through the capillary tube needed to be replaced by a capillary tube-suction line heat exchanger model that was based on first principles. The ct-sl hx model was incorporated in a way such that the model was not overly sensitive to initial guesses, in order to preserve the robustness of the system equations, and to ensure that the numerous additional equations did not drastically increase solution time. Second, it was necessary to improve the accuracy of the charge conservation equations. This was accomplished by comparing the predictions of several different void fraction correlations to experimental results to determine which was most accurate, and accounting for charge in the previously neglected single-phase components and in the lubricating oil.

Lastly, the model incorporated the results of research conducted on heat transfer in condensers and evaporators (Wattelet, 1993; Dobson, 1994; Admiraal and Bullard, 1993; Cavallaro and Bullard, 1994) which allowed the calculation of system variables, such as overall heat transfer coefficients in the heat exchanger zones, that were previously user-specified parameters. The user-specified pressure drops in the system were also replaced by accurate pressure drop correlations (Souza et. al., 1992).

This report describes the way in which each of the components is modeled. That is followed by a brief discussion about the relationship between the system model, RFSIM, and the ACRC solver, developed by Mullen and Bullard (1994), which is used. Next the accuracy of the model is examined on first a component and then a system level by comparing experimental results to predicted model results. Finally, the ability of the model to simulate alternative refrigerants is tested.

Chapter 2: Model Description

There are four components in the RFSIM model: a compressor, a condenser, a capillary tube-suction line heat exchanger, and an evaporator. They are shown in Figure 2.1 along with the various state points defined throughout the system. The model also contains three groups of system equations which define the thermodynamic properties and states in the system, relate the refrigeration load to the cooling capacity, and calculate the total system charge. All of the aforementioned governing equations are listed together and solved as one simultaneous 124 equation set. This chapter describes the modeling strategies and correlations used for each of the component models. For a more in detailed description refer to the ACRC Refrigerator/Freezer Model User's Reference in Appendix D.

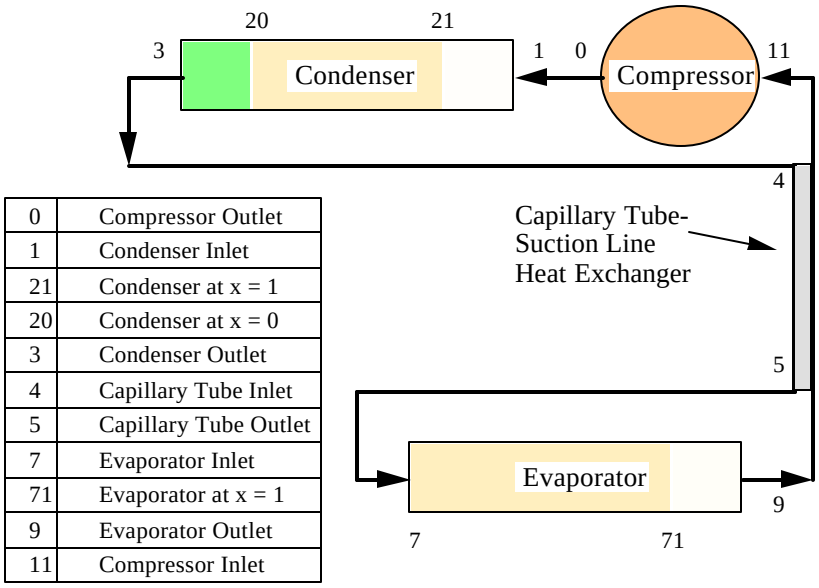

0	Compressor Outlet
1	Condenser Inlet
21	Condenser at x = 1
20	Condenser at x = 0
3	Condenser Outlet
4	Capillary Tube Inlet
5	Capillary Tube Outlet
7	Evaporator Inlet
71	Evaporator at x = 1
9	Evaporator Outlet
11	Compressor Inlet

Figure 2.1 Schematic diagram of refrigeration system showing state points

2.1 Compressor

The compressor is a map-based model which was developed from experimental data provided by the manufacturer. Both the compressor power and the mass flow rate are biquadratic curve fits that are functions of the saturation temperatures at the inlet and outlet pressures of the compressor. The coefficients for the curve fit are input by the user for each compressor/refrigerant combination which is used. When alternative refrigerants are used with the same compressor, the maps are revised assuming constant isentropic and volumetric efficiencies for different refrigerants at the same pressure ratios. The compressor shell heat loss is modeled with an empirical correlation developed by Cavallaro (1994) which assumes that the heat transfer from the shell is a function of the velocity of the air flowing over the shell, and the temperature difference between the shell and air.

2.2 Condenser

The condenser is modeled as a three zone parallel counterflow heat exchanger that consists of a desuperheating zone, two-phase zone, and subcooled zone. Each of these zones is governed by three energy equations: a refrigerant-side energy balance, an air-side energy balance, and an effectiveness-NTU rate equation.

The relative size of each zones is determined from the area in the UA expression of the effectiveness equation. The heat transfer coefficients on both the air- and refrigerant-side as well as pressure drops are calculated for each zone from refrigerant and air mass flow rates and temperature dependent transport properties. Extensive experimental and analytical research by Admiraal (1993) on the modeled refrigeration system, concluded that the correlations listed in Table 2.1 were most accurate at predicting the refrigerant-side heat transfer. Likewise, the air-side heat transfer is calculated using an empirical correlation developed by Cavallaro (1994). The volumetric air flow rate was also estimated by Cavallaro.

2.3 Capillary Tube-Suction Line Heat Exchanger

The capillary tube-suction line heat exchanger (ct-sl hx) model is based on the finite-difference model developed by Piexoto and Bullard (1994). The ct-sl hx model is similar to the condenser model in that it is divided into zones for modeling purposes, but in this case the ct-sl hx model is split into regions which are determined from the geometry of the component rather than the state of the refrigerant in the component. Thus, it is separated into three distinct regions: the capillary tube adiabatic inlet region, the heat exchanger region, and the adiabatic capillary tube outlet region. In each of these regions a group of governing equations, which consist of mass, momentum, and energy conservation equations, describe the physical processes which are occurring in the component. The key assumptions of this model are homogeneous equilibrium two-phase flow, and choked flow at the capillary tube outlet where the Mach number of the homogeneous liquid and vapor mixture is one.

Table 2.1 Correlations used by RFSIM

Condenser Heat Transfer	
Superheated	Gnielinski (Incropera and DeWitt, 1990)
Two-phase	Dobson (1994)
Subcooled	Gnielinski (Incropera and DeWitt, 1990)
Air-side	Cavallaro and Bullard (1994)
Evaporator Heat Transfer	
Superheated	Gnielinski (Incropera and DeWitt, 1990)
Two-phase	Wattelet (1994)
Air-side	Cavallaro and Bullard (1994)
Capillary Tube Heat Transfer	
Single-phase	Gnielinski (Incropera and DeWitt, 1990)
Two-phase	Gnielinski (Incropera and DeWitt, 1990)
Suction Line Heat Transfer	
Single-phase	Gnielinski (Incropera and DeWitt, 1990)
Evaporator & Condenser Pressure Drop	
Two-phase	Souza et. al. (1992)
Single-phase	Moody friction factor
Single-phase return bends	Ito (1960)
Two-phase return bends	Christofferson et. al. (1993)
Capillary Tube Friction Factors	
Single-phase	Blasius (ASHRAE, 1993)
Two-phase	Souza et. al. (1992)

The governing equations for this component model are not included in the system model with the other component governing equations. The reason for this is twofold. One, being significantly larger than the other components with 250^{+} equations, the ct-sl hx more than doubles the total number of equations in the remainder of the system and would significantly increase the solution time. Second, and more importantly, the simultaneous solution of the ct-sl hx equation set would require very accurate initial guesses for the many thermodynamic and transport properties in the model.

It is possible, however, to reduce the set of 250^{+} equations to only six equations that must be solved simultaneously in the system model, and to solve the remaining equations "sequentially" in a separate routine. Therefore, a subroutine was written that uses a specific set of inputs and sequentially determines the output variables. These prescribed inputs and outputs for the subroutine are shown in Figure C.3 in Appendix C. Now the numerous property variables are explicit intermediate variables which do not require initial guesses. A few of these "sequential" operations actually require the solution of one- and two- variable implicit equations, which are solved by internal iteration.

This subroutine can be considered as six explicit functions which are executed in parallel. The outputs of these functions are then present in the system model in the form of six governing equations. These six equations compare the subroutine outputs to user-defined parameters and select variables in the system model. The exact form of these equations along with a comprehensive description of the ct-sl hx model can be found in Appendix C.

The correlations used for heat transfer coefficients and friction factors shown in Table 2.1 were found to give the best model results when compared to experimental results.

2.4 Evaporator

The evaporator is modeled as a counterflow heat exchanger. It is modeled as consecutive zones, as was done in the condenser, except that only the two-phase and superheated zones are present in this case. Likewise, each zone is described by the same three energy equations that were used before. The refrigerant-side heat transfer correlations in Table 2.1 were determined to provide the most accurate modeling results by Admiraal (1993), while the air-side empirical correlations were once again taken from Cavallaro (1994). The value used for volumetric air flow rate was also estimated by Cavallaro. Finally, the pressure drop correlations are excactly the same as those used in the condenser.

2.5 System Equations

The system equations are classified into three groups. The first and largest group determines the thermodynamic properties which define the states in the system. These equations are entirely independent of the component model equations. Properties such as enthalpy and specific volume that are needed for the mass and energy equations are calculated by calls to the NIST REFPROP property routines. Pressure drop equations also relate the state point pressures throughout the system to one another.

Also included in these system equations is a simple cabinet model that relates the heat load to the cooling capacity provided by the evaporator. There are two components to the refrigerator heat load: the heat transfer through the cabinet walls and the heat load provided by electrical heaters for experimental purposes. The cabinet heat load is calculated using overall heat transfer coefficients, or UA's, for each cabinet which were experimentally

determined from reverse heat leak tests by Rubas (1993). The heater were used to achieve steady-state operation at specified compartment temperatures. The model assumes that the air streams from each cabinet thoroughly mix in the refrigerator mullion prior to entering the evaporator and calculates the fraction of the air flow through each cabinet. The effects of temperature stratification in the cabinets can also be examined with these equations.

Finally, the charge conservation equation, which is the last group of system equations, accounts for the amount of refrigerant in each component of the system as well as that dissolved in the oil. Simple volume and density calculations are used to calculate the amount of refrigerant in the single-phase components of the system. The dimensions of the system components as well as the value for each component volume can be found in Appendix A. The amount of refrigerant in the two-phase zones of the heat exchangers is calculated with the Hughmark (1962) void fraction correlation. This void fraction correlation was chosen over several others because it was found by experiment to be the most accurate, which is consistent with findings by Rice (1987). The comparision of four different types of void fraction correlations using component models and experimental data can be found in Appendix B. An empirical correlation by Grebner and Crawford (1992) which predicts the pressure-temperature-concentration relationships for various refrigerant/oil mixtures, is used to calculate the amount of refrigerant dissolved in the oil.

Chapter 3: RFSIM and the ACRC Solver

The ACRC equation solver handles most input and output for RFSIM and solves its governing equations with a modified Newton-Raphson method. The ACRC solver also performs ASME and Monte Carlo uncertainty analyses and a simple sensitivity analysis of the governing equations.

The organizational framework of the ACRC solver is based on the TrueBasic sensitivity analysis program by Porter and Bullard (1992). The ACRC solver includes modifications to the Newton-Raphson algorithm that improve its ability to solve equations when poor guesses for variable values are given. A simple means of "swapping" variables and parameters in the governing equations is also implemented. Sparse-matrix Jacobian calculation was implemented by Hahn and Bullard (1993) and has been modified slightly in the present version.

Additional information on the ACRC solver can be found in Mullen and Bullard (1994).

3.1 Model-Solver Relationship

The structure and organization of the ACRC refrigerator/freezer model as implemented with the ACRC solver is depicted in Figure 3.1. The separate subroutines for model initialization, checking, and equation evaluation allow this structure to handle special problems that arise in thermal system simulations. For instance, the boundary checking in RFSIM determines whether the refrigerant at the evaporator exit is currently two-phase or superheated and switches to a slightly modified equation set if the condition has changed since the last iteration. Because the equations are listed separately and in an order-independent fashion, it is relatively easy to modify them or to replace a component model with a new one.

3.2 Swapping Parameters and Variables

The basic requirement of the Newton-Raphson method is that there as many governing equations as variables and that the equations be independent and non-singular. Thus a given variable can become a parameter if a former parameter simultaneously becomes a variable (in order to maintain the same number of equations and variables), as long as the equations remain independent and have no singularities.

For example, Figure 3.2 depicts a set of three equations, requiring three variables for solution. Conventionally, a designer might specify the evaporator area (A_{evap}) and solve for the COP, but "swapping" allows the NR method to solve for the A_{evap} that will yield a particular COP. Examples of using "swapping" with RFSIM include specifying capacity while solving for evaporator size or the length or diameter of the capillary tube. Total system refrigerant charge can be specified, solving for condenser subcooling, or vice-versa.

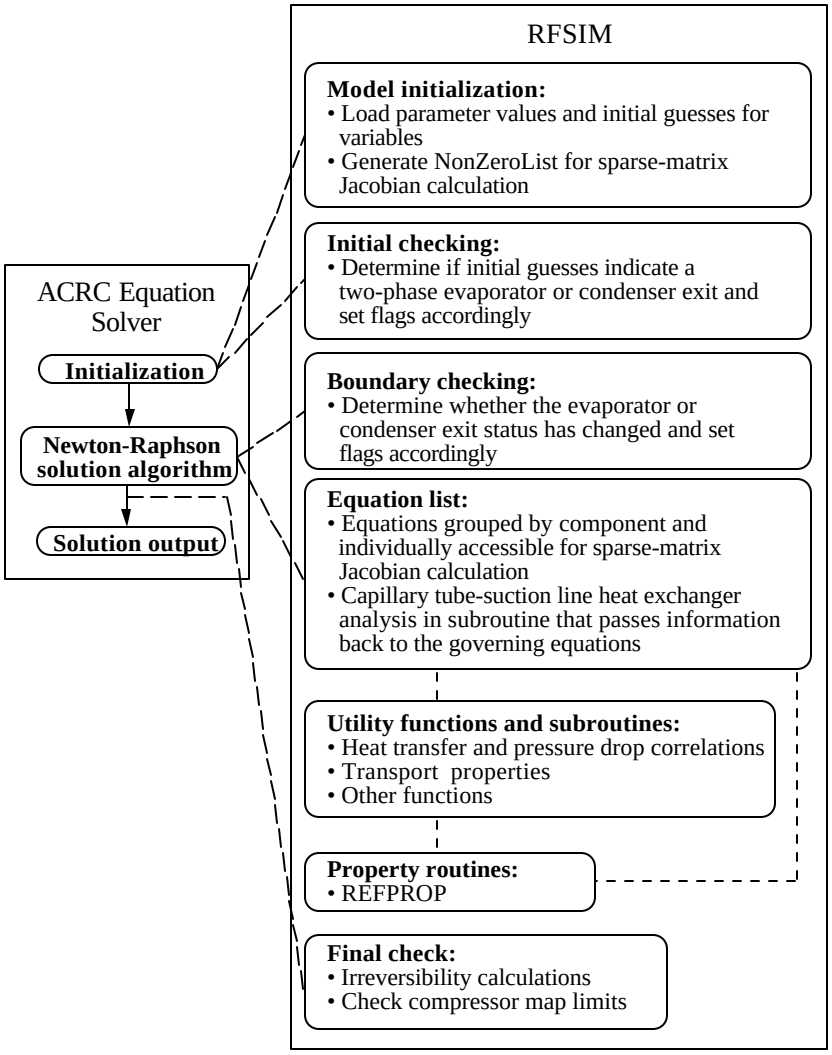

Figure 3.1 Organization of RFSIM and the ACRC solver

Variable-parameter swapping can also be used for parameter estimation. For example, the outlet conditions of a heat exchanger may be specified to allow a heat transfer coefficient to be solved for.

The ACRC solver allows swapping of a parameter and a variable by simply changing two flags in the input file. There is no need to change the program or recompile, making it simple to change the model from a simulation to a variety of design configurations.

Equation set:	**Normal configuration:**		**After swapping:**	
$COP = \frac{Q_{evap}}{\dot{W}_{comp}}$	Variables:	Parameters:	Variables:	Parameters:
	COP	U	A_{evap}	U
$Q_{evap}=U, A_{evap}$?T	Q_{evap}	A_{evap}	Q_{evap}	COP
$\dot{W}_{comp} = f(\Delta T)$	$\dot{W}_{comp}$	?T	$\dot{W}_{comp}$	?T

Figure 3.2 Example of parameter-variable "swapping"

3.3 Speed Enhancements in the Model and Solver

The refrigerator/freezer model consists of 124 governing equations, many of which involve lengthy calls to property routines or pressure drop functions. A straightforward evaluation of the Jacobian matrix for the 124 equations would require considerable execution time for the 15,376 (= 124^2) partial derivative calculations. However, most of those equations contain only a few variables, so the majority of the partial derivatives are always zero. Such a system of equations is termed "sparse."

To improve execution time, the non-zero elements of the Jacobian are mapped in advance by the ACRC solver, and that information is used to ensure that only those partial derivatives that may be non-zero are evaluated when the Jacobian is calculated. The remainder of the Jacobian elements are always zero and no time is wasted by calculating them.

Similarly, a sparse-matrix Gaussian elimination routine given by Stoecker uses full pivoting and linked lists to speed that step of the Newton-Raphson solution (Stoecker, 1989). The results of the speed enhancements are presented in Table 3.1 for RFSIM operating on a Convex C240 machine. A typical simulation run which uses a previous solution at similar conditions for the initial guesses, takes around one minute on average to solve. Actual execution times vary by computer, but it is clearly demonstrated that while the sparse-matrix Gaussian elimination saves a significant amount of time per NR iteration, the largest enhancement is obtained through the sparse-matrix Jacobian calculation.

Table 3.1 Speed enhancement results

	Sec/iteration
RFSIMwith no enhancement:	180
Adding sparse Gaussian elimination:	170
Adding sparse Jacobian calculation:	20

3.4 Automated Step Relaxation to Enhance Solution Robustness

The Newton-Raphson method is not globally convergent–a NR step may be calculated that does not bring the variables closer to a solution, particularly when the initial guesses are poor. A NR step may even result in an attempt to evaluate a function (e.g. a thermodynamic or transport property) outside of its domain. Common examples include attempting to calculate a refrigerant quality above the critical temperature or attempting to raise a negative number to a non-integer power (e.g. in a heat transfer or pressure drop correlation).

When either of the above instances occurs, the ACRC Newton-Raphson implementation recognizes it, retraces the step, reduces the NR step size by half, and retakes the shorter step. This technique greatly increases the model's robustness and somewhat reduces the need for good initial guesses.

Chapter 4: Component Model Validations

The validation of each of the component models is an important step towards validating the system model. Obviously the ability of the system model to accurately predict the refrigerator's performance is limited by the accuracy of the component models. Therefore, one can only hope that any deficiencies in a component model will not have a pronounced effect on the system as a whole. Hopefully, the examination of these components on an individual level will provide some insight into possible deficiencies in the first-principles based models and guide future improvement efforts. In order to evaluate the performance of each component model, a comparison of experimental and simulation results was conducted. An Amana TC18MBL top-mount refrigerator/freezer was run under steady-state conditions for a wide variety of ambient, fresh food compartment, and freezer temperatures.

4.1 Compressor Model

The biquadratic curve fits which are used in the compressor modeling equations (described in section 2.1) were examined by Cavallaro (1994) for their accuracy. The refrigerant mass flow rate map results were compared against two experimentally obtained values for mass flow rate.

The first mass flow rate was measured using a Sponsler turbine mass flow meter located at the exit of the condenser. This device determines the mass flow rate by measuring the volumetric flow rate of the liquid refrigerant. Problems arise when bubbles are present at the exit of the condenser, causing the mass flow meter to give inaccurate results. Another souce of error could be caused by the inaccuracy of the calibration to convert volumetric flow rate to mass flow rate. Therefore, another method of determining the mass flow rate was used to examine the accuracy.

The second mass flow rate is calculated from a refrigerant-side energy balance on a control volume of only the evaporator and ct-sl hx. The evaporative load (Q_{evap}) can be determined from the cabinet UA's and heater powers, while the enthalpies at the inlet to the capillary tube (h3) and the inlet to the compressor (h11) are found from measured values. Temperatures at the inlet to the capillary tube and compressor were measured with immersion thermocouples and their respective pressures were determined from pressure transducers. The mass flow rate was then calculated using the following equation

$$Q_{evap} = w_{calc}(h_{11} - h_3) \tag{4.1}$$

Cavallaro's results showed that the compressor map overestimates the energy balance by up to 5%. The mass flow meter results were disregarded, pending calibration of the device the next time the system is disassembled. These results are consistent with the compressor manufacture's claims that the map data are accurate to within 5% of the actual value. Cavallaro also reports that errors in the mass flow rate have the most significant effect on the condensing temperature in system models.

The compressor power map was found to be very accurate (within ±7.5 Watts) when compared with exprimental results from a power transducer.

4.2 Heat Exchanger Models

Research was conducted at the ACRC to develop multi-zone heat exchanger models which utilize both refrigerant- and air-side heat transfer coefficients correlations to obtain overall conductance values. It is these heat

exchanger models which are used in RFSIM. The results of these studies are summarized in the remainder of this secton.

Admiraal (1993) examined both the evaporator and condenser in the Amana experimental refrigerator assuming constant air-side and tube heat transfer resistances. His results showed that the use of variable refrigerant-side conductance models were more accurate than simple constant-conductance models, which were previously used in the refrigerator/freezer model. The evaporator model was able to predict loads within 4 %, which translates into only a 0.5 % error in the calculation of COP. When the model is run in design mode ,where subcooling and superheat are specified, such small uncertainties in heat exchanger conductances and other parameters cancel one another out and combine with other parametric uncertainties in ways that permit accurate prediction of COP and system energy use (Porter and Bullard, 1993).

In the condenser on the other hand, Admiraal reports that calculated heat transfer coefficients may be a significant source of modeling error, due to the complex air-flow patterns in the condenser. However, this method is superior to a constant conductance model. Therefore, the system model validation is conducted with a simpler air flow pattern by eliminating leaks and preventing any outlet air from recirculating into the condenser compartment. However, regardless of how accurate the refrigerant-side heat transfer coefficients can be predicted, the most important factors to consider are air-side values since they dominate the total heat transfer resistance in both heat exchangers.

Cavallaro (1994) demonstrated that heat exchanger performance could be predicted with similar accuracy over a wide range of air flow rates produced by variable speed fans.

4.3 Capillary Tube-Suction Line Heat Exchanger Model

The ct-sl hx model and simulation theory are briefly described in Section 2.3 and explained in detail in Appendix C. The data which are used in this validation were taken in the spring of 1994 using the aforementioned Amana top mount refrigerator operating with the manufacturer's recommended 8 oz. of R-12. This data set includes 16 steady-state operation points at four different ambient temperatures of 100°F, 90°F, 75°F, and 60°F. Only 7 of these 16 data points could be used for validating the stand-alone ct-sl hx model because the refrigerant must be subcooled at the exit of the condenser in order to measure the state of the refrigerant at the inlet to the capillary tube. The remaining points, however, are used in the system model validation because the outlet state of the condenser is calculated by the condenser model, thus alleviating this problem.

The inlet states of the refrigerant in both the capillary tube and suction line were specifed, along with the diameters of both the capillary tube and suction line and the lengths of each region in the ct-sl hx (listed in section 2.3). In the condenser, the condensing pressure and degrees of subcooling were given, while in the evaporator, the inlet pressure and temperature were given (all of the points contained a large amount of superheating in the evaporator). The model calculated the pressure and temperature steps in each region, the capillary tube exit state (specified by pressure and quality), and the mass flow rate through the capillary tube. The results of the simulations also allowed many of the variables along the component, such as temperatures and qualities, to be examined.

4.3.1 Refrigerant Mass Flow Rate

The primary purpose of the capillary tube is to regulate the flow of refrigerant to the evaporator. This component, in conjunction with the compressor, determines the mass flow rate in the entire system, which is a crucial part of each component model. Therefore, a necessary requirement of a ct-sl hx simulation model is to be able to predict the mass flow rate very accurately over a wide range of operating conditions. For these reasons, the values which are predicted by the ACRC ct-sl hx model are compared to mass flow values calculated from an energy balance, which was determined in section 4.1 to be most accurate method to measure mass flow rate.

The results of this comparison are shown in Figure 4.1. The data points are numbered 9-12 for the 75° ambient temperatures and 13-16 for the 60° ambients (data point 14 was not included because of measurement errors which had occured). In both sets of ambient temperatures, the air temperature at the evaporator inlet decreases with increasing data point number. The figure shows clearly that the model underpredicts mass flow by 20% on average.

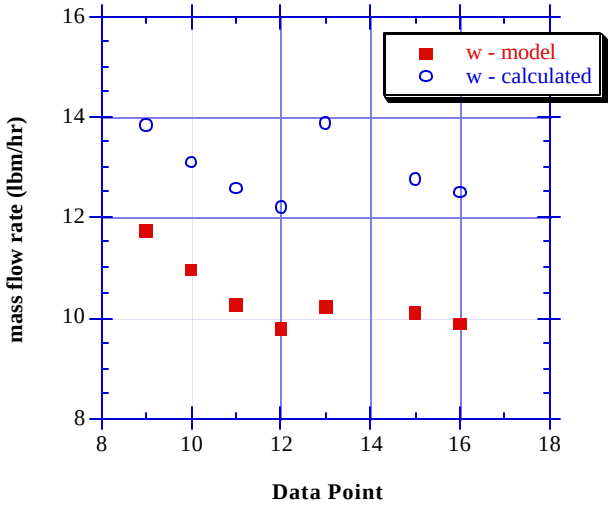

Figure 4.1 Comparison of mass flow rates

The factors which influence the mass flow rate in the capillary tube the most are the friction factor correlation and the capillary tube diameter. The former was modified with several different friction factor correlations (see section C.3.3 in Appendix C), but it had very little effect on the mass flow rate. The original model from Peixoto used a friction factor correlation developed by Pate (1982). However, this correlation was not a function of the tube roughness and was only accurate for R-12. Therefore, it was first replaced by an explicit formulation of the Colebrook single-phase friction factor (Swamee and Jain, 1976). To adapt this correlation to two-phase flow, an average friction factor was used that was a mass weighted average of the liquid and vapor phases. This assumes that both phases are traveling at the bulk velocity, and that forces are proportional to the volumes of liquid and vapor slugs (see Appendix C). A more accurate friction factor was obtained using a two-phase pressure drop correlation developed by Souza (1992). The frictional pressure drop is computed as if the flow were a single-phase flow, except for the introduction of modifiers to the properties inside the single-phase friction coefficient. This empirical correlation has been validated experimentally for inner tube diameters down to 0.118 in. It is this correlation which is used to obtain all of the results in this paper. As a best case scenario, the Blasius smooth tube friction factor was used throughout

the capillary tube to see how the smallest possible frictional resistance would affect mass flow. But even then, the predictions still remained well below the calculated value.

The capillary tube diameter also has a very pronounced effect on the mass flow rate. For some insight into the importance that the input parameters have on mass flow rate, a sensitivity analysis was performed. The results showed that the tube diameter has by far the largest effect on mass flow rate than any other parameter, with a 1% increase in diameter resulting in a 2.9% increase in mass flow rate. A Monte Carlo uncertainty analysis indicates that the mass flow calculation should be accurate to within 10% if the tolerances on diameter and inlet region length are within 1%. A tolerance for the tube diameter could not be found from the manufacturers specification drawings. The roughness for the tube was also absent in the manufacturer's drawings and was assumed, for the Colebrook calculation, to be 2.36E-5 in. (Melo et. al., 1994).

4.3.2 Outlet States

The remaining model variables are very difficult to compare because of the lack of experimental data measurements which are available for this component. It is very difficult to get precise measurements for capillary tube studies without elaborate measurement devices throughout the component. The Amana experimental refrigerator was ill-equiped to handle such demands, since the primary focus was to obtain accurate system measurements that were the least intrusive to the system. Therefore the comparative data are limited to the temperature at the suction line outlet and the energy gain in suction line. Ideally, the state of the refrigerant at the outlet of the capillary tube would be compared but flow conditions at the choked (sonic) exit of the capillary tube make the conditions at this point independent of the evaporator conditions. Upon exiting, the refrigerant expands to the evaporator pressure from the critical exit pressure. This isenthalpic expansion then sets the inlet evaporator quality, which can not be determined experimentally. It can be inferred, however, from measurements of the enthalpy change in the heat exchanger region.

Figure 4.2 shows a comparison of the suction line outlet temperature predicted by the model and the temperature at the suction line oulet which was measured with an immersion thermocouple with an accuracy of ± 1°F. This is a good indicator of the accuracy of the heat exchanger region's governing equations. Once again the model's predictions are below the data. This would tend to point to a deficiency in the heat transfer equations. Therefore, the Gnielinski heat transfer correlations were replaced by the Dittus-Boelter correlations in both the suction line and capillary tube, but were found to have a minimal effect on the results. Nonetheless, it is difficult to discern whether the heat transfer correlation is the source of error since all variables have such a strong dependence on mass flow rate.

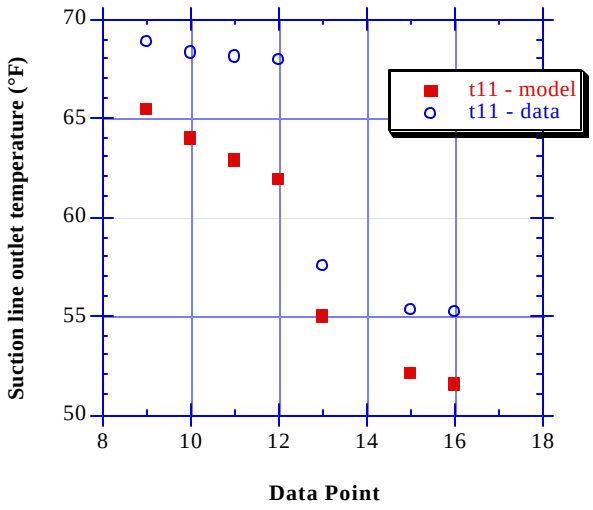

Figure 4.2 Comparison of suction line outlet temperatures

The wall temperature at the inlet and outlet of the heat exchanger region were also compared. The comparison of the predicted and measured wall temperatures at the suction line outlet (and capillary tube inlet) to the ct-sl hx are shown in Figure 4.3. This graph shows that the agreement for the 75°F ambient points is not as good as at the 60°F ambient points. This is consistent with findings by Peixoto and Bullard (1994) that the operating conditions having greater subcooling at the exit of the condenser are predicted better by the modeling equations. It is believed that this is because the equations in the liquid region are more accurate than the equations that describe the two-phase regions. Once again the general trend is similar to that of the mass flow rate results and is probably significantly affected by that variable. Otherwise, Figure 4.3 indicates that the heat transfer is underpredicted in the heat exchanger zone. Comparisons of the wall temperature at the suction line inlet to the ct-sl hx reflect the same deficiency in heat transfer, as the model predicts a wall temperature higher than the measured value.

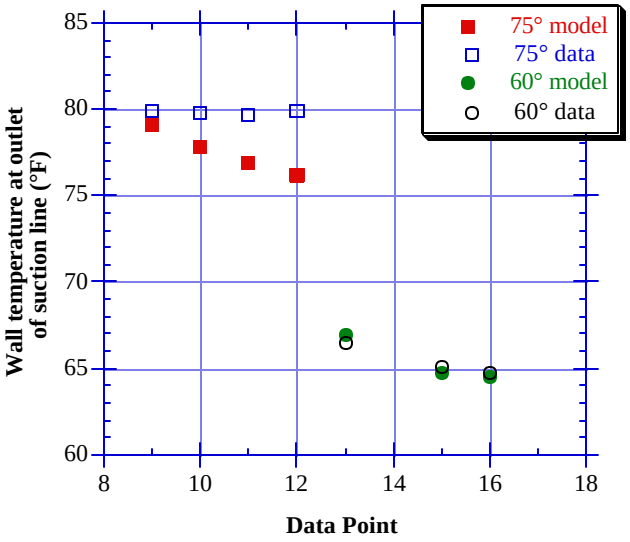

Figure 4.3 Comparison of wall temperatures at suction line outlet

4.3.3 Enthalpy Gain in Suction Line

The final comparison, shown in Figure 4.4, is along the lines of the last one, in that it attempts to examine the accuracy of the heat exchange region. It shows the enthalpy gain in the suction line. Not surprisingly, the model underpredicts the measured value. Any efforts at increasing or decreasing the heat transfer between the two tubes would be wise to concentrate on the suction line heat transfer coefficients since the superheated vapor dominates the total resistance. Predictably, changing the heat transfer coefficient in the capillary tube had very little effect on the heat exchanger performance.

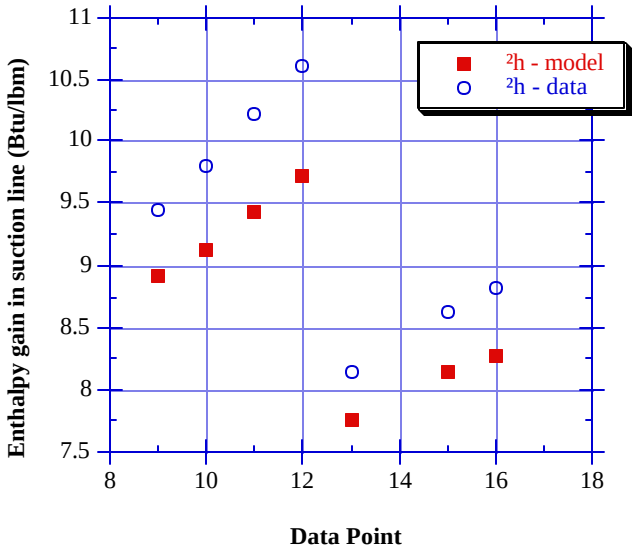

Figure 4.4 Comparison of enthalpy gains in suction line

4.3.4 Evaluation of Results

All of the aforementioned comparisons imply that the primary error in the model is the predicted mass flow rate. The assumption that the flow is homogeneous is perhaps an underlying source of error, since the mass flow is calculated from the critical liquid and vapor mass fluxes. The results are inconclusive as to whether the heat exchanger region is modeled correctly. A possible source of modeling error could be attributable to the geometry of the actual component in the Amana refrigerator. In actuality, the first 16 in. of the inlet region is slightly non-adiabatic and is exposed to the condenser air flow (a rough calculation predicts less than a 1°F temperature increase). Thus, it is questionable whether that assumption is suitable for accurate modeling.

Although these results are preliminary, the model appears to be more accurate in the lower ambient temperatures where there are large amounts of subcooling. Encouragingly, all of the results in general follow the same trend as the measured data values. This would seem to imply that the governing equations are correct but that the calculated values for such things as heat transfer coefficients, friction factors, and speed of sound may be inaccurate. Ideally, measurements are needed along the entire length of the component so that individual regions may be analyzed. Such examinations are currently underway at the ACRC using an experimental facility developed by Johnson and Dunn (1993). Until extensive experimental data is analyzed, it will be difficult to decide which areas to concentrate future improvements on this component model.

Chapter 5: System Model Validation

Results from the system model are compared to experimental data now that the component models have been examined for their accuracy. The accuracy of the system model is obviously limited by the accuracy of the component models (discussed in Chapter 4). However, the errors which occur on the component level may either cancel or be magnified at the system level. The results of this analysis should provide insight into which components of the system model should be improved to obtain accurate simulation results. This section will also test the ability of the model to predict the performance of the system using an alternative refrigerant.

5.1 Experimental Results

A comparison of experimental and predicted results was conducted to examine the accuracy of the system model. The previously mentioned, steady-state data set that was taken in the spring of 1994 is also used for this analysis. The methods which were used to obtain this data are described by Rubas and Bullard (1993). The refrigerator was operated with the manufacturer's recommended 8 oz. of R-12 over a wide range of ambient and evaporator inlet temperatures. The data set consists of 16 data points, four at each of the following ambient temperatures: 100°F, 90°F, 75°F, and 60°F. For each ambient temperature group, the evaporator inlet air temperature was decreased over a range of values which are representative of normal cycling operation. Thus, the first data point in each ambient temperature group has the highest evaporator inlet air temperature while the last has the lowest. For all eight data points in the 100°F and 90°F ambient temperature groups, the refrigerant at the exit of the condenser is two-phase and the refrigerant at the exit of the evaporator is slightly superheated (1-5°F). For the remaining eight data points in the 75°F and 60°F ambient temperature groups, however, the condenser exit is subcooled and the evaporator is significantly superheated (12-18°F).

5.2 Design Model Validation

The first step in validating the system model is to test its accuracy while operating in design mode. In this configuration, the user specifies the exit conditions of both the condenser and evaporator and the model assumes that the system charge and capillary tube are optimized to achieve these specified steady-state conditions. A design model, therefore, cannot predict the performance of the system over a range of ambient temperatures or during off-design conditions such as those experienced during cycling. Since the state of the refrigerant at the exits of the heat exchangers must be specified as inputs to the design model, the validation was performed only using the data points where the condenser is subcooled and the evaporator is superheated (i.e., at 75°F and 60°F ambient temperatures).

The predicted values of several key system variables are compared to measured values in section F.1 of Appendix F. These results, which are summarized in Figure 5.1, show that the design model overpredicts the efficiency of the system by roughly 3% on average. A closer examination of the data, provides some insight into possible causes for errors.

The evaporator capacity, shown in Figure F.2, is quite accurate while the system power, shown in Figure F.3, is consistently underpredicted. In regards to the latter, one can not expect a smaller error since the accuracy of the compressor power is well within the limits of the map data which were specified by the compressor manufacturer. The slight error in capacity, on the other hand, is traceable to another important and influential system variable, mass flow rate (labeled as w in Figure 5.1). The results of the mass flow rate comparison support the finding of Cavallaro

(1994) which stated that the compressor map overpredicted the actual value by about 5% (also within the range of the map accuracy). Therefore, one possible explanation is that the error in the compressor map is causing the evaporating temperature to be too high because the temperature difference in the evaporator must decrease in order to satisfy the specified evaporative load. This explanation is in fact consistent with the results found in Figure 5.1.

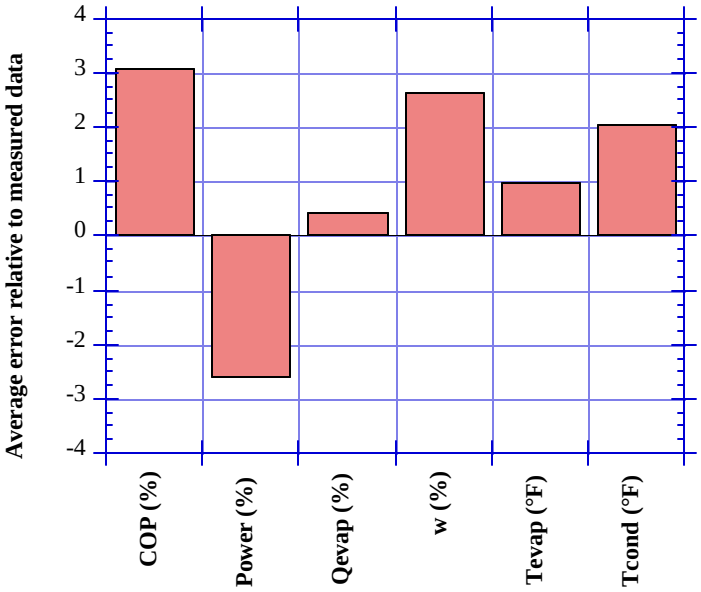

Figure 5.1 Error of system variables relative to measured data in design mode

Any attempt at reducing the error in the prediction of system performance should therefore concentrate on obtaining more accurate compressor maps. The accuracy of the remaining component models was established in earlier test (Reeves et. al., 1992; Admiraal and Bullard, 1993; Cavallaro and Bullard, 1994) and is verified with these results. In summary, these results show that the RFSIM design model is predicting as accurately as the compressor maps will allow. Examination of the system variable comparisons in Appendix F show that the predicted results follow the same trends as the data, demonstrating that the system model in design mode is accurate.

5.3 Simulation Model Validation

The next step in validating the system model is to test its accuracy while operating in simulation mode. As was previously discussed, the model can be changed from a design model to a simulation model by adding two sets of equations: a capillary tube-suction line heat exchanger model (described in Appendix C) and a charge conservation equation (described in Appendix B). In simulation mode, the system model solves for the states of the evaporator and condenser outlets rather than having them specified by the user. Therefore, all 16 data points were used for this analysis. For each simulation point, the ambient temperature, the average fresh food and freezer compartment temperatures, and the heater loads were inputs to the model.

The effect of these two sets of equations on the accuracy of the model can be found by comparing the simulation results to the previously discussed design results. Once again, the predicted values for several key system variables were compared to the measured values and are shown in section F.2 of Appendix F. These results

are summarized in Figure 5.2. As expected, the accuracy of the system model is much worse when operating in simulation mode. The primary cause for the poor accuracy can be traced back to the component validation of the capillary tube-suction line heat exchanger, which quantified the error in the ct-sl hx mass flow predictions. The error in mass flow rate is so dramatic that it dominates the rest of the system variables causing them to be inaccurate. The model also predicted better at the highest ambient temperatures, where there is the least amount of condenser subcooling and evaporator superheating.

The effect of the mass flow rate can be seen in the results of some of the predicted variables shown in Appendix F. The mass flow rate, which is consistently very low, is causing a larger superheat zone of the evaporator, and consequently an undersized two-phase zone. This condition requires that the temperature difference between the air and the refrigerant increase, causing the evaporating temperature to be too low. In fact, the model's predictions of evaporating temperature are also consistently low. The relatively good agreement in condensing temperature is a result of the relatively small effect that condensing temperature has on the mass flow rate through the compressor. Or in other words, the compressor map for mass flow rate is much more sensitive to the evaporating than the condensing temperature.

In summary, the accuracy of the design model, described above, demonstrated that the inaccuracies in the simulation model's predictions cannot be attributed to the other component models (the compressor, condenser, and evaporator), but instead must lie with the capillary tube-suction line heat exchanger model and/or the charge conservation equations. The results of the void fraction analysis in Appendix B suggest that it is unlikely that the charge conservation equations are contributing significantly to the error, and experiments are currently underway to separate and eliminate the remaining uncertainties so that the model's accuracy in simulation mode is as good as design mode.

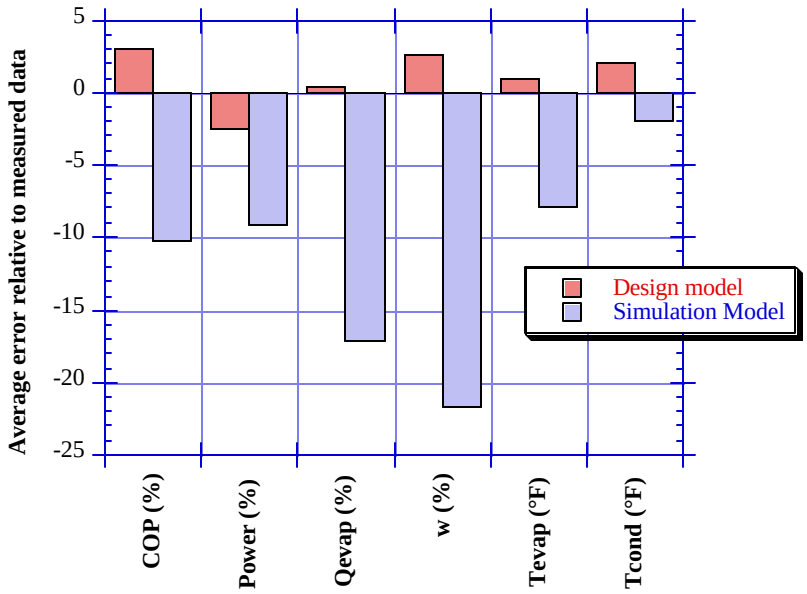

Figure 5.2 Error of system variables in design and simulation mode

5.4 Simulation Model Using Alternative Refrigerant

This section discusses the ability of the system model to accurately simulate the performance of the system with an alternative refrigerant. The steps which are necessary to modify the system model for this operation are described in section D.7 of Appendix D. In summary, all that is required are new property functions, new compressor maps, and new refrigerant-oil solubility coefficients. The alternative refrigerant which was chosen for this analysis is a natural hydrocarbon, propane (R290), and a flammable substance. However its combination of lower liquid density and higher heat of vaporization at typical operating conditions mean that a comparable refrigerating capacity can be achieved with less total system charge.

There are a few uncertainties which are introduced into the model up front when simulating propane. First, information was not available for propane/mineral oil mixtures, so the coefficients for R-12 are used as a rough approximation. More significantly, there is no compressor data for the compressor operating with propane. Therefore, new compressor maps for mass flow rate and power were generated assuming that the isentropic and volumetric efficiencies were a function of pressure ratio alone, and were refrigerant-independent. Obviously these assumptions will reduce the accuracy of the system model when compared the simulation results for R-12. Nevertheless, the model should provide accurate qualitative results and the same trends should be present when comparing the predicted results to the measured data.

The measured data was obtained from the same Amana experimental refrigerator that was used to obtain the data for R-12. None of the components of the system were altered in any way to account for the different operating fluid. For the 16 point data set, the refrigerator was operated with an experimentally determined optimal charge of 4.5 oz., found by minimizing the energy usage for normal cycling operation at an interpolated 5°F freezer temperature. And once again, the refrigerator was run at steady-state at the same four ambient temperatures as for R12 (100°F, 90°F, 75°F, and 60°F) and a range of evaporator inlet air temperatures. One interesting result of the experiments was that the impurities in "natural grade" propane were found to have a drastic effect on the vapor-pressure curve. Therefore, 99.5% pure propane was used for these experiments.

The model predictions and experimental data are compared in section F.3 of Appendix F. The same variables which were examined to determine the simulation and design model accuracies are included, with the exception of the mass flow rate. Because none of the data points have subcooled condenser exits, the actual mass flow rate could not be measured by the turbine mass flow meter in the liquid line or calculated using an energy balance.

The results of the variable comparisons, summarize in Figure 5.3, are somewhat inconclusive, showing a reverse trend from the R-12 results. The graph of evaporating temperatures shows that the simulation model is predicting a temperature that is an average of 5°F too high, as opposed to the results of the R-12 simulations which predicted this temperature to be too low. There are two possible explanations. First, the compressor maps which were generated from the R-12 maps are significant sources of errors. The compressor power map underpredicted the measured compressor power, by about 33%, at each of the measured condensing and evaporating temperatures. Therefore it is highly probable that the mass flow rate map is equally, if not more, inaccurate.

Second, it was not possible to separately validate the capillary tube-suction line heat exchanger component model when using propane, since no subcooled data points were obtained. Until the ct-sl hx model can be examined on a component level, its contribution to system-level errors is unknown. It is encouraging, however, to see that

aside from these errors, the model accurately predicted that the exits of both the condenser and evaporator would be two-phase for all of the data points.

Experiments are currently underway to address these problems. The refrigerator will be overcharged in order to obtain subcooled refrigerant at the condenser exit. This will allow the actual mass flow rate to be measured from an energy balance so that new compressor maps can be constructed for both power and mass flow rate. Knowledge of the state of the refrigerant at the outlet of the condenser will also allow the ct-sl hx component to be analyzed against experimental data.

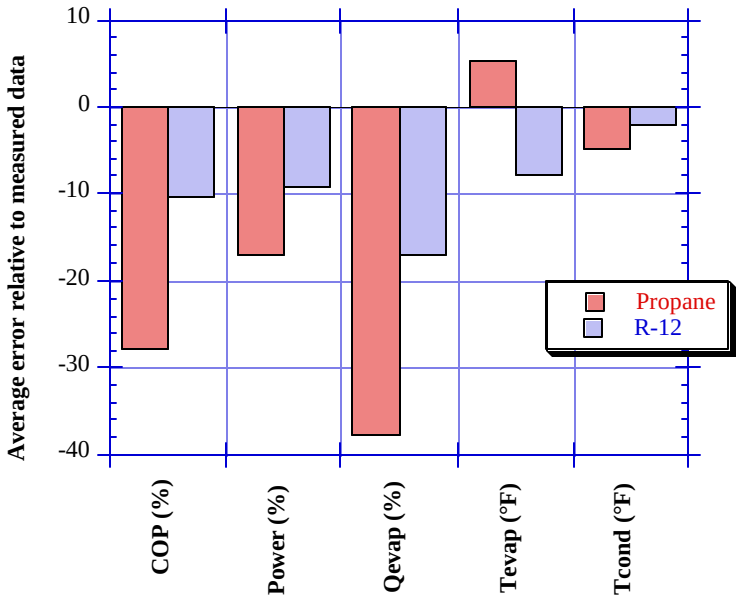

Figure 5.3 Error of system variables for R12 and propane in simulation mode

Chapter 6: Summary and Conclusions

A refrigerator/freezer model (RFSIM) was developed from the ACRC2 model by Porter and Bullard (1992) that is capable of running in either design mode or simulation mode. This model is solved using the ACRC solver (Mullen and Bullard, 1994), which is capable of switching equations during the course of a solution. The ACRC solver also uses several speed enhancement techniques which reduce the average solution time of the 124 equation set to under a minute. Several modifications were made to the ACRC2 model to develop a more generalized, and refrigerant-independent, model.

A capillary tube-suction line heat exchanger (ct-sl hx) model (Piexoto and Bullard, 1994), based on first principles, replaced a curve fit of experimental data that had previously calculated the mass flow rate through the capillary tube. By specifying a particular set of input variables to the ct-sl hx component model, the 250^{+} simultaneous equations could be backsubstituted into just six functions which appear in the system model. These six functions could then be solved "sequentially", and eliminate the need for initial guesses for all but six ct-sl hx variables. This technique minimized the solution time while maintaining the system model's robustness.

A study of several void fraction correlations was conducted to determine which one would most accurately calculate the refrigerant in the two-phase zones of the condenser and evaporator. A comparison of component model results versus experimental data revealed that the Hughmark (1962) correlation was more accurate than the Zivi (1964) or homogeneous correlations that were previously used. The refrigerant inventory equations for the single-phase components and the lubrication oil were also included. Lastly, heat transfer and pressure drop correlations were added as functions external to the system equations, like the NIST property routines, REFPROP. This allowed the calculation of the overall heat transfer coefficients and pressure drops in each zone of the evaporator and condenser to be calculated rather than user-specified.

The predictions of the model in both design and simulation mode were compared to experimental data to test RFSIM's accuracy. The results of the design mode analysis showed that the model predicted several system variables, including efficiency and evaporator capacity, very accurately. The slight discrepancies in some of the results were the result of the compressor maps used to obtain power and mass flow rate. The accuracy of the design model, therefore, could only be improved by using more accurate maps.

The simulation model results reflected the errors in the ct-sl hx component model, which underpredicts the mass flow rate by up to 20%. The source of error has been narrowed to either the two-phase friction factor correlation or the homogeneous assumption in the speed of sound calculation. Comparisons to experimental data show that the simulation model underpredicts efficiency by 10% on average, primarily due to a substantial error in the mass flow rate. Simulation results using propane are consistent with these findings, but reflect additional errors associated with the lack of compressor map data obtained with propane. Experiments currently underway are designed to correct these deficiencies.

References

ASHRAE, ASHRAE Handbook of Fundamentals, Atlanta GA, 1993.

Arthur D. Little, Inc., Refrigerator and Freezer Computer Model User's Guide, U.S. Department of Energy, Washington D.C., 1982..

Admiraal, D.M. and C.W. Bullard, "Heat Transfer in Refrigerator Condensers and Evaporators," University of Illinois at Urbana-Champaign, ACRC TR-48, 1993.

Cavallaro, A.R., "Effects of Varying Fan Speed on a Refrigerator/Freezer System," University of Illinois at Urbana-Champaign, ACRC TR-63, 1994.

Christoffersen, Brian, J. C. Chato, J.P. Wattelet, and A.L. de Souza, "Heat Transfer and Flow Characteristics of R-22, R-32/R-125 and R-134a in Smooth and Micro-fin Tubes," University of Illinois at Urbana-Champaign, ACRC TR-47, 1993.

Dobson, M. K., "Heat Transfer and Flow Regimes During Condensation in Horizontal Tubes," University of Illinois at Urbana-Champaign, ACRC TR-57, 1994.

Grebner, J.J. and R.R. Crawford, "The Effects of Oil on the Thermodynamic Properties of Dichlorodifluoromethane (R-12) and Tertrafluoroethane (R-134a)," University of Illinois at Urbana-Champaign, ACRC TR-13, 1992.

Hahn, G. W. and C. W. Bullard, "Modeling Room Air Conditioner Performance," University of Illinois at Urbana-Champaign, ACRC TR-40, 1993.

Hughmark, G.A., "Hold-up in Gas-liquid Flow," Chemical Engineering Progress, Vol. 58, No. 4, pp. 62-65, 1962.

Incropera, F.P. and D.P. DeWitt, Fundamentals of Heat and Mass Transfer, 3rd ed., John Wiley & Sons, Inc., New York, 1990.

Ito, H., "Pressure Losses in Smooth Pipe Bends," Journal of Basic Engineering: Transactions of the ASME, March 1960, p.135.

Johnson, M.J. and W.E. Dunn ,"Design of an Experimental Apparatus for Studying the Flow of Refrigerant R-134a in a Capillary Tube Refrigeration System," University of Illinois at Urbana-Champaign, ACRC TR-51, 1993.

Melo, C., Ferreira, R.T.S., Boabaid Neto, C., Goncalves, J.M., and M.R. Thiessen, "Experimental Analysis of Capillary Tubes for CFC-12 and HFC-134a," Proceedings of the 1994 International Refrigeration Conference, Purdue University.

Merriam, R., Varone, A. and H. Feng, EPA Refrigerator Analysis Program User Manual, Version 1.0, Arthur D. Little, Inc., 1993.

Mullen, C. E. and C. W. Bullard, "Room Air Conditioner System Modeling," University of Illinois at Urbana-Champaign, ACRC TR-60, 1994.

Peixoto, R. and C. W. Bullard, "A Design Model for Capillary Tube-Suction Line Heat Exhangers," University of Illinois at Urbana-Champaign, ACRC TR-53, 1994.

Porter, K. J. and C. W. Bullard, "Modeling and Sensitivity Analysis of a Refrigerator/Freezer System," University of Illinois at Urbana-Champaign, ACRC TR-31, 1992.

Reeves, R.N., Bullard, C.W., and R.R. Crawford, "Modeling and Experimental Parameter Estimation of a Refrigerator/Freezer System," University of Illinois at Urbana-Champaign, ACRC TR-9, 1992.

Rice, C.K., "The Effect of Void Fraction Correlation and Heat Flux Assumption on Refrigerant Charge Inventory Predictions," ASHRAE Transactions, Vol. 93, Part 1, 1987, pp. 341-367.

Rubas, P.J. and C.W. Bullard, "Assessment of Factors Contributing to Refrigerator Cycling Losses," University of Illinois at Urbana-Champaign, ACRC TR-45, 1993.

Souza, A. L., J. C. Chato, J. M. S. Jabardo, J. P. Wattelet, J. Panek, B. Christoffersen, and N. Rhines, "Pressure Drop During Two-Phase Flow of Refrigerants in Horizontal Smooth Tubes," University of Illinois at Urbana-Champaign, ACRC TR-25, 1992.

Stoecker, W. F., Design of Thermal Systems , 3rd ed., New York: McGraw-Hill, 1989.

Wattelet, J. P., "Heat Transfer Flow Regimes of Refrigerants in a Horizontal-Tube Evaporator," University of Illinois at Urbana-Champaign, ACRC TR-55, 1994.

Zivi, S.M., "Estimation of steady-state steam void-fraction by means of the principle of minimum entropy production," ASME Transactions, Journal of Heat Transfer, Series C, Vol. 86, May, pp. 247-252, 1964.

Appendix A: Component Dimensions and Volume Calculations

A.1 Introduction

When the model is operating in simulation mode, as opposed to design mode, the total amount of charge in the system is specified rather than calculated (i.e. mtotal is a parameter (K) rather than a variable (X)). Therefore, it is important to be able to accurately calculate the amount of charge in each of the components to be able to compare with the user-specified total amount of refrigerant charge. It is this charge inventory equation which allows the model to be solved at off-design conditions.

The two pieces of information that are needed to calculate the amount of refrigerant in a single component are: (1) the refrigerant's state, and (2) the volume that it occupies in that state. The former is exactly specified by any two of the properties which are variables of the model. Once the state is known, it is a simple matter to find the refrigerant's density. The volume is a constant which is specified by the user in the parameter list. Thus, if the state points of the various refrigerant-side components in the system aren't correct then the component masses will not add up to the total specified charge. Obviously, this makes it very important to have accurate values for the component volumes.

A.2 Procedure

The volume calculations were made in one of two ways. Either the hardware was directly measured or the dimensions were taken from a dimensioned drawing from the manufacturer, and in some instances a combination thereof. Figure A.1 is a schematic diagram of the refrigerant system showing each component that is accounted for in the mass inventory. Even though some of the components contain a negligible amount of refrigerant during steady-state operation, it is important to monitor the redistribution of the refrigerant in the system during transient operation, making each component important.

The total volume of the system has increased from its original amount as a result of the instrumentation and modifications which were made for the purpose of data acquisition. In some instances, the original components have been replaced by newer ones and are thus noted. A detailed description of each component will follow and summarize the procedure that was used in each case.

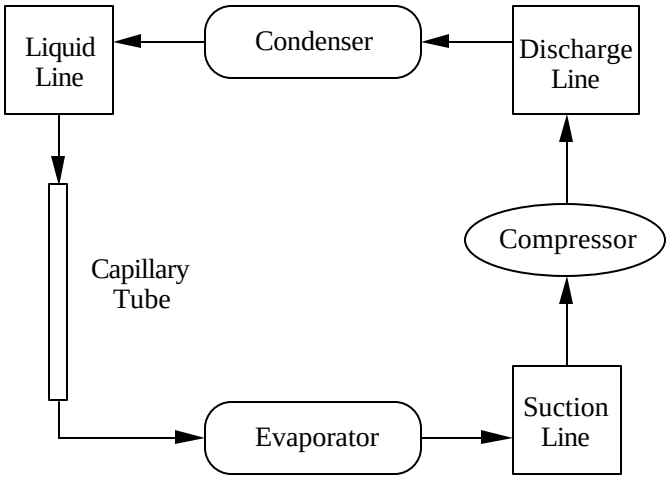

Figure A.1 Schematic diagram of components in charge inventory

A.2.1 Compressor

The compressor in the Amana experimental refrigerator is a Tecumseh reciprocating compressor, model AE1390V. It originally contained 13oz of grade 32 Naphthenic mineral oil, but it was estimated that six ounces may have been lost during the course of experimentation, leaving as little as seven ounces currently (Coulter, 1994).

The compressor housing encloses the compression mechanism and windings which are surrounded by an empty volume open to the suction line. Therefore, the refrigerant occupies the empty volume in the housing at the suction line pressure and temperature, which is always at a single-phase superheated vapor state when operating at steady-state. This makes the density very low, and as a result, a relatively small amount of mass resides in the compressor shell. Without the benefit of being able to open the compressor housing to directly measure the empty volume, it was determined through personal communication with the manufacturer to be 164 in^3 (Rubas, 1993). This value is not intended to include the volume of space which is occupied by the oil in the sump.

A.2.2 Discharge Line

The discharge line is a short copper tube which carries the high pressure refrigerant from the compressor to the condenser. It follows from this fact that the refrigerant is also always superheated vapor and has a very low density. Thus, the amount of mass in this component is very small. Nevertheless, it is included in the charge inventory to be rigorous. The dimensions and total volume are summarized in Table A.1.

A.2.3 Condenser

The condenser is a wire and tube type and had all dimensions specified in a dimensioned drawing from the manufacturer. The geometric input parameters for the condenser which are used in the volume calculations as well as some utility functions, such as pressure drops, are shown in Table A.2. The total volume is 18.535 in^3. The condenser is an important component in the mass inventory equation because the refrigerant can accumulate as high density subcooled liquid in the outlet region. In fact, during normal steady-state operation, it has been found that as much as half of the total mass is in the condenser.

A.2.4 Liquid Line

The liquid line region includes the tubing as well as other assorted components from the condenser to the entrance to the capillary tube. As was stated in the preceding section, the refrigerant at the exit of the condenser is often subcooled liquid with a very high density. Therefore it is very important to account for all the mass of refrigerant in this region as accurately as possible. This is a challenging task since the current liquid line has had extensive modifications made from the original one.

A turbine mass flow meter with two adaptive connectors was put directly after the condenser exit. The mass flow meter itself does not have a significant internal volume but the connectors at each end do, and as a result are accounted for. Figure A.2 shows the dimensions of the connectors. The total combined volume is 0.1657 in^3.

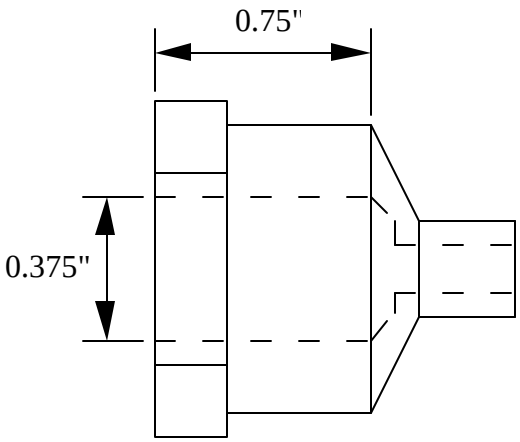

Figure A.2 Connector on mass flow meter

Following the mass flow meter is a filter-dryer that removes any water from the system. It contains several small desiccant spheres in between two screens and additional empty volume where refrigerant could reside. The empty volume in the desiccant region was calculated while taking into account the volume occupied by the spheres. Figure A.3 shows a profile of the filter-dryer and the necessary dimensions to calculate the volume. The total volume of the component is 1.253 in^3, while the volume that the spheres occupy was found to be 0.427 in^3. Hence, the total empty volume is 0.826 in3, neglecting the volume occupied by the screens.

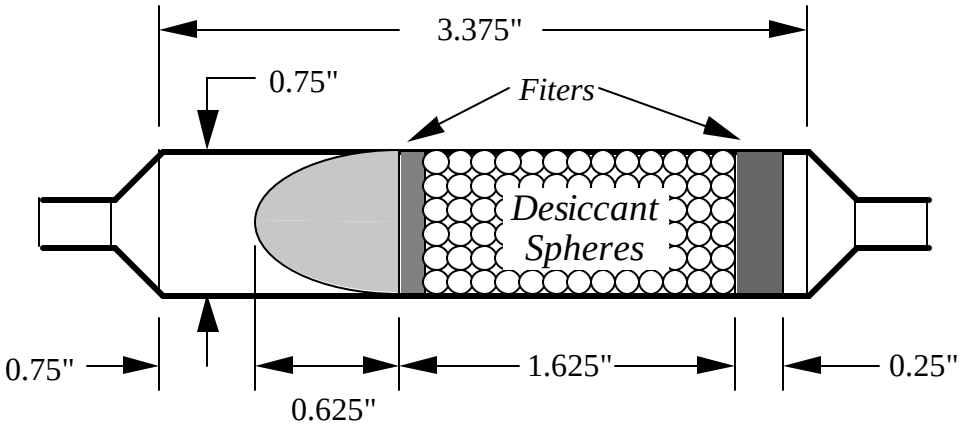

Figure A.3 Filter-dryer

It is possible that this liquid line region, which was not included in earlier model versions, could be responsible for calculated mass inventories which were previously below the known amount. The dimensions of the liquid line tubing are shown in Table A.1.

A.2.5 Capillary Tube

The capillary tube is also a two-phase component like the condenser and evaporator. However, unlike the other heat exchangers, the internal volume is very small so a rough approximation is made concerning the ratio of the mass of liquid to the mass of vapor in the component. The charge equation assumes that half the capillary tube is liquid and uses an average density. The dimensions of the capillary tube are summarized in Table A.1. The capillary tube has been replaced but it was verified through measurements that an exact replica of the original part was used.

A.2.6 Evaporator

The Peerless evaporator that is currently in use in the Amana was installed in June, 1992, and is a duplicate of the original. It is a fin and tube counterflow heat exchanger. The total volume is the largest of any other component at 37.396 in^3. A summary of the dimensions is shown in Table A.2. Directly downstream of the evaporator is an additional 7.57 in. of tubing (0.115 in^3), followed by an accumulator (5.984 $in^{3)}$ which prevents any liquid from entering the suction line. All of the aforementioned values were calculated from the dimensioned drawings from the manufacturer and verified on the unit which was replaced. After the condenser, the evaporator is the next largest site for mass accumulation, and during normal steady-state operation, approximately 25% of the refrigerant resides there.

A.2.7 Suction Line

The suction line is partially brazed to the capillary tube to form a counterflow heat exchanger. It connects the evaporator to the compressor inlet, hence the name suction line. Although the refrigerant may leave the evaporator as a two-phase liquid, it is always heated to superheated vapor by the warmer capillary tube. Therefore, it contains a negligible amount of refrigerant. The dimensions are summarized in Table A.1.

Table A.1 Summary of tubing dimensions

Tubing Type	**Discharge Line**	**Liquid Line**	**Capillary tube**	**Suction Line**
Total length	16"	18"	125.5" inlet: 47.0" hx: 50.485" outlet: 28.0"	67.6875"
Wall thickness	0.028"	0.028"	N/A	0.028"
Outer diameter	0.3125"	0.3125	0.081"	0.3125"
Inner diameter	0.2565"	0.2565	0.033"	0.2565"
Volume	0.8268 in^3	0.930 in^3	0.10734 in^3	3.497 in^3

Table A.2 Summary of heat exchanger dimensions

Component	**Condenser**	**Evaporator**
# of straight tube lengths	35	18
Straight tube length	14.5"	24"
# of return bends	35	17
Diameter of return bends	1.5"	1.0"
Total length	590.0"	466.3"
Wall thickness	0.025"	0.028"
Inner diameter	0.2"	0.319"
Volume	18.535 in^3	37.27 in^3

A.2.8 Total Volume

Obviously, the total system volume is simply the sum of the components that were just described. This gives a total system volume of 232.25 in^3.

A.3 Verification

The procedure just described is a good approximation at calculating the total system volume. However, there are many uncertainties that are not easily cleared up, for example, tubing which is insulated and not easily

examined. In some instances, components have been replaced or added and not well documented. Therefore, an experimental test was undertaken to verify the calculated system volume.

The theory behind the experiment is as follows. When the refrigerator is not running, the entire system begins to warm to the ambient temperature. In a typical ambient temperature between 70°F and 100°F, the refrigerant becomes superheated vapor throughout the isothermal system. Since it is a superheated vapor, its specific volume is known for a given pressure and temperature. If the refrigerator is carefully filled with an exact amount of charge (M_{vap}), then the volume of the entire system can be solved.

However, there is an added complication because of the oil in the system. The oil which is primarily used for compressor lubrication also absorbs a fraction of the R12 and reduces the vapor pressure in the system. Special empirical models must be used to predict the solubility relations for refrigerant-oil mixtures at equilibrium (Grebner, 1992). The dissolved refrigerant is a function of the temperature, pressure, and mass of oil in the system (M_{oil}). Therefore the total amount of refrigerant is now the sum of the vapor refrigerant and the amount dissolved in the oil (Mdis).

$$M_{total} = M_{vap} + M_{dis} = \frac{V}{\upsilon(P,T)} + f(T,P,M_{oil}) \qquad \text{(A.1)}$$

Unfortunately, the Grebner/Crawford empirical model introduced too much uncertainty to accurately calculate the system volume, because at ambient temperatures a significant fraction of the refrigerant was dissolved in the oil (up to ~35%). In addition, we were also unsure of the exact amount of oil in the compressor (see section A.2.1).

Therefore, to remove the added uncertainty of the amount of refrigerant dissolved in the oil, a refrigerant was sought that was non-soluble in the Naphthene oil present in the Amana compressor. Ironically, the successor to R-12, R-134a, fit that criterion. Now all that needed to be accounted for was the refrigerant that existed in the system in the form of vapor.

First, the refrigerator was filled with exactly 0.194 lbm of R-134a. Then the system was allowed to come to complete thermal equilibrium at a constant ambient temperature. Finally, the pressure and temperature measurements within the system at that ambient temperature, were taken by the data acquisition system and recorded. This procedure was followed at three different ambient temperatures: 60°F, 75°F, and 90°F. The results are shown in Table A.3. These measurements were then used in Engineering Equation Solver (EES) to determine the specific volume of the refrigerant at each state. Multiplying the mass by the specific volume then produced the total volume values shown in Table A.3.

Table A.3 Experimental results

Ambient Temperature (°F)	System Pressure (psia)	System Temperature (°F)	Internal Volume (in^3)
60	62.3	59.9	261.1
75	68.9	75.2	243.5
90	75.2	90.6	230.3

It was somewhat unsettling to discover that the three values for volume were not nearly identical. Nevertheless, it was encouraging to discover that the values were in the range of the total volume that was calculated using the component dimensions (232.14 $in^{3)}$. Here are some hypotheses to explain why a discrepancy exits between the calculated and experimental total volume values.

First, the accuracy of the measurement devices could be a cause for absolute error in the experimental values. A change in the temperature by one degree Fahrenheit causes a 0.3% change in specific volume, while a change in pressure by 1 psia causes a 1.8% change in specific volume. Thus, the pressure has a much larger effect on the accuracy than the temperature does. Since the thermocouples on the refrigerator are accurate to within 1°F, it is not believed that this is a source of significant error. On the other hand, the pressure transducers are only accurate to within up to 2.0 psia at high pressures. Therefore, it is possible that the uncertainty in the pressure measurements could cause the absolute values to be off.

Second, it is possible that trace amounts of R-134a dissolved in the Naphthenic mineral oil. This could explain why there is a relative error between the experimental values. Examination of the Grebner/Crawford refrigerant oil mixture solubility correlation shows that for the range of pressures measured, it is the temperature that has the largest effect on the amount of refrigerant that dissolves in the oil. This is easily seen in a plot of dissolved refrigerant versus pressure and temperature (Rubas, 1993). If the coefficients and properties of R-12 are used in the correlation, the amount of refrigerant that is dissolved in the oil decreases with increasing ambient temperature. Comparing to the amount of dissolved refrigerant predicted at 60°F, there is 58% less at 75°F and 74% less at 90°F. Therefore, allowing for slight amounts dissolved in the oil could possibly explain the differences in the experimental results.

A.4 Conclusions

The dimensions of every component in the system were either directly measured or taken from a dimensioned drawing from the manufacturer. These dimensions were then used to calculate each of the component volumes and summed to determine a total system volume of 232 in^3. In order to verify this result, an experiment was run that would produce an experimental total volume for comparison. The experimental results ranged from 261 in^3 to 230 in^3, with an average of 245 in^3. However, since the instrument measurements and oil were believed to have a slight effect on the accuracy of the experimental values, the value calculated from the component dimensions is believed to be more accurate. Most importantly, the volumes of the condenser and evaporator, which contain approximately 75% of the total charge, are believed to be accurate.

References

Coulter, W., personal communication, University of Illinois, Urbana, IL, 1994.

Grebner, J.J. and R.R. Crawford, "The Effects of Oil on the Thermodynamic Properties of Dichlorodifluoromethane (R-12) and Tetrafluoroethane (R-134a)," University of Illinois at Urbana-Champaign, ACRC TR-13, 1992.

Rubas, P.J. and C.W. Bullard, "Assessment of Factors Contributing to Refrigerator Cycling Losses," University of Illinois at Urbana-Champaign, ACRC TR-45, 1993.

Appendix B: Void Fraction Correlation Analysis

B.1 Introduction

The ability to analytically predict the refrigerant charge inventory is an important part in the development of a simulation model for a refrigeration system, because the off-design performance is determined by the amount of total charge in the system. In order to design the system to operate efficiently at both the design and off-design conditions charge inventory predictions must be accurate. For dynamic modeling, the need for accurate inventory of the refrigerant is crucial. This capability also provides a design tool for determining ways to minimize total system refrigerant charge which has many beneficial implications.

B.2 Refrigerant Mass Equations

Single phase components can be modeled rather simply and accurate results can be obtained by having precise volume measurements (Appendix A). However, predicting the refrigerant charge inventory in a two-phase component is a significantly more difficult task. There are two basic uncertainties: the degree of vapor-to-liquid slip at each cross section in the two-phase region, and the variation of refrigerant quality with length through the two-phase region. The two factors which affect the accuracy of this calculation are the void fraction representation and the two-phase heat flux assumption. The latter has been found to be insignificant for forced flow evaporators and of secondary importance to choice of void fraction correlation for condensers. In regards to the former, charge inventory predictions have ranged by as much as a factor of 10 for evaporators in heat pump applications (Rice, 1987).

The single phase refrigerant mass, m, contained in a length of tubing, L, of cross sectional area A_c and total volume, V is given by Equation B.1

$$m = A_c L \frac{\int_0^L \rho \cdot dl}{\int_0^L dl} = V \cdot \rho_{ave} \tag{B.1}$$

where ρ_{ave} is a suitably averaged refrigerant density over the tube length. This equation is used to calculate the refrigerant mass in the subcooled liquid or superheated vapor sections of a heat exchanger.

When determining mass in two-phase regions the total is the sum of the vapor, g, and liquid, f, contributions occupying each cross sectional area over the length of the region. The void fraction, α, is the ratio of the cross-sectional area of the vapor phase to the total cross-sectional area. Therefore the total mass, m_t, can be expressed in terms of tube volume V

$$m_t = \frac{V \cdot \left[\rho_g \int_0^L \alpha \cdot dl + \rho_f \int_0^L (1-\alpha) \cdot dl\right]}{\int_0^L dl} \tag{B.2}$$

The void fraction α in Equation B.2 is generally represented as some function of refrigerant quality, x, as $\alpha = f_\alpha(x)$. Hence, to evaluate the total mass equation above a relationship between tube length and quality must be established. Traditionally this is accomplished by writing an expression regarding the heat flow variation, dQ, with differential length, dl, in the two phase region.

$$dQ = \dot{m}_r h_{fg} dx = f_Q(x) dl \tag{B.3}$$

where

$\dot{m}_r$ = refrigerant mass flow rate

h_{fg} = enthalpy of vaporization, and

$f_Q(x)$ = assumed heat flux equation

The total mass equation can now be written as

$$m_t = V \cdot \left[\rho_g W_g + \rho_f (1 - W_g)\right] \tag{B.4}$$

where

$$W_g = \frac{\int_{x_i}^{x_o} \frac{f_\alpha(x)}{f_Q(x)} \cdot dx}{\int_{x_i}^{x_o} \frac{1}{f_Q(x)} \cdot dx} \tag{B.5}$$

and x_i and x_o are inlet and outlet refrigerant qualities. Wg is called the refrigerant vapor density weighting factor. Thus the evaluation of the total mass in the two-phase region is reduced to the problem of evaluating the above integrals and selecting the appropriate void fraction correlation and heat flux assumption (Rice, 1987).

B.3 Void Fraction Correlations

For the purposes of this analysis, four void fraction correlations were examined to see which yielded the most accurate results. Existing void fraction correlations can be classified into four categories: homogeneous, slip-ratio-correlated, X_{tt}-correlated, and mass-flux-dependent. A void fraction correlation was taken from each group to be evaluated and compared. The models increase in complexity from the homogenous model to the empirically based Hughmark correlation.

B.3.1 Homogeneous

Generally the void fraction is represented as some function of mass quality and several properties which are constant at a given average saturation temperature. Several void fraction representations of this kind have been developed, and the most simplified of which is the homogeneous model. This model assumes that the two phases are a homogeneous mixture traveling at the same velocity. Thus, the relationship between quality and void fraction are derived as

$$\alpha = \frac{1}{1 + \left(\frac{1-x}{x}\right)\frac{\rho_g}{\rho_f}} \tag{B.6}$$

B.3.2 Slip-Ratio-Correlated

A slightly more complex model assumes that the two phases are separated into two exclusive streams that are flowing at different velocities, u_f and u_g. The ratio of the two defines a property called the slip ratio, $S = u_g/u_f$. A new relationship is now derived from equation (B.6) and is slightly modified to include the slip ratio

$$\alpha = \frac{1}{1 + \left(\frac{1-x}{x}\right)\frac{\rho_g}{\rho_f} \cdot S} \tag{B.7}$$

The slip ratio has been estimated by several investigators. For the purpose of this analysis, a void fraction developed by Zivi was used. The slip ratio is defined as

$$S = \left(\frac{\rho_g}{\rho_f}\right)^{-1/3} \tag{B.8}$$

This relationship was developed for annular flow based on principles of minimum entropy production under conditions of zero wall friction and zero liquid entrainment (Zivi, 1964).

B.3.3 X_{tt}-Correlated

Another type of correlation uses the Lockhart-Martinelli correlating parameter X_{tt} defined as

$$X_{tt} = \left(\frac{1-x}{x}\right)^{0.9} \cdot \left(\left(\frac{\mu_f}{\mu_g}\right)^{0.2} \cdot \frac{\rho_g}{\rho_f}\right)^{0.5} \tag{B.9}$$

and the void fraction is defined over the following ranges developed by Wallis (1969), and refined by Domanski and Didion (1983) for $X_{tt} > 10$.

$$\alpha = \left(1 + X_{tt}^{0.8}\right)^{-0.378} \qquad \text{for } X_{tt} = 10$$

$$\alpha = 0.823 - 0.157 \ln\left(X_{tt}\right) \qquad \text{for } X_{tt} > 10$$

B.3.4 Mass-Flux-Dependent

Lastly, the Hughmark correlation was used. It is an empirical correlation that assumes a bubble flow regime with a radial gradient of bubbles across the channel. Although developed for vertical upward flow with air-liquid systems near atmospheric pressure, it was found to predict other flow regimes and geometries as well. It is based on a form of the homogenous correlation with the exception of the correction factor K_H found in the numerator

$$\alpha = \frac{K_H}{1 + \left(\frac{1-x}{x}\right) \cdot \frac{\rho_g}{\rho_f}} \tag{B.10}$$

In turn, K_H is a function of the correlating parameter Z which is dependent upon a viscosity-averaged, α-weighted Reynolds number, the Froude number, and the liquid volume fraction.

$$Z = \frac{Re_\alpha^{1/6}\, Fr^{1/8}}{y_L^{1/4}} \tag{B.11}$$

Then K_H is found by using a curve fit of K_H as a function of Z. The solution requires an iterative procedure since Z contains a dependence on void fraction through the averaged Reynolds number.

B.4 Heat Flux Assumption

As was previously mentioned, the accuracy of charge inventory predictions is not heavily dependent on the two-phase heat flux assumption. For this analysis a constant heat flux assumption was used. This implies that the quality varies linearly along the tube length. Thus, the heat flux weighting factor becomes a constant equal to 1.

B.5 Procedure

The void fraction correlations just described were examined in a domestic refrigeration system to determine which would give the most accurate and consistent results. This was accomplished by comparing the results of component models which use the void fraction correlations with actual experimental results. These experimental data contain several measurements throughout the system operating at steady-state under a specific set of operating conditions. Since the amount of refrigerant in just the two-phase components of the system (the evaporator and condenser) cannot be determined from the experimental data, it is only possible to compare the actual total amount of charge to the predicted total. Therefore, the data are used to calculate the amounts of refrigerant in each component at several operating points. These individual amount are then summed to get a total predicted amount at each data point. All these predicted amounts should then match the actual system charge used in the experiment.

The component models of the condenser and evaporator were taken from the ACRC refrigeration model (Porter and Bullard, 1992) which assumes multi-zone heat exchangers having constant overall heat transfer coefficients and pressure drops. The components in which the refrigerant was single-phase, such as tubing between components, simply calculated the mass by using the average density and the volume of the component (Eqn B.1). Finally, the amount of refrigerant dissolved in the systems lubrication was calculated using a refrigerant/oil mixture solubility model (Grebner and Crawford, 1992).

The experimental data which were used to make the charge inventory calculations were obtained from ACRC Project 12. They consisted of two data sets comprised of steady-state points at ambient temperatures ranging from 100°F to 60°F and a wide range of compartment temperatures.

The component models were run using Engineering Equation Solver (EES). In addition to the many parameters which had to be specified, several variables were specified by the experimental data. In the heat exchangers, both the refrigerant and air inlet states were specified, but not the outlet states. It was also necessary to use the correct set of equations by specifying whether the outlets of the evaporator and condenser were superheated or subcooled, respectively. Conversely, in the single-phase components, both the inlet and outlet states were specified so that the average density could be calculated. Finally, the power to the condenser fan and the refrigerant mass flow rate were specified from the data. The integrals in the total mass equation (Eqn. 4) to calculate the weighting factor, W_g, were evaluated using a Gaussian-Legandre quadrature method for numerical integration (Porter and Bullard, 1992). This procedure was followed for each of the void fraction correlations.

B.6 Results

The results of the analysis are shown in the several figures which follow. Figure B.1 shows the total predicted charge for each void fraction correlation calculated at each of the steady-state points from one of the data sets. Due to the two-phase conditions found at the evaporator and condenser exits in several of the points in the other data set, it was not used further in the analysis. Obviously the Hughmark void fraction correlation predicts the

highest amount of total charge which is consistent with published reports (Rice, 1987). The exact amount of charge in the refrigerator at the time of the experiment was 12 oz.

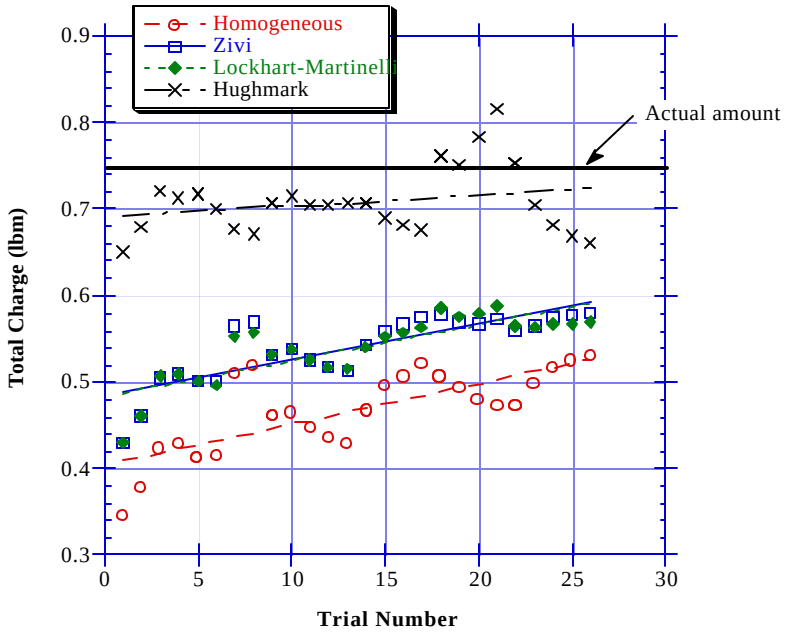

Figure B.1 Comparison of void fraction correlations

So it appears that the all the void fraction correlations except for Hughmark seriously underpredict the total amount of charge. Additionally, the total charge is more consistent with Hughmark than the other three, as can be seen from the linear curve fits of the data points for each method. The line for Hughmark is much flatter than the others. The only discrepancy in the Hughmark data are the five points at the end which are considerably higher than the rest. Interestingly, these point are for a low (60°F) ambient temperature and low cabinet temperatures where the system is at a low cooling capacity.

Figure B.2 shows the amount of charge in each of the components of the system for the Hughmark correlation. Note that most of the charge is present in the evaporator and condenser, and the mass in the evaporator fluctuates more than any of the other components. Additionally, the questionable points appear to be the result of the evaporator calculation.

For comparison, Figure B.3 shows the breakdown of the component masses for the Zivi void fraction correlation. The graphs shows that the underprediction is due to the charge which is calculated for the evaporator. The difference between the Hughmark and Zivi correlations for the evaporator accounts for most of the difference in total system charge.

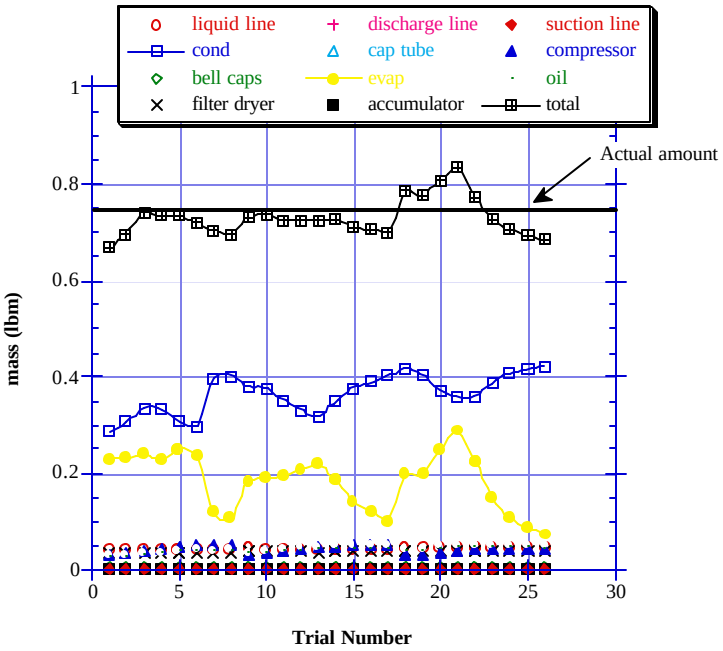

Figure B.2 Component charge distribution using Hughmark correlation

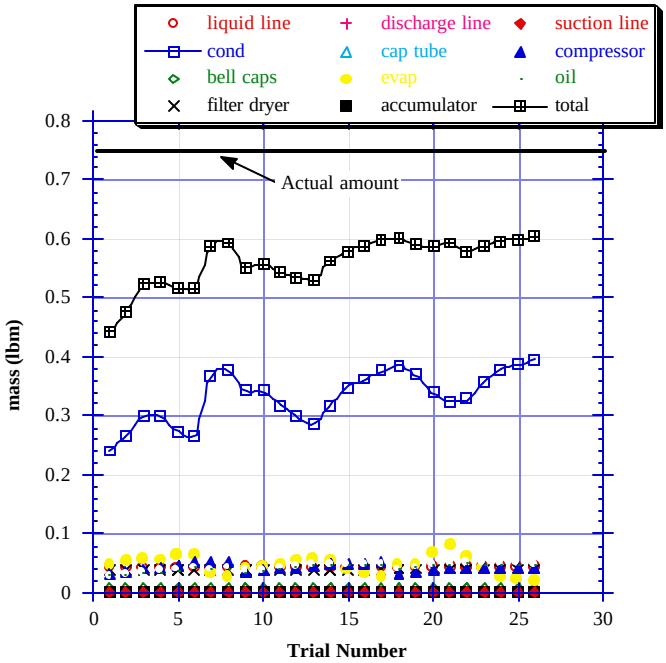

Figure B.3 Component charge distribution using Zivi correlation

The remainder of the components consisting of the single phase components and the refrigerant dissolved in the oil are shown in Figure B.4. The largest contributors to total charge are the subcooled components, filter-dryer and liquid line tubing, and the charge in the compressor can and oil. As expected the latter contributors follow

closely to the suction pressure of the compressor. Most of the other components are seemingly insignificant to the total charge.

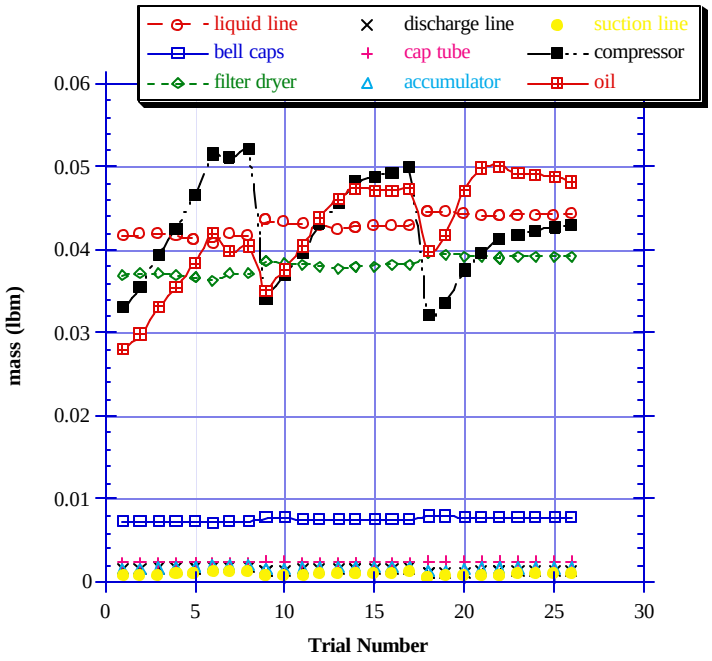

Figure B.4 Masses of Single phase components and refrigerant in oil

B.7 Conclusions

As has been shown, the Hughmark void fraction correlation is the most accurate at predicting the refrigerant charge when doing a component simulation. The others significantly underpredict the total mass in the system, especially in the evaporator. Another criterion for which the Hughmark correlation outperformed the others was in providing a more consistent total mass for the 26 trial runs. There is less variance from the mean and could be even less if the askew points at the end could be disregarded. The next step in validating the Hughmark correlation will be to use it in a simulation model in which the states in the system are not specified from a data set but rather solved for by the system model.

References

Domanski, P. and D. Didion, "Computer Modeling of the Vapor Compression Cycle with Constant Flow Area Expansion Device," NBS Building Science Series 155, 1983.

Grebner, J.J. and R.R. Crawford, "The Effects of Oil on the Thermodynamic Properties of Dichlorodifluoromethane (R-12) and Tetrafluoroethane (R-134a)," University of Illinois at Urbana-Champaign, ACRC TR-13, 1992.

Porter, K.J. and C.W. Bullard, "Modeling and Sensitivity Analysis of a Refrigerator/Freezer System," University of Illinois at Urbana-Champaign, ACRC TR-31, 1992..

Rice, C.K., "The effect of void fraction correlation and heat flux assumption on refrigerant charge inventory predictions," ASHRAE Transactions, Vol. 93, Part 1, 1987, pp.341 - 367.

Wallis, G.B., One-Dimensional Two-Phase Flow, New York, McGraw-Hill, pp.51-54, 1969.

Zivi, S.M., "Estimation of steady-state steam void-fraction by means of the principle of minimum entropy production," ASME Transactions, Journal of Heat Transfer, Series C, Vol. 86, May, pp.247-252, 1964.

Appendix C: Capillary Tube - Suction Line Heat Exchanger Model and Simulation Theory

C.1 Introduction

The capillary tube-suction line heat exchanger (ct-sl hx), shown in Figure C.1, is one of the four major components of the refrigeration system being modeled. This counterflow heat exchanger consists of the capillary tube soldered to the outside of the larger diameter suction line to the compressor. The capillary tube is broken up into three distinct regions for modeling purposes. First is the adiabatic inlet region, followed by the heat exchanger region with the suction line, and finally the outlet adiabatic region. The capillary tube is a very important part of the system because it must: 1) reduce the pressure of the liquid refrigerant, and, 2) regulate the flow of refrigerant to the evaporator. (Stoecker, 1986)

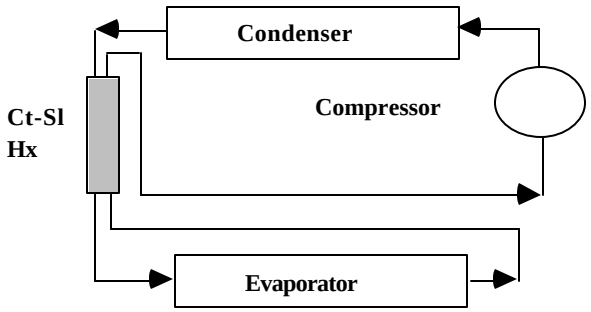

Figure C.1 Vapor compression cycle with ct-sl hx

Capillary tube-suction line heat exchangers are very common in household refrigerators because they can increase system capacity by using the colder suction line to lower the enthalpy of the fluid entering the evaporator, with only a modest increase in compressor power. Thus there is a slight improvement in the system COP. It also has the added benefit of preventing liquid refrigerant from entering the compressor.

When operating in design mode, the system model assumes that the total amount of refrigerant and the sizing of the capillary tube have been optimized at that operating condition. Thus, the ct-sl hx model is very important when running the system model in simulation mode. It enables the system model to be solved at a range of operating temperatures, with a fixed amount of charge, by calculating the mass flow rate through the user specified capillary tube at off-design conditions.

C.2 Description of Process

Unlike its simple appearance, the capillary tube-suction line heat exchanger is a very difficult component to model. The refrigerant in the suction line is typically superheated vapor and is easily modeled as a single-phase fluid. However, depending upon the inlet conditions to the heat exchanger, there can be a combination of processes occurring in the capillary tube. For instance, the refrigerant can undergo such complex processes as flashing two-phase flow and critical (choked) flow. Therefore, a model must have the capability to run in several possible modes

to account for operating points at off-design conditions in which different combinations of processes may be occurring. This section will explain all the possible processes which are accounted for as the refrigerant travels through each region of the capillary tube.

First consider the inlet adiabatic region of the capillary tube. The entering refrigerant, from the condenser, is either a two-phase mixture or a subcooled liquid. If the former is true then the mixture pressure continues to decrease isothermally and the entire adiabatic region can be modeled as a two-phase mixture. If the latter is true then the refrigerant decreases pressure almost linearly until the flash point is reached so that the remainder of the region is two-phase. Fortunately, the system being modeled rarely operated with large amounts of subcooling at the exit of the condenser when properly charged. Therefore the model assumes that flashing never occurs in the heat exchanger region.

Therefore the refrigerant always enters the heat exchanger region of the capillary tube as a two-phase mixture. However, the flow is no longer adiabatic, because of the exchange of energy with the suction line, causing two opposing mechanisms to counteract one another. The flashing of the refrigerant tries to increase the quality while the energy exchange tries to decrease it. If the refrigerant enters the heat exchanger region with too low a quality, the heat exchange with the suction line may cause recondensation to occur. Otherwise, the refrigerant will remain two-phase throughout the remainder of the heat exchange region.

Finally the refrigerant enters the adiabatic outlet region. If recondensation has occurred in the heat exchanger region then the refrigerant will once again flash into a two-phase mixture. As the two-phase mixture continues to vaporize, the increase in specific volume will cause an increase in the velocity of the refrigerant. Previous experiments on domestic refrigerators have shown that the velocity normally increases until critical flow is reached. At a fixed condenser pressure, further reductions of the evaporator pressure below this point will not increase the mass flow rate. Thus it is assumed that there is a condition of choked flow at the exit of the outlet region.

C.3 Description of Model

The modeling equations used for this simulation code were taken from work which was done on capillary tubes at the ACRC (Peixoto, 1994). The approach taken here builds on most of the assumptions and correlations that have been verified in the literature, and employs a solution technique that makes it unnecessary to assume a linear quality profile as other authors have done. The following sections state the assumptions, define the variables, and list the governing equations.

C.3.1 Assumptions

The assumptions for adiabatic flow are:

a. negligible heat exchange with the ambient;
b. steady state, pure refrigerant one-dimensional flow;
c. homogeneous equilibrium two-phase flow;
d. critical conditions reached when Mach number of the homogeneous liquid and vapor mixture at exit of the outlet region is equal 1.0.

The additional assumptions for the heat exchanger region are:

e. negligible axial heat conduction in the capillary tube and suction line walls;

f. negligible thermal resistance in the capillary tube and suction line walls,

g. radially and axisymetrically isothermal capillary tube and suction line walls.

C.3.2 Diagram of Model with Variables and Parameters Defined

Figure C.2 only defines the parameters (shown in boldface) and variables which are present in the system model. The flashing point is shown to lie in the inlet region, but it could also be absent in the case of a two-phase inlet condition. Lsub and DL, which are outputs of the model, show what fraction of the inlet region is liquid and what fraction is two-phase.

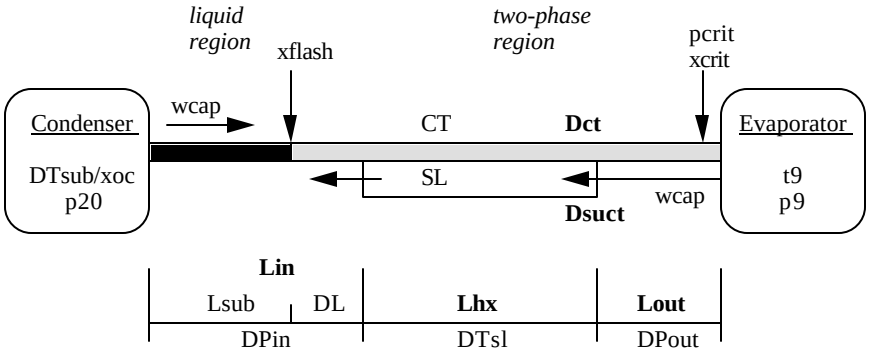

Figure C.2 Variables and parameters used in the ct-sl hx model

Where the parameters are defined as

Dct - Diameter of the capillary tube

Dsuct - Diameter of the suction line

Lin - Length of the adiabatic inlet region of capillary tube

Lhx - Length of the heat exchanger region of the ct-sl hx

Lout - Length of the adiabatic outlet region of the capillary tube

and the variables are defined as

DPin - Pressure steps in inlet region of capillary tube

DTsl - Temperature steps in suction line of heat exchanger region

DPout - Pressure steps in the outlet region of capillary tube

DTsub - Degrees of subcooling at exit of condenser

p20 - Condensing pressure

p9 - Pressure at inlet of suction line

pcrit - Pressure at exit of capillary tube (choked flow)

t9 - Temperature at inlet of suction line

wcap - Mass flow rate calculated by ct-sl hx subroutine

xcrit - Quality at exit of capillary tube (choked flow)

xflash - Quality of refrigerant at flash point

xoc - Quality of refrigerant at exit of condenser/inlet to capillary tube

C.3.3 Governing Equations

The equations which were used for this model are presented in this section. The governing equations for the adiabatic inlet and outlet regions of the capillary tube are identical. They consist of the mass, momentum and energy conservation equations, presented below:

$$\frac{\dot{m}_r}{A_{ct}} = G_{ct} = \text{const} \tag{C.1}$$

$$\frac{-dp}{dx} = \frac{f\upsilon G_{ct}^2}{2D_{ct}} + G_{ct}^2 \frac{d\upsilon}{dx} \tag{C.2}$$

$$\frac{dh}{dx} = \frac{-G_{ct}^2}{2} \frac{d\left(\upsilon^2\right)}{dx} \tag{C.3}$$

Next are the governing equations used in the heat exchanger region. Once again the mass, momentum, and energy conservation equations for the capillary tube are used. However there is the addition of the mass and energy conservation equation for the suction line, and an energy equation for the heat exchanger. These six governing equations are listed below:

$$\frac{\dot{m}_r}{A_{ct}} = G_{ct} = \text{const} \tag{C.4}$$

$$\frac{\dot{m}_r}{A_{sl}} = G_{sl} = \text{const} \tag{C.5}$$

$$\frac{-dp}{dx} = \frac{f\upsilon G_{ct}^2}{2D_{ct}} + G_{ct}^2 \frac{d\upsilon}{dx} \tag{C.6}$$

$$\frac{dh}{dx} + \frac{G_{ct}^2}{2} \frac{d\left(\upsilon^2\right)}{dx} = cp_{sl} \frac{dT_{sl}}{dx} \tag{C.7}$$

$$\dot{m}_r cp_{sl} \frac{dT_{sl}}{dx} = -h_{sl}\pi D_{sl}(T_w - T_{sl}) \tag{C.8}$$

$$h_{ct}\pi D_{ct}(T_{ct} - T_w) - h_{sl}\pi D_{sl}(T_w - T_{sl}) = 0 \tag{C.9}$$

The pressure drop at the entrance of the capillary tube due to the abrupt contraction in tube size from the larger diameter liquid line tube to the capillary tube is calculated with Eqn. C.10. The entrance loss factor, K, is equal to 0.5 (Melo, 1992).

$$Dp = (1+K)\frac{V_{in}^2}{2\upsilon_{in}} \tag{C.10}$$

The thermodynamic properties for the two-phase region, listed below, are calculated using the NIST REFPROP property routines for the liquid and vapor phases.

$$h = (1-x)h_f + xh_g \tag{C.11}$$

$$s = (1-x)s_f + xs_g \tag{C.12}$$

$$\upsilon = (1-x)\upsilon_f + x\upsilon_g \tag{C.13}$$

Liquid thermal conductivities and specific heats are used to calculate the heat transfer coefficients in the two-phase capillary tube since the perimeter of the tube is assumed to always be wetted. Therefore the heat transfer is dependent upon the thin liquid film. The suction line, on the other hand, is assumed to always be superheated, therefore vapor properties are used. The viscosities for both phases are used in the capillary tube to calculate the friction factor. These transport properties for the liquid and vapor phases are calculated using cubic curve fits developed from data in the 1993 ASHRAE Fundamentals handbook.

$$\begin{aligned} k_{ct} &= k_f \\ k_{sl} &= k_g \end{aligned} \tag{C.14}$$

$$\begin{aligned} c_{p_{ct}} &= c_{p_f} \\ c_{p_{sl}} &= c_{p_g} \end{aligned} \tag{C.15}$$

$$\begin{aligned} \mu_{sl} &= \mu_g \\ \mu_{ctf} &= \mu_f \\ \mu_{ctg} &= \mu_g \end{aligned} \tag{C.16}$$

The friction factor in the liquid regions is calculated using the correlation in Equation. C.17 for turbulent flow in smo oth tubes (ASHRAE, 1993).

$$f_{liq} = 0.3164\ Re^{-0.25} \tag{C.17}$$

The model developed by Piexoto uses a two-phase friction factor developed by Pate (1982). However, this correlation is only applicable for capillary tubes which are the same as Pate's, since it has no dependence on tube roughness. Piexoto also suggests that Pate's friction factor should probably not be used for refrigerants other than CFC-12. Therefore, a two-phase friction factor was developed which is a mass weighted average of the liquid and vapor friction factors that assumes that both the liquid and vapor phases are traveling at the bulk fluid velocity. This result is derived from a flow-regime assumption in which liquid and vapor slugs traveling at the bulk velocity exert friction forces independently. The pressure drops are therefore weighted by void fraction (similar to Dukler's (1964) weighting of viscosity in homogeneous two-phase flow which was used to calculate the Reynolds number in Pate's friction factor). The single-phase friction factors are calculated using Equation. C.18a (Swamee and Jain, 1976), which is a curve fit that approximates the transcendental Colebrook friction factor correlation for single-phase turbulent flow, with the appropriate single-phase Reynolds number.

$$f = 0.25\left[\log\left(\frac{e/D}{3.7} + \frac{5.74}{Re^{0.9}}\right)\right]^{-2} \tag{C.18a}$$

When the pressure drops due to the liquid and vapor slugs are added and terms rearranged, the void fraction disappears and the following "average friction factor" results.

$$\bar{f} = (1-x)f_f + x \cdot f_g \tag{C.18b}$$

A two-phase frictional pressure drop correlation developed by Souza, et. al. (1992), which uses the Lockhart-Martinelli parameter (X_{tt}) and the Froude number, was also used. It is based on a homogeneous flow model in which both phases are assumed in equilibrium and traveling at the same velocity. The pressure drop is computed as if the flow were a single-phase flow but modifiers are introduced to the properties inside the single-phase friction coefficient. This empirical correlation was chosen over the others for the model validation since it has been validated experimentally for internal tube diameters down to 0.118 in.

The single- and two-phase heat transfer coefficients were calculated using the Gnielinski equation (Incropera and DeWitt, 1990) in Equation. C.19. This correlation was chosen over the Dittus-Boelter equation (Incropera and DeWitt, 1990) and a heat transfer coefficient correlation by Sleicher and Rouse (1975). All three equations provided similar results, but the Gnielinski equation was chosen because it is more accurate in the ct-sl hx model's range of operating conditions and it provided slightly better results when compared to experimental data.

$$Nu_D = \frac{(f/8)(Re_D - 1000)Pr}{1 + 12.7(f/8)^{0.5}\left(Pr^{2/3} - 1\right)}$$
$$f = \left(0.79 \ln Re_D - 1.64\right)^{-2} \tag{C.19}$$

The mass flow rate and the critical mass flux are calculated by the relations:

$$\dot{m}_r = G_{crit} A_{ct} \tag{C.20}$$

$$G_{crit} = \left(\frac{x}{G_{cg}^2} + \frac{1-x}{G_{cl}^2} \right)^{-0.5}$$

$$G_{cg}^2 = \left| \frac{-1}{\left(\frac{\partial v}{\partial p}\right)_g - \left(\frac{v_g - v_f}{s_g - s_f}\right)\left(\frac{\partial s}{\partial p}\right)_g} \right|$$

$$G_{cl}^2 = \left| \frac{-1}{\left(\frac{\partial v}{\partial p}\right)_l - \left(\frac{v_g - v_f}{s_g - s_f}\right)\left(\frac{\partial s}{\partial p}\right)_l} \right| \tag{C.21}$$

C.4 Solution Strategy for CT-SL HX Model in System Model

There are two significant problems that are encountered when the governing equations for the ct-sl hx are placed in the system model along with the other component equations. First, unlike the other component submodels, the ct-sl hx model is very large, having 250^+ simultaneous equations. That would more than triple the number of equations which the equation solver must handle and significantly increase the execution time. Second, and more importantly, the solution is not very robust. Most of the thermodynamic and transport property variables associated with the ct-sl hx require very accurate initial guesses to converge on a solution. This makes the model equations

very sensitive to the initial guesses and will not allow the model to converge if the guesses aren't close to the solution.

Normally, the state of the refrigerant at the inlet to the capillary tube and suction line, as well as the dimensions of the component, are considered inputs to the model and the state of the refrigerant at the outlet of the capillary tube and suction line and mass flow rate are considered the outputs of the model (Figure C.3). However, if a specific combination of various variables and parameters is specified (shown by the characters in boldface in Figure C.3), then the equations may be rewritten such that the six remaining variables and parameters (not in boldface) may be determined sequentially.

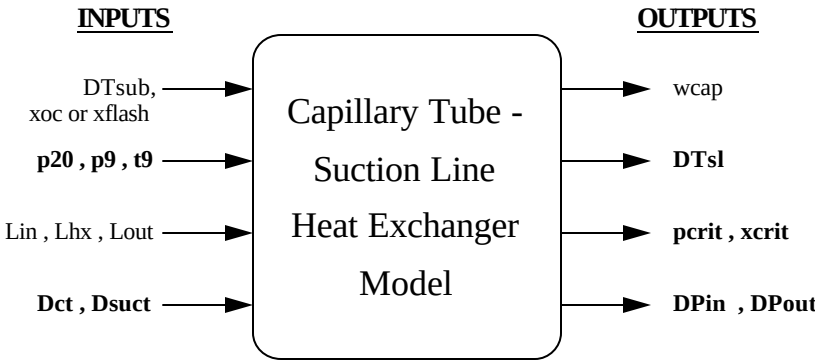

Figure C.3 Diagram of inputs and outputs to ct-sl hx model

Some of these "sequential" operations actually require the solution of one-variable implicit equations or sets of two equations and two unknowns, which can be solved by internal iteration. Once the equations are in a "sequential" format, the entire model could theoretically be reduced by back substitution from 250^{+} equations into six functions which are solved explicitly.

$wcap = f_W(p20,p9,t9,Dct,Dsuct,pcrit,xcrit,DPin,DTsl,DPout)$

$Lin = f_{L1}(p20,p9,t9,Dct,Dsuct,pcrit,xcrit,DPin,DTsl,DPout)$

$Lhx = f_{L2}(p20,p9,t9,Dct,Dsuct,pcrit,xcrit,DPin,DTsl,DPout)$

$Lout = f_{L3}(p20,p9,t9,Dct,Dsuct,pcrit,xcrit,DPin,DTsl,DPout)$

$xflash \text{ or } xoc = f_X(p20,p9,t9,Dct,Dsuct,pcrit,xcrit,DPin,DTsl,DPout)$

$DTsub = f_D(p20,p9,t9,Dct,Dsuct,pcrit,xcrit,DPin,DTsl,DPout)$

This makes all of the property variables explicit intermediate variables that do not require initial guesses. Because these six functions share many of the same intermediate calculations and variables, a subroutine was written that returns the values of all six functions. This subroutine is, in effect, six functions which are executed in parallel These function values can then be compared with either parameters or variables in the governing equations in the system model, which are described in the next section.

Therefore, the governing equations for the ct-sl hx are located in a subroutine rather than in the system model with the other governing equations. This helps to keep the number of equations in the system model to a manageable size and minimizes the number of initial guesses needed by the Newton-Raphson (NR) equation solver.

C.5 System Model Governing Equations

As was previously mentioned, the numerous equations in the ct-sl hx model have been reduced down to six governing equations which are present in the system model. Each governing equation is a comparison of the ct-sl hx subroutine outputs to either user-specified parameters or variables present in the system model. There are also now six new variables which are introduced into the system model since they previously were not present in the system equations. These six variables are: wcap, pcrit, xcrit, DPin, DTsl, and DPout. These variables all require initial guesses, just like the other NR system variables, and can be obtained from a previous solution of the system.

The first equation compares the refrigerant mass flow rate predicted by the capillary tube (wcap) to the system mass flow rate variable (w)

```
R(int+3) = wcap - w
```

This is a very crucial equation in the system model since the ct-sl hx model, along with the compressor model, determine the mass flow rate of the entire system. There is only a single value for mass flow rate where operation is steady-state because the mass flow rate through each component varies inversely to one another with pressure difference. The precise method in which mass flow rate is calculated is explained in section C.6.1.

The next equation is a comparison of the user-defined length of the inlet region (Lin) to the length which is calculated by the subroutine (Ling). The subscript g signifies that the variable is an ouput of the ct-sl hx subroutine and distinguishes it from the user-specified parameter.

```
R(int+4) = Lin - Ling
```

Depending on what the input values are, the ct-sl hx model calculates a length for this region, but it does not necessarily match the actual length. Therefore, the input variables are adjusted by the NR solver until the calculated length is equal to the actual length of the inlet region.

Similar to the last equation, the third and fourth equations are length comparisons, but this time they are for the heat exchanger and outlet regions, respectively

```
R(int+5) = Lhx - Lhxg
R(int+6) = Lout - Loutg
```

where Lhx and Lout are the user-defined lengths and Lhxg and Loutg are the calculated lengths.

The fifth and sixth equations are more easily explained together since they are both dependent upon the exit condition of the condenser. In both instances, if the refrigerant leaving the condenser is a two-phase mixture then Cond2phX is true and the first option is used, else the refrigerant is subcooled and the second option is used.

```
IF (Cond2phX) THEN
   R(int+7) = xoc - xocg
ELSE
   R(int+7) = 0.0 - Xflashg
END IF

IF (Cond2phX) THEN
```

```
   R(int+8) = 0 - dTsubg
ELSE
   R(int+8) = setsub - dTsubg
END IF
```

First examine the equations for a two-phase condition. The first equation compares the quality at the inlet of the capillary tube calculated by the ct-sl hx subroutine (xocg) to the outlet quality of the condenser (xoc), which is a variable in the system model. The second equation then compares the subcooling calculated by the ct-sl hx model (dTsubg) to the amount of subcooling in the model (setsub), which should be zero for a two-phase inlet. Conversely, if the subcooled condition exists, then the inlet quality to the capillary tube is obviously zero. Therefore, the first equation can no longer be used for comparison. Instead, the quality at the flash point calculated by the ct-sl hx model is compared to what the actual value should be, zero. The second equation then becomes a measure of how closely the calculated degrees of subcooling (dTsubg) matches the system variable for degrees subcooling at the condenser exit (setsub). Therefore, the equations check the inlet state by either comparing the temperature and the quality when the inlet is two-phase, or the degrees of subcooling and flash point quality when the inlet is subcooled.

C.6 Solution Algorithm for CT-SL HX Model

The manner in which the ct-sl hx model calculates the output variables for the six equations just described is explained in more detail below, for each of the three regions of the ct-sl hx. Since there are many possible modes of operation for the ct-sl hx, as mentioned in section C.2, this discussion will assume the most common mode of operation where there is no recondensation in the heat exchanger region and flashing is occurring in the adiabatic inlet region. Also, the number of segments in each region is fixed. The solution begins by starting at the outlet of the capillary tube and solving for the state of the refrigerant at the ends of each segment by taking pressure steps backwards towards the heat exchanger region. Once in the heat exchanger region, the states at each segment are found by taking temperature steps along the suction line. Finally, pressure steps are once again taken until the state of the refrigerant at the entrance of the capillary tube is calculated. Research done by Peixoto at the ACRC found that three segments (steps) in each region was sufficient for modeling accuracy. For reasons that will soon be clear, the outlet region of the capillary tube is examined first.

C.6.1 Adiabatic Outlet Region of the Capillary Tube

The first objective is to determine the mass flow rate of refrigerant, which will facilitate the solution of each segment. Referring back to the model description in section C.3, a choked flow condition is present at the exit of the capillary tube. The state of the refrigerant at this point is related to the state of the refrigerant at the entrance to the evaporator in the system model by the assumption that there is an isenthalpic expansion between the two states. Therefore, the pressure at the exit of the capillary tube (pcrit) will always be higher than the evaporating pressure, and the quality at the exit of the capillry tube (xcrit) will be lower than the quality at the entrance to the evaporator, since enthalpy remains constant. By using the initial guesses from the system model for the state of the refrigerant at this critical condition (pcrit and xcrit), Eqn. C.20 can be used to calculate the mass flow rate as a function of the critical mass flux (G_{crit}), calculated in Eqn C.21. Now that the mass flow rate has been determined, it is possible to begin marching backwards down the capillary tube to solve each individual segment.

Each region of the ct-sl hx is divided into segments, which are completely filled with refrigerant as either a subcooled liquid or two-phase mixture. In this case, where there is no recondenstion occurring, the refrigerant in the entire adiabatic outlet region is a two-phase mixture. A typical segment from this region of the capillary tube is shown in Figure C.4, where the refrigerant is two-phase, w is the mass flow rate, D_{ct} is the diameter, and L is the length of the segment. Since the refrigerant is two-phase, the pressure (P) and temperature (T) are not independent so the quality (x) is used to specify the thermodynamic state.

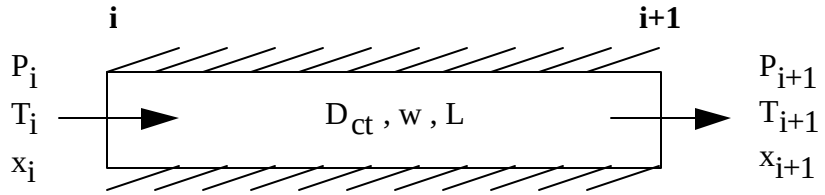

Figure C.4 Segment from adiabatic outlet region of capillary tube

This segment is described by the three governing equations listed in section C.3.3 (Eqns. C.1 - C.3). Now suppose that the state of the refrigerant at end (i+1) is known by specifying either the pressure, P, or temperature, T, and the quality, x. Then either P or T and x at (i) can be found by using the momentum and energy equations shown in forward finite difference form below (2 equations and 2 unknowns).

$$(P_i - P_{i+1}) = \frac{L f_{avg} \upsilon_{avg} G_{ct}^2}{2 D_{ct}} + G_{ct}^2 (\upsilon_{i+1} - \upsilon_i)$$
$$\text{where, } L = (x_{i+1} - x_i) \qquad \text{(C.22)}$$

$$(h_{i+1} - h_i) = \frac{-G_{ct}^2}{2} (\upsilon_{i+1}^2 - \upsilon_i^2) \qquad \text{(C.23)}$$

Obviously, if it were possible to specify an additional variable, such as T or P at (i), then only one equation would be needed to calculate the quality. That is precisely what is done to facilitate a sequential solution of the segments. One of the property variables (in this case the pressure steps in this region, DPout) is a variable in the system model and is determined by the NR solver, external to the subroutine, while the other variable (the quality) is found internal to the subroutine from the energy equation using a one-dimensional variable NR code.

Thus, the procedure goes as follows. The system model provides the subroutine with a guess for the pressure drop in the segment. This pressure drop is then put in the energy equation to solve for the quality. Once the quality is determined, there must be something to check the accuracy of the specified pressure drop. Even though the energy equation is satisfied, the pressure drop guess may not describe the actual physical segment. In this case the length, L, found from the momentum equation serves that function. Close examination of this equation will reveal that the length of each segment is still unknown at this point. However, although each individual segment length is unknown, the total length of a region is known. Therefore, all the segments in a region are solved, using the method just stated, and summed to give a total region length (Loutg). This length is then an output from the subroutine and compared to the user-specified actual length in the system equations (4th governing equation in section C.5). If they do not match, then the next iteration the NR solver will make a new guess and the process will repeat until no difference exists.

Now that the inlet state to the outlet region is calculated it is possible to continue to the next region. Unfortunately, the heat exchanger region is a somewhat more complicated matter.

C.6.2 Heat Exchanger Region

A segment from the heat exchanger region is shown in Figure C.5 where the refrigerant in both the capillary tube and suction line is two-phase. The capillary tube has the same thermodynamic property inputs and outputs as before, except this time it is exchanging heat with the suction line. This introduces several new variables into the system. As was previously stated in the model assumptions (section C.3.1), the refrigerant in the suction line is assumed to be always superheated vapor with negligible pressure drop, so that if the pressure (P_{sl}) is known, and only the temperature needs to be found to specify the state. The wall temperature between the two tubes (T_w) is also a variable at the inlet and outlet of the segment. And just like the adiabatic segment, the mass flow rate and diameter of both tubes are known. Now that the variables of the segment are set up, it is time to examine the governing equations.

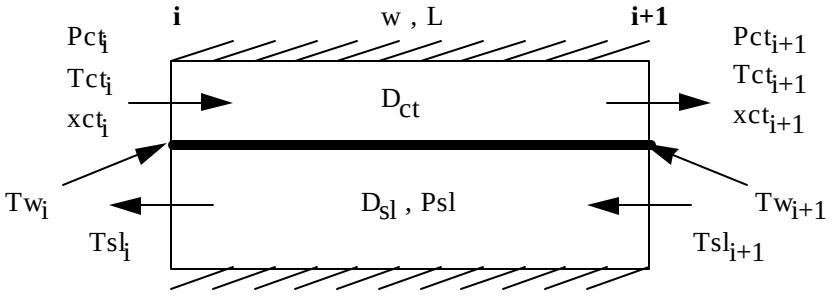

Figure C.5 Segment from heat exchanger region of ct-sl hx

The governing equations shown in section C.3.3 for this heat exchanger region are also somewhat different and more numerous than those for the adiabatic segment. First look at the capillary tube equations. The momentum equation remains the same, but now the energy equation has an additional term which accounts for the energy exchange with the suction line, expressed as the change in energy of the refrigerant in the suction line. The forward finite difference forms of these two equations are shown in equations C.24 and C.25. There is also now an energy equation for the suction line, shown in Equation C.26. It states that the energy change of the refrigerant is due to the convective heat exchange with the connecting wall. Finally, equations C.27 and C.28 maintain that at a point, the convective heat transfer from the refrigerant in the capillary tube to the connecting wall is equal to the convective heat transfer from the wall to the refrigerant in the suction line.

$$(P_i - P_{i+1}) = \frac{Lf_{avg}\upsilon_{avg}G_{ct}^2}{2D_{ct}} + G_{ct}^2(\upsilon_{i+1} - \upsilon_i)$$
$$\text{where, } L = (x_{i+1} - x_i) \qquad \text{(C.24)}$$

$$(h_{i+1} - h_i) + \frac{G_{ct}^2}{2}(\upsilon_{i+1}^2 - \upsilon_i^2) = C_{p_{sl}}(T_{sl_{i+1}} - T_{sl_i}) \qquad \text{(C.25)}$$

$$\dot{m}_r C_{p_{sl}}(T_{sl_{i+1}} - T_{sl_i}) = -h_{sl_{avg}}\pi D_{sl} L(T_{w_{avg}} - T_{sl_{avg}}) \qquad \text{(C.26)}$$

$$h_{ct_i}\pi D_{ct}(T_{ct_i} - T_{w_i}) = h_{sl_i}\pi D_{sl}(T_{w_i} - T_{sl_i}) \quad \text{(C.27)}$$

$$h_{ct_{i+1}}\pi D_{ct}(T_{ct_{i+1}} - T_{w_{i+1}}) = h_{sl_{i+1}}\pi D_{sl}(T_{w_{i+1}} - T_{sl_{i+1}}) \quad \text{(C.28)}$$

The strategy used for this heat exchanger region is the same as that which was used in the adiabatic region: to reduce the number of variables that need to be determined. Just as before, assume that all the variables are known at end (i+1) of the segment in Figure C.5. That leaves five variables unknown at end (i) (T_{ct} or $P_{ct,}$ x_{ct}, Tw, and $T_{sl,}$), and the first four equations shown above.

Now observe what happens when one of the properties at end (i) is specified as was done in the previous section, only this time make it the temperature of the suction line. The momentum equation is solved explicitly for the length, and Equation C.27 is explicitly solved for the wall temperature at (i). Using backsubstitution, the governing equations can be reduced from four to two by substituting the expressions for L and Tw into Equation C.26. Now the only unknowns that remain in the two equations are the temperature or pressure and quality of the capillary tube. This two-equation, two-variable system is solved using a NR solution method which exists in another subroutine call. The temperature and quality at end (i) of the capillary tube thus determined are returned to the ct-sl hx subroutine. And once again, the momentum equation is used to determine the length of the segment.

This procedure continues until all of the segments in the heat exchanger region are solved and then the individual lengths are added up to get a total heat exchanger length (Lhxg). This length is then used in 3rd governing equation in section C.5 and compared to the actual user-specified length. If they are not equal, the NR solver updates the old guess with a new one, and starts the procedure over again until the lengths match. Hence, the procedure is very similar to that used for the adiabatic segments, except that the NR system variable is now the temperature gain in the suction line (DTsl) rather than the pressure drop in the capillary tube.

C.6.3 Adiabatic Inlet Region of the Capillary Tube

This region of the ct-sl hx is identical in form to the outlet region which was already described in section C.6.1. Thus, Figure C.4 should be referred to in all discussion about the individual two-phase segments of this region, since there are the same property variables present. Following from the calculations in the heat exchanger region, the state of the refrigerant is known at the outlet of the adiabatic inlet region of capillary tube. Therefore, the two-phase segments are solved backwards in succession just as was done before in the outlet region, but this time using the pressrue step, DPin, instead. The only difference between the solution methods of the two regions is caused by the subcooled liquid refrigerant segment at the entrance of the capillary tube.

The three segments in the inlet region are divided such that the first segment from the inlet is entirely filled with liquid refrigerant, while the remaining two segments are entirely filled with a two-phase mixture. In the liquid segment, the temperature of the refrigerant remains constant and the pressure drop is caused by friction losses in the tube, which is shown in the forward finite difference form of the momentum equation below.

$$(P_i - P_{i+1}) = \frac{L_{sub} f_{i+1} \upsilon_{i+1} G_{ct}^2}{2D_{ct}} \quad \text{(C.29)}$$

First, the two two-phase sections are solved backwards sequentially, just as before, until the quality at the entrance to the first section is found. The pressure steps in this region, DPin, only apply to the two-phase segments,

not the liquid segment. This point, which is the boundary between the liquid and two-phase segments, is the flash point and the quality is, by definition, supposed to be zero. Therefore, the value for quality which is calculated (xflash) is sent to the system equations to compare with the desired zero value (5th governing equation in section C.5). Second, the degrees of subcooling (DTsub) are calculated by using the saturation temperature at the condensing pressure of the system model (p20) and the temperature calculated at the flash point. Then this information is used in the system model and compared with the system variable for degrees of subcooling at the exit of the condenser (setsub) in the sixth governing equation. The combination of these two equations is what determines the state of the refrigerant at the inlet to the capillary tube.

Now all that remains is to solve the momentum equation in the remaining liquid segment to determine the total inlet length. Both the lengths in the two-phase region were calculated as before and summed to give a value for DL. Once, the subcooled length is found, it is added to DL and returned to the system model for comparison with the user-specified inlet region length (4th governing equation), thus concluding the ct-sl hx model calculations.

C.7 Conclusion

The capillary tube-suction line heat exchanger appears to be a very simple device, but in actuality, it is possibly the most complex component in the refrigeration system to model. The multiple combinations of the two-phase processes which may occur require a robust model which can operate in several modes. The approach taken here places the governing equations of the model in a subroutine and specifies certain inputs such that the solution of the outputs is seemingly sequential. Further development of the model should include more possible modes of operation, such as flashing in the heat exchanger region and a two-phase inlet to the suction line.

References

ASHRAE, ASHRAE Handbook of Fundamentals, Atlanta GA, 1993.

Dukler, A.E., et al., "Pressure Drop and Hold Up in Two-Phase Flow," A. I. Ch. Journal, Vol. 10, pp. 38-51, 1964.

Incropera, F.P. and D.P. DeWitt, Fundamentals of Heat and Mass Transfer, 3rd ed., John Wiley & Sons, Inc., New York, 1990.

Melo, C., R.T.S. Ferreira and R. H. Pereira, "Modeling Adiabatic Capillary Tubes: A Critical Analysis," Proceedings of the International Refrigeration Conference, Purdue University, p. 118, 1992.

Pate, M.B., "A Theoretical and Experimental Analysis of Capillary Tube-Suction Line Heat Exchangers," Ph.D., Thesis, Purdue University, 1982.

Piexoto, R.A. and C.W. Bullard, "A Simulation and Design Model for Capillary Tube-Suction Line Heat Exchangers," Proceedings of the International Refrigeration Conference, Purdue University, p.335-340, 1994.

Sleicher, C.A. and M.W. Rouse, "A Convenient Correlation for Heat Transfer to Constant and Variable Property Fluids in Turbulent Pipe Flow," International Journal of Heat and Mass Transfer, Vol. 18, p.677-683, 1975.

Souza, A.L., J.C. Chato, J.M.S. Jabardo, J.P. Wattelet, J. Panek, B. Christofferson, and N. Rhines, "Pressure Drop During Two-Phase Flow of Refrigerants in Horizontal Smooth Tubes," University of Illinois at Urbana-Champaign, ACRC TR-25, 1992.

Stoecker, W.F., Refrigeration and Air Conditioning, Second Edition, McGraw-Hill, New York, 1986.

Swamee, P.K., and Jain, A.K., "Explicit Equations for Pipe-Flow Problems," Proceedings of the ASCE, Journal of the Hydraulics Division, 102, HY5, p.657-664, May 1976.

Appendix D: ACRC Refrigerator/Freezer Model User's Reference

D.1 Reading the Equations

D.1.1 Form of Equations

The system governing equations are located in the EQNS.f file. However, they appear in a slightly different form so that they may be used by the ACRC Equation Solver. Thus, the equations are converted into residual formats, which moves both sides of the equation over to the same side and sets that sum to zero. Here is an example of a governing equation written in standard form

Eqn #1 : LHS = RHS

where LHS and RHS are the left- and right-hand sides of the equation, respectively. This equation can then be changed into the residual form

R(1) = RHS - LHS

The equation solver then considers this equation solved once the residual value is less than a specified tolerance (near zero).

D.1.2 Computed GOTO Structure

The EQNS.f file uses a computed GOTO structure to evaluate individual equations. This feature enables the program to save time by calculating only the non-zero partial derivatives in the Jacobian matrix; most of the other NxN partial derivatives are always zero. That is why each residual equation is preceded by a line number. When the equation solver wants to evaluate a particular residual equation, the corresponding residual number of that equation is assigned to the variable EQNUM. This value for EQNUM is then used in the computed GOTO to determine which line number corresponds to that residual number. Therefore it is very important to make sure that all the residual equations has a line number in the computed GOTO statement. For example, examine the three equation model below.

```
1     EQNUM = NonZeroList(ELEMENT,VariableNum)
      GOTO(10, 30, 20),EQNUM
10    R(1) = x + y - 7
         Goto 1
30    R(2) = x^2 - 16
         Goto 1
20    R(3) = y^2 - 9
         Goto 1
```

First the array NonZeroList is used to select an equation to evaluate (for either partial derivative calculations or for an iteration). If, for instance, the equation solver wished to evaluate the second residual R(2), then EQNUM would be set to the number 2 and would be used in the computed GOTO statement shown above. The computed GOTO would then direct the program to go to line 30 (which not coincidentally is the second line number listed in the GOTO argument list) and the correct line number would be chosen (The line numbers in the GOTO statement are purposely out of numerical order to show that there is no dependence on the order of the line numbers). The residual is then evaluated and the program is directed to return to line 1 where instructions for the next residual equation to evaluate can be obtained. For a more detailed discussion see Mullen (1994).

D.1.3 Equation Switching

The form of the evaporator and condenser models requires that the modeling equations be able to switch during a solution. Since the heat exchangers are modeled in zones (subcooled, two-phase, etc.), there are instances where a zone in a heat exchanger will diminish until it completely disappears. This is the case when the initial guesses assume that the solution will include, for instance, a subcooled zone of the condenser. If, in fact, the solution does not have a subcooled zone, then the equations must be able to switch to exclude that zone. Otherwise, the solution will be forced to contain a subcooled zone, which it should not have.

Therefore, logical equation flags, which specify which equation to use, are used with the residuals that are dependent upon the state of the refrigerant at the exit of a heat exchanger. The only two equation flags which used are for the evaporator (Evap2phX) and condenser (Cond2phX). For example, if the exit of the evaporator is two-phase, then Evap2phX will be true. Conversely, if the exit of the evaporator is superheated, Evap2phX will be false. Here is an example taken directly from the condenser equations.

```
IF (Cond2phX) THEN
   R(cond+2) = 0 - qsub
ELSE
   R(cond+2) = w*(h20 - h3) - qsub
END IF
```

The manner in which the equations are switched and how it is determined to switch the equations, is discussed in section D.4.2 on boundary checking.

D.1.4 NonZeroFlag

The NonZeroFlag is used to indicate when the NonZeroList is being calculated. It is necessary because of the equation switching capabilities which were just explained in section D.1.3. Let's take the example just used in the previous section on equation switching.

```
2040   IF (.not.NonZeroFlag) THEN
          IF (Cond2phX) THEN
             R(cond+2) = 0 - qsub
          ELSE
             R(cond+2) = w*(h20 - h3) - qsub
          END IF
       ELSE
          R(cond+2) = qsub + w + h20 + h3
       END IF
        GOTO 1
```

The equation flags tell us that when the condenser is subcooled the second equation is used. Otherwise, for a two-phase exit, the first one is used. But, this poses a problem for the Jacobian matrix. Since the nonzerolist is only calculated once, at the beginning of a solution, the zones which are present in the heat exchangers at that time are used to determine which elements in the partial derivative matrix are zero and do not need to be calculated during the solution. Thus, if the nonzerolist thinks that the only variable in this residual equation is qsub, the variables w, h20, and h3 will not ever be considered in the partial derivative calculations.

Therefore the NonZeroFlag indicates when the nonzerolist is being calculated. In that case, all of the variables which appear in the two equations combined, are listed in a dummy residual equation. The form of this equation is irrelevant since the nonzerolist only checks to see if the residual changes as a result of a change in the variable. All other times, the NonZeroFlag will be false and the actual residual equations will be used.

D.1.5 Equation Counters

One of the advantages of using a Newton-Raphson solver is that the equations do not have to be in any particular order. However, the ACRC Refrigerator/Freezer model (RFSIM) places the residual equations into groups by component or sub-model. If it is necessary to insert an equation into the middle of the residual equations, then all of the equations following that one will need to be renumbered by adding one to their current number. Therefore, counter variables are used to indicate the residual number of the first equation in each group. If, for example, an equation is added to the end of the condenser equations, then only the counter variables for all the groups following that component will increase by one. For instance, cond = 54, indicates that the first condenser residual equation, R(cond+0), is R(54). Then R(55) will be denoted, R(cond+1), and so on.

D.2 Component Models

There are four components present in RFSIM: a compressor, a condenser, a capillary tube - suction line heat exchanger, and an evaporator. Each one of these components will be described in great detail in the sections which follow. First, a complete description is given that explains the manner in which the component is being modeled. Then, when appropriate, a diagram shows the configuration of the component and the variables which are being used. Finally, the governing equations are shown exactly as they appear in the EQNS.f file, along with a brief description of each.

D.2.1 Compressor

The compressor model is based on data which was supplied by the compressor manufacturer. Biquadratic curve fits were made for the power consumption and the mass flow rate through the component. These equations are functions of saturation temperatures corresponding to the pressure at the inlet and outlet of the compressor. They appear only as function calls in the system model but they can be found as functions wf and Pcompf in the EQNSUBS.f file. Since the original data was for a compressor operating with CFC-12, the curve fits had to be adjusted for different refrigerants. This was accomplished by assuming constant isentropic and volumetric efficiencies for different refrigerants at the same pressure ratios. The definition of isentropic efficiency, η_s, is shown in Equation D.1

$$\eta_s = \frac{P_s}{P} \tag{D.1}$$

where Ps is the isentropic power and P is the actual compressor power. With the compressor maps of CFC-12, it was possible to use this relation to calculate the power that compressor would consume with a new refrigerant. Similarly, the definition for volumetric efficiency, η_v, in Equation D.2 was used to calculate the mass flow rate for different refrigerants through the compressor.

$$\eta_v = \frac{w \cdot \upsilon_{suc}}{\dot{V}_{disp}} \tag{D.2}$$

The heat loss from the compressor shell is assumed to be proportional to the temperature difference between the discharge temperature and the temperature of the air flowing over the compressor shell. In turn, this constant of proportionality is a function of the velocity of the air flowing over the compressor shell (Cavallaro, 1994). The equations for the heat loss appear in the condenser model rather than the compressor model, since they play an important role in the energy exchange in the air flow through the condenser.

The governing equations for this component are marked with the counter variable `comp`.

```
  R(comp+0) = MDisLine - Mass(1,Acond,asubcond,a2ph1,a2ph2,
&  asupcond,Aevap,a2phevap,asupevap,Dcond,Devap,dpsuction,w,xoc,
&  xi,xoe,t20,t21,t3,p3,t7,t71,t9,p9,t11,rho1,rho20,rho21,rho70,
&  rho71,rho11,voldisline,Volcond,volbcap,volliqline,volfltr,
&  volcap,Volevap,volaccum,volsuctline,volcomp)

  R(comp+1) = MComp - Mass(8,Acond,asubcond,a2ph1,a2ph2,
&  asupcond,Aevap,a2phevap,asupevap,Dcond,Devap,dpsuction,w,xoc,
&  xi,xoe,t20,t21,t3,p3,t7,t71,t9,p9,t11,rho1,rho20,rho21,rho70,
&  rho71,rho11,voldisline,Volcond,volbcap,volliqline,volfltr,
&  volcap,Volevap,volaccum,volsuctline,volcomp)
```

These two equations calculate the mass of refrigerant that is present in the discharge line and compressor, respectively, by using the function Mass. The equation

```
  R(comp+2) = wf(tsat1,tsat11) - w
```

calculates the compressor refrigerant mass flow rate that is predicted by the compressor map function, wf. The equation

```
  R(comp+3) = Pcompf(tsat1,tsat11) - pcomp
```

calculates the compressor power consumption that is predicted by the compressor map funciton, Pcompf. The equation

```
  R(comp+4) = h11 + (BTU(pcomp) - qcomp)/w - h1
```

calculates the enthalpy difference across the compressor, which is equal to the power minus the heat loss from the compressor shell.

D.2.2 Condenser

The condenser model is divided into three zones: a subcooled, a two-phase, and a desuperheating zone. Each of these zones is governed by three energy equations: a refrigerant-side energy balance, an air-side energy balance, and an effectiveness rate equation. The value for the overall heat transfer coefficient used to calculate the effectiveness is calculated in the subroutine UsCond in the EQNSUBS.f file. This subroutine calculates a refrigerant-side heat transfer correlation using the Gnielinski correlation. Likewise, the air-side heat transfer coefficient is

calculated using an empirical correlation developed by Cavallaro (1994). The area of each zone is calculated by the model, and used in the UA expression. The total area is constrained by the user-defined parameter acond, which is the total external surface area of the condenser.

The configuration of the compressor and condenser, as well as the air flow patterns through the compartment, are shown in Figure D.1. The condenser spans the entire width of the compartment and is split by a dividing wall. The region which is located at the air inlet of the condenser is referred to as the inlet section, while the other region is aptly named the outlet section. Starting in the outlet section, the refrigerant travels first through the desuperheating zone and then into the second two-phase zone before crossing over into the inlet section. Once in this section, the refrigerant travels through tubes that are vertically stacked into three banks, which orients the subcooled zone above the first two-phase zone.

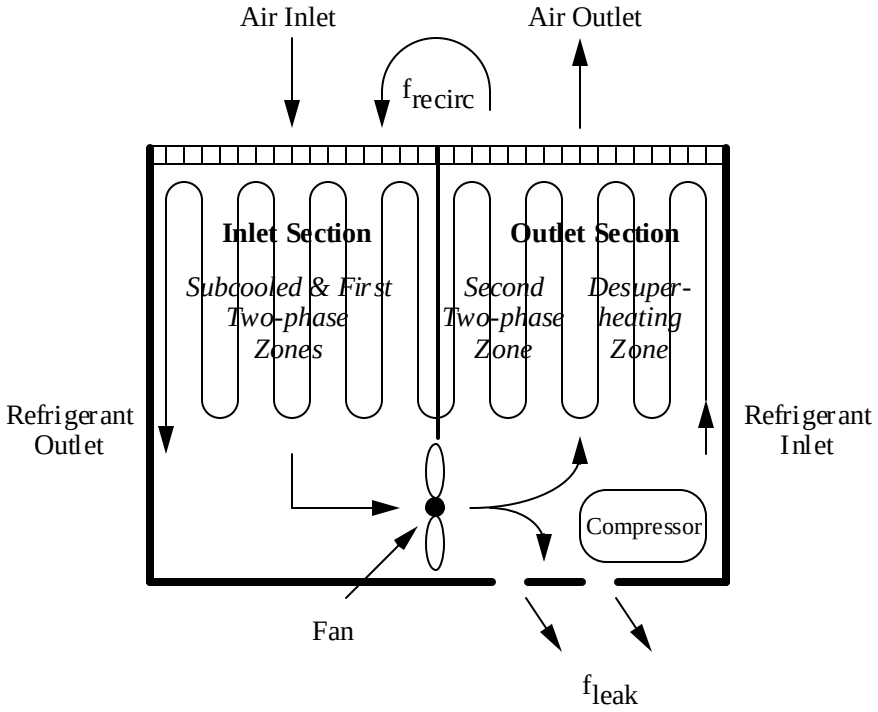

Figure D.1 Condenser/compressor configuration and air flow patterns

The air entering the condenser consists of air from the room at ambient temperature and air which recalculates from the outlet back into the inlet. After it flows over the inlet section and through the fan, the air stream splits and a fraction of it exits out the back of the compartment while the other part flows over the compressor towards the outlet section. The single-phase zones are modeled as parallel counterflow heat exchangers. Figure D.2 shows a schematic of the condenser with the air temperature variable names.

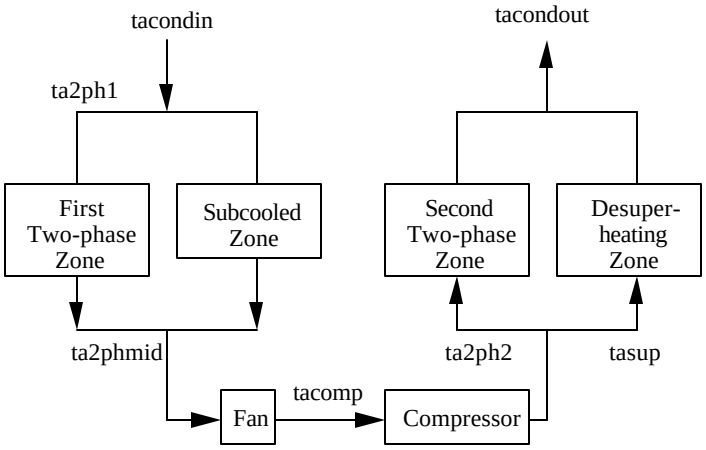

Figure D.2 Schematic of condenser with air temperatures

The governing equations for this component are marked with the counter variable `cond`.

D.2.2.1 Conservation Equations

```
R(cond+0) = qsub + q2ph1 + q2ph2 + qsupcond - qcond
```

This equation calculates the overall heat transfer rate for the condenser by summing the heat transfer rates in each zone.

```
  R(cond+1) = MCond - Mass(2,Acond,asubcond,a2ph1,a2ph2,
&  asupcond,Aevap,a2phevap,asupevap,Dcond,Devap,dpsuction,w,xoc,
&  xi,xoe,t20,t21,t3,p3,t7,t71,t9,p9,t11,rho1,rho20,rho21,rho70,
&  rho71,rho11,voldisline,Volcond,volbcap,volliqline,volfltr,
&  volcap,Volevap,volaccum,volsuctline,volcomp)
```

This equation calculates the total refrigerant mass in the condenser by using the function Mass. This total consists of the mass in the superheated, two-phase, and when applicable, the subcooled zones.

D.2.2.2 Subcooled Zone

```
IF (Cond2phX) THEN
   R(cond+2) = 0 - qsub
ELSE
   R(cond+2) = w*(h20 - h3) - qsub
END IF
```

These equations calculate the heat transfer rate in the subcooled zone by using a refrigerant-side energy balance.

```
R(cond+3) = tacondin - ta2ph1
```

This equation states that the air temperature at the entrance to the first two-phase zone is the same as the air entering the subcooled zone. Therefore the air-side energy balance for this zone is included in the first two-phase zone's equations.

```
R(cond+4) = esubcond*cminsub*(t20 - tacondin) - qsub
```

```
  R(cond+5) = epc(usubcond*asubcond,cminsub,cmaxsub) - esubcond

  Call UsCond(1,w,(t1+t21)/2.,(t20+t21)/2.,(t20+t3)/2.,Dcond,
&   crtmult,NSECTC,w*4/(pi()*Dcond**2),vdotcond,AAF1C,alphacond,
&   Usubcondc,U2phcondc,Usupcondc)
  R(cond+6) = usubcondc - usubcond

  IF (Cond2phX) THEN
     R(cond+7) = 0.9 - cminsub
  ELSE
     R(cond+7) = min((qsub/(t20 - t3)),(cacondin*fsubcond))
&              - cminsub
  END IF

  IF (Cond2phX) THEN
     R(cond+8) = 1 - cmaxsub
  ELSE
     R(cond+8) = max((qsub/(t20 - t3)),(cacondin*fsubcond))
&              - cmaxsub
  END IF

  mdotacond = vdotcond*60/va(patm,tacondin)
  R(cond+9) = mdotacond*cpa(tacondin) - cacondin

  R(cond+10) = asubcond/(asubcond + a2ph1) - fsubcond
```

This group of equations calculates the heat transfer rate in the subcooled zone by using an effectiveness rate equation. First, the effectiveness of the heat exchanger in this zone is calculated using the parallel counterflow equation. Then the overall heat transfer coefficient is obtained by calling the subroutine UsCond. The output of this subroutine, usubcondc, is then set equal to the system variable, usubcond. Next, the minimum and maximum heat capacity values between the refrigerant and air flow streams are determined. If the exit of the condenser is two-phase, dummy values are assigned to assure that the variables are stored as non-zero values. If these variables were set to zero, the effectiveness in the rate equation (R(cond+4)), would not be zero. As a result, that would prevent the area of the subcooled zone, asubcond, from becoming zero, and the solution would not converge. The last two equations calculate the heat capacity of the condenser inlet air and the fraction of the inlet section of the condenser occupied by the subcooled zone.

D.2.2.3 Two-Phase Zone

```
  IF (Cond2phX) THEN
     R(cond+11) = w*(h21 - h3) - q2ph1 - q2ph2
  ELSE
     R(cond+11) = w*(h21 - h20) - q2ph1 - q2ph2
  END IF
```

These equations calculate the heat transfer rates of both the first and second sections of the two-phase zone using a refrigerant-side energy balance.

```
  R(cond+12) = e2ph1*cacond2ph1*(t21 - ta2ph1) - q2ph1
```

```
      R(cond+13) = cacondin*(1 - fsubcond) - cacond2ph1

      R(cond+14) = e2p(u2ph1cond*a2ph1,cacond2ph1) - e2ph1

      Call UsCond(2,w,(t1+t21)/2.,(t20+t21)/2.,(t20+t3)/2.,Dcond,
     &   crtmult,NSECTC,w*4/(pi()*Dcond**2),vdotcond,AAF1C,alphacond,
     &   Usubcondc,U2phcondc,Usupcondc)
      R(cond+15) = u2phcondc - u2ph1cond

      R(cond+16) = fupstream*acond - asubcond - a2ph1
```

This group of equations calculates the heat transfer rate in the first section of the two-phase zone using an effectiveness rate equation. The heat capacity of the air at the inlet of the first two-phase section is calculated along with the effectiveness of the heat exchanger, using the two-phase heat exchanger effectiveness function, e2p. The overall heat transfer coefficient for this section of the two-phase zone is once again found by calling the subroutine UsCond. The final equation specifies that the sum of the subcooled area and first section of the two-phase area are equal to the fraction of the total condenser area which is in the inlet section of the condenser.

```
      R(cond+17) = cacondin*(ta2phmid-tacondin) - qsub - q2ph1
```

This equation calculates the heat transfer in the combined subcooled and first two-phase zones using an air-side energy balance.

```
      R(cond+18) = cacondin*(1 - fleak)*(ta2ph2 - tacomp) - qcomp
```

This equation calculates the heat transfer from the compressor shell to the air stream in the condenser using an air-side energy balance, where fleak is the fraction of the inlet air flow that leaks out of the back of the compartment prior to reaching the compressor.

```
      Vaircomp = vdotcond*4/(pi()*DfanC**2*60)
      ts = 0.855*t1 - 24.7
      R(cond+19) = 2.121*Vaircomp**0.5*(1.21)*(ts - tacomp) - qcomp
C
```

This equation also calculates the heat transfer from the compressor shell to the air stream in the condenser. Except, this time it is proportional to the temperature difference between the compressor shell temperature and the temperature of the air flowing over the shell by an empirical correlation developed by Cavallaro (1994). First the velocity of the air is calculated from the volumetric flow rate and the cross-sectional area of the condenser fan. Then, the temperature of the compressor shell is calculated as a function of the discharge temperature, since the manufacturer's compressor data provides no information on this value.

```
      R(cond+20) = cacondin*(tacomp - ta2phmid) - BTU(pcond)
```

This equation calculates the amount of energy transferred to the air stream from the condenser fan.

```
      R(cond+21) = e2ph2*cacond2ph2*(t21 - ta2ph2) - q2ph2
```

```
      R(cond+22) = cacondin*(1 - fleak)*(1 - fsupcond) - cacond2ph2

      R(cond+23) = e2p(u2ph2cond*a2ph2,cacond2ph2) - e2ph2

      Call UsCond(2,w,(t1+t21)/2.,(t20+t21)/2.,(t20+t3)/2.,Dcond,
     &   crtmult,NSECTC,w*4/(pi()*Dcond**2),vdotcond*(1-fleak),AAF2C,
     &   alphacond,Usubcondc,U2phcondc,Usupcondc)
      R(cond+24) = u2phcondc - u2ph2cond

      R(cond+25) = (1 - fupstream)*acond  - asupcond - a2ph2
```

This equation calculates the heat transfer rate in the second section of the two-phase zone using an effectiveness rate equation. The heat capacity of the inlet air, the effectiveness of the heat exchanger, and the overall heat transfer coefficient are calculated as they were in the inlet section. The final equation specifies that the sum of the superheated area and second section of the two-phase area are equal to the fraction of the total condenser area which is in the outlet section of the condenser.

D.2.2.4 Superheated Zone

```
      R(cond+26)= w*(h1 - h21) - qsupcond
```

This equation calculates the heat transfer rate in the superheated zone by using a refrigerant-side energy balance.

```
      R(cond+27) = esupcond*cminsupcond*(t1 - tasup)  - qsupcond

      R(cond+28) = ta2ph2 - tasup

      R(cond+29) = epc(usupcond*asupcond,cminsupcond,cmaxsupcond)
     &           - esupcond

      Call UsCond(3,w,(t1+t21)/2.,(t20+t21)/2.,(t20+t3)/2.,Dcond,
     &   crtmult,NSECTC,w*4/(pi()*Dcond**2),vdotcond*(1-fleak),AAF2C,
     &   alphacond,Usubcondc,U2phcondc,Usupcondc)
      R(cond+30) = usupcondc - usupcond

      R(cond+31) = min(qsupcond/(t1 - t21),cacondin*(1 - fleak)*
     &            fsupcond) - cminsupcond

      R(cond+32) = max(qsupcond/(t1 - t21),cacondin*(1 - fleak)*
     &           fsupcond) - cmaxsupcond

      R(cond+33) = asupcond/(asupcond + a2ph2) - fsupcond
```

This group of equations calculates the heat transfer rate in the superheated zone by using an effectiveness rate equation. First, the air temperatures at the entrance to the superheated and second two-phase zones are set equal. The air-side energy balance for this zone is included with the second section of the two-phase zone later in the equations. Then the effectiveness, the overall heat transfer coefficient, and the minimum and maximum heat capacities are calculated. The final equation calculates the fraction of the outlet section of the condenser that is occupied by the superheated zone.

```
      R(cond+34)= cacondin*(1 - fleak)*(tacondout - ta2ph2) - q2ph2 -
     &            qsupcond
```

This equation calculates the heat transfer in the combined superheated and second two-phase zones using an air-side energy balance.

```
      R(cond+35)= frecirc*tacondout + (1 - frecirc)*tamb - tacondin
```

The final condenser equation calculates the temperature of the inlet air to the condenser using the fraction of air which recalculates back into the condenser, frecirc.

D.2.3 Capillary Tube - Suction Line Heat Exchanger

The capillary tube-suction line heat exchanger is a counterflow heat exchanger that consists of the capillary tube soldered to the outside of the larger diameter suction line leading to the compressor. A diagram of this component along with the parameters and variables which are associated with it, are shown in Figure C.2 in Appendix C. A complete description of this component model and the simulation theory can be found in Appendix C.

The form of the governing equations for the ct-sl hx are implemented somewhat differently than the other component models. The 250^{+} equations in this model have been back substituted into six functions that are included in the ctslhx subroutine. The outputs of these functions are used in the system goveming equations below. The governing equations for this component are marked with the counter variable `int`, denoting "interchanger".

D.2.3.1 System Governing Equations

```
      R(int+0) = MLiqLine - Mass(3,Acond,asubcond,a2ph1,a2ph2,
     &  asupcond,Aevap,a2phevap,asupevap,Dcond,Devap,dpsuction,w,xoc,
     &  xi,xoe,t20,t21,t3,p3,t7,t71,t9,p9,t11,rho1,rho20,rho21,rho70,
     &  rho71,rho11,voldisline,Volcond,volbcap,volliqline,volfltr,
     &  volcap,Volevap,volaccum,volsuctline,volcomp)

      R(int+1) = MCapTube - Mass(4,Acond,asubcond,a2ph1,a2ph2,
     &  asupcond,Aevap,a2phevap,asupevap,Dcond,Devap,dpsuction,w,xoc,
     &  xi,xoe,t20,t21,t3,p3,t7,t71,t9,p9,t11,rho1,rho20,rho21,rho70,
     &  rho71,rho11,voldisline,Volcond,volbcap,volliqline,volfltr,
     &  volcap,Volevap,volaccum,volsuctline,volcomp)

      R(int+2) = MSuctLine - Mass(7,Acond,asubcond,a2ph1,a2ph2,
     &  asupcond,Aevap,a2phevap,asupevap,Dcond,Devap,dpsuction,w,xoc,
     &  xi,xoe,t20,t21,t3,p3,t7,t71,t9,p9,t11,rho1,rho20,rho21,rho70,
     &  rho71,rho11,voldisline,Volcond,volbcap,volliqline,volfltr,
     &  volcap,Volevap,volaccum,volsuctline,volcomp)
```

This group of equations calculates the total refrigerant mass in the liquid line, capillary tube, and suction line by using the function Mass.

```
      IF (design.ne.1.0) THEN
         IF (.not.ctsldone)
     &    Call ctslhx(ectslhx,pcrit,xcrit,DPout,DTsl,DPin,Dct,Dsuct,t9,
     &      p9,p20,Ling,Lhxg,Loutg,xocg,xflashg,dTsubg,wcap,Lsub,DL)
         ctsldone = .true.
```

```
      R(int+3) = wcap - w
   ELSE
      IF (.not.Evap2phX) THEN
         R(int+3) = t9 - t71 - setsup
      ELSE
         R(int+3) = xoe - setsup
      END IF
   END IF
```

This equation calculates the mass flow rate when the model is in simulation mode and compares it to the system mass flow rate, w. If the model is in design mode, the exit of the evaporator is specified by either degrees of superheat (if Evap2phX is false) or quality (if Evap2phX is true). Thus, the equation that is used depends upon which mode of operation the model is in (see section D.8 on Operation Modes).

```
   IF (design.ne.1.0) THEN
      IF (.not.ctsldone)
&     Call ctslhx(ectslhx,pcrit,xcrit,DPout,DTsl,DPin,Dct,Dsuct,t9,
&       p9,p20,Ling,Lhxg,Loutg,xocg,xflashg,dTsubg,wcap,Lsub,DL)
      ctsldone = .true.
      R(int+4) = Lin - Ling
   ELSE
      R(int+4) = pcrit - 27.0
   END IF

   IF (design.ne.1.0) THEN
      IF (.not.ctsldone)
&     Call ctslhx(ectslhx,pcrit,xcrit,DPout,DTsl,DPin,Dct,Dsuct,t9,
&       p9,p20,Ling,Lhxg,Loutg,xocg,xflashg,dTsubg,wcap,Lsub,DL)
      ctsldone = .true.
      R(int+5) = Lhx - Lhxg
   ELSE
      R(int+5) = xcrit - 0.25
   END IF

   IF (design.ne.1.0) THEN
      IF (.not.ctsldone)
&     Call ctslhx(ectslhx,pcrit,xcrit,DPout,DTsl,DPin,Dct,Dsuct,t9,
&       p9,p20,Ling,Lhxg,Loutg,xocg,xflashg,dTsubg,wcap,Lsub,DL)
      ctsldone = .true.
      R(int+6) = Lout - Loutg
   ELSE
      R(int+6) = DPout - 16.0
   END IF
```

The preceding three equations compare the three user-specified lengths to the three lengths calculated by the ctslhx subroutine when the model is in simulation mode. When these equations are satisfied, the calculated total length of the capillary tube will be the same as the length of the actual capillary tube. If the model is in design mode, the ctslhx variables which only appear in these equations are set to values which are representative to a simulation run. This way, new initial guesses will not be required if the user switches into simulation mode for the next run.

```
  IF (design.ne.1.0) THEN
     IF (.not.ctsldone)
&    Call ctslhx(ectslhx,pcrit,xcrit,DPout,DTsl,DPin,Dct,Dsuct,t9,
&      p9,p20,Ling,Lhxg,Loutg,xocg,xflashg,dTsubg,wcap,Lsub,DL)
     ctsldone = .true.
     IF (.not.NonZeroFlag) THEN
        IF (Cond2phX) THEN
           R(int+7) = xoc - xocg
        ELSE
           R(int+7) = 0.0 - Xflashg
        END IF
     ELSE
        R(int+7) = xoc + xocg + Xflashg
     END IF
  ELSE
     R(int+7) = DTsl - 24.0
  END IF

  IF (design.ne.1.0) THEN
     IF (.not.ctsldone)
&    Call ctslhx(ectslhx,pcrit,xcrit,DPout,DTsl,DPin,Dct,Dsuct,t9,
&      p9,p20,Ling,Lhxg,Loutg,xocg,xflashg,dTsubg,wcap,Lsub,DL)
     ctsldone = .true.
     IF (.not.NonZeroFlag) THEN
        IF (Cond2phX) THEN
           R(int+8) = 0 - dTsubg
        ELSE
           R(int+8) = setsub - dTsubg
        END IF
     ELSE
        R(int+8) = setsub + dTsubg
     END IF
  ELSE
     R(int+8) = DPin - 10.0
  END IF
```

These last two equations compare the outlet state that is predicted by the ctslhx subroutine to the state which is present in the system model. If the model is in design mode, the ctslhx variables are set to dummy values just as was done in the previous three equations. If the model is in simulation mode, the equations depend upon the exit of the condenser (Cond2phX). If the entrance to the capillary tube is two-phase, then (1) entrance quality calculated by the ctslhx subroutine is compared to the system entrance quality, and (2) the degrees of subcooling calculated by the ctslhx subroutine is compared to zero (which is true for a two-phase entrance condition). If the entrance to the capillary tube is subcooled, then (1) the quality at the flash point is compared to zero (which is the actual value that it should be), and (2) the degrees of subcooling calculated by the ctslhx subroutine is compared to the system subcooling.

These two equations are not found in the ct-sl hx governing equations because they are equations which relate the inlet and outlet of the component to other components. Therefore they are included in the thermodynamic property and state equations, marked by the counter variable `prop`.

```
IF (design.ne.1.0) THEN
   R(prop+27) = hpx(pcrit,xcrit) - h5
ELSE
   R(prop+27) = ectslhx*(hpt(p11,t3) - h9) - (h11 - h9)
END IF
R(prop+28) = Xhp(h5,p7) - xi
```

When the model is operating in simulation mode, their purpose is to couple the outlet of the capillary tube to the inlet of the evaporator. The first equation calculates the enthalpy at the exit of the capillary tube (where the flow is choked). This enthalpy along with the evaporating pressure, p7, are used in the function Xhp to determine the quality at the inlet of the evaporator. This method assumes that there is isenthalpic expansion from the critical pressure at the outlet of the capillary tube to the evaporating pressure. When the model is operated in design mode, the ct-sl hx model is no longer available to calculate the state of the refrigerant at the outlet of the capillary tube. Therefore, the user specified effectiveness of the ct-sl hx is used to specify the state of the refrigerant at the outlet of the suction line.

```
R(prop+42) = h3 - h5 - h11 + h9
```

This final equation states that the energy which the capillary tube looses is gained by the suction line. This is represented by equating the change in enthalpy for each component. When the model is operating in simulation mode, the enthalpy change across the capillary tube is determined by the ctslhx subroutine and this equation calculates the enthalpy at the exit of the suction line. When the model is operating in design mode, the ct-sl hx effectiveness determines the enthalpy change across the suction line and this equation calculates the enthalpy at the exit of the capillary tube.

D.2.3.2 CTSLHX Subroutine

This section explains the code which is found in the ctslhx subroutine. A complete explanation of the solution algorithm that is used for a ct-sl hx operating with a subcooled entrance and flashing in the inlet region with no recondensation is in section C.6 of Appendix C. However, since the ct-sl hx model can operate in several different modes other than the one described, the logic and solution strategy are explained. Rather than listing all of the code in this section, only the explanation is presented and the code can be found in the complete model listing in Appendix G.

First the subroutine takes the pressure and quality at the exit of the capillary tube (pcrit and xcrit), which were input to the subroutine, and calculates the mass flow rate assuming choked flow. Since the state at the outlet has already been specified, then solution proceeds by stepping down the capillary tube in three pressure increments. It begins by assuming that recondensation will not occur and starts to solve for the inlet state of the segment at the outlet. This is accomplished through the use of the **tpact** subroutine (which stands for two-phase adiabatic capillary tube segments). This subroutine is given the outlet pressure and quality along with the inlet pressure and various other previously calculated outlet properties and returns the quality at the inlet of the segment. The subroutine uses the energy equation and iterates on inlet quality until it is satisfied. Once the outlet state is specified (by p and x), the momentum equation is solved for the length of the segment, which is also an output of the tpact subroutine. This

procedure continues until either the entire outlet region is solved or the quality at the entrance to a segment is found to be less than zero (meaning recondensation occurs).

If the quality does go below zero, the subroutine sets the recondensation flag true and essentially untakes its last step by trying to find the fraction of the DPout pressure step which coincides with the flash point where the quality is zero. This is done with the **ract** subroutine (which stands for recondensation in an adiabatic capillary tube segment). If the quality is found to be less than zero before the inlet of the outlet region, a warning is printed to the screen since the model is not written to handle this case. First an initial guess is made, based on the negative quality which was already found, which assumes that the quality in that segment is linear with pressure. This guess, along with various other properties at the outlet, are input to the ract subroutine. The subroutine also uses the energy equation and iterates on pressure until the equation is solved, and calculates the length of a segment with that pressure drop. Then the remaining pressure step which completes the remainder of the pressure step DPout is taken. This subcooled liquid partial step is solved using the **spact** subroutine (which stands for single-phase adiabatic capillary tube segment). This subroutine calculates the length from the momentum equation and various other properties at the inlet from the inlet and outlet pressures. At this point the entire outlet region has been solved and the solution can proceed to the heat exchanger region.

The path which the solution takes at this point depends on whether recondensation was found to occur in the outlet region. Since there are several more governing equations in this region, some additional capillary tube properties need to be calculated at the already specified outlet before continuing. Let us begin by assuming that recondensation did not occur. First the temperature steps in the suction line are taken so that all the properties and variables in the suction line can be calculated. These suction line variables along with the outlet state of the capillary tube are input into the hxsolver subroutine (which stands for heat exchanger segment solver). This subroutine uses two governing equations and a Newton-Raphson solution method to find the temperature and quality at the inlet to the capillary tube given the temperature at the suction line outlet. This proceeds until all of the segments in this region are solved. If the quality at the entrance of any segment is found to be less than zero, the subroutine prints a warning to the screen since it is not equipped to handle this situation. However, sometimes when marching towards a solution this phenomenon may occur and then disappear, which is acceptable.

If recondensation was found to occur in the outlet region, then the recondensation point needs to be found. This is done by using the same two governing equations as before, except this time the temperatures at the capillary tube inlet and suction line outlet need to be found given that the quality at the inlet of the capillary tube is zero. After these temperatures are found, the remaining temperature step from the DTsl step is taken and the remaining two-phase segments are solved in the same way as before as if no recondensation had occurred. The same hxsolver subroutine is used in both cases but the Newton-Raphson variables are determined by the logical flags recond and recondone. If recond is true and the recondone flag is false, the hxsolver subroutine will solve this liquid step. Once recondone is true, the two-phase segments are all that remain and capillary tube temperature and quality are again the variables.

The solution of the remainder of the ct-sl hx depends upon the state of the refrigerant at the inlet to the capillary tube. This is indicated by the equation flag, Cond2phX (see section D.1.3). If the entrance is two-phase

then all of the segments in the inlet region are solved taking pressure steps like was already done in the outlet region. The outlet state and the inlet pressure are input to the tpact subroutine and the inlet quality and length are output. After the first inlet section has been solved, the inlet quality and the degrees of subcooling are calculated and output to the system model along with the region lengths and mass flow rate.

If the inlet to the capillary tube is subcooled, the two-phase segments are solved backwards in succession using the tpact subroutine until the very first segment is reached. This segment contains subcooled refrigerant and is solved using the spact subroutine. Next the length of this segment is combined with the two-phase segments to get the inlet region total length, and the inlet state is calculated. Except this time the calculated degrees of subcooling is supposed to match the subcooling in the system model, and the quality which was calculated at the flash point is sent to the system model rather than the inlet quality.

D.2.4 Evaporator

The evaporator, which is shown in Figure D.3, is essentially a counterflow heat exchanger. The refrigerant enters from the top and flows downwards through the two-phase and subcooled zones, while the air coming from the two cabinets is first mixed and then flows upwards in the opposite direction. It is modeled as consecutive zones, just as was done in the condenser, except this time only the two-phase and superheating zones are present. Likewise, each zone is modeled with the same three energy equations that were used before: a refrigerant-side energy balance, an air-side energy balance, and an effectiveness rate equation. The overall heat transfer coefficients in the effectiveness equations are calculated using the subroutine UsEvap in the EQNSUBS.f file.

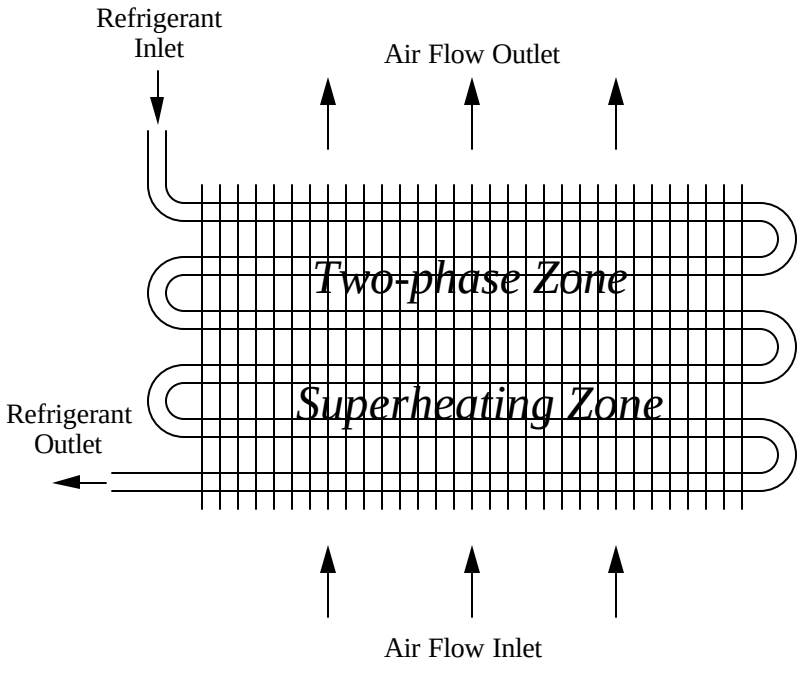

Figure D.3 Evaporator configuration

The governing equations for this component are marked with the counter variable `evap`.

D.2.4.1 Conservation Equations

```
R(evap+0) = MEvap - Mass(5,Acond,asubcond,a2ph1,a2ph2,
```

```
&  asupcond,Aevap,a2phevap,asupevap,Dcond,Devap,dpsuction,w,xoc,
&  xi,xoe,t20,t21,t3,p3,t7,t71,t9,p9,t11,rho1,rho20,rho21,rho70,
&  rho71,rho11,voldisline,Volcond,volbcap,volliqline,volfltr,
&  volcap,Volevap,volaccum,volsuctline,volcomp)

  R(evap+1) = MAccum - Mass(6,Acond,asubcond,a2ph1,a2ph2,
&  asupcond,Aevap,a2phevap,asupevap,Dcond,Devap,dpsuction,w,xoc,
&  xi,xoe,t20,t21,t3,p3,t7,t71,t9,p9,t11,rho1,rho20,rho21,rho70,
&  rho71,rho11,voldisline,Volcond,volbcap,volliqline,volfltr,
&  volcap,Volevap,volaccum,volsuctline,volcomp)
```

These equations calculate the total refrigerant mass in the evaporator and accumulator by using the function Mass. This total evaporator mass consists of the mass in the two-phase and, when applicable, the superheated zones. The accumulator and some additional tubing are located just downstream of the evaporator exit.

```
R(evap+2) = a2phevap + asupevap - aevap
 GOTO 1
```

This equation specifies that the total area of the evaporator is equal to the sum of the superheated and two-phase areas.

```
R(evap+3) = q2phevap + qsupevap - qevap
 GOTO 1
```

This equation calculates the overall heat transfer rate for the evaporator by summing the heat transfer rates in each zone.

D.2.4.2 Two-Phase Zone

```
IF (Evap2phX) THEN
   R(evap+4) = w*(h9 - h5) - q2phevap
ELSE
   R(evap+4) = w*(h71 - h5) - q2phevap
END IF
```

This equation calculates the heat transfer rate in the two-phase zone by using a refrigerant-side energy balance.

```
R(evap+5) = e2phevap*caevap*(ta2ph - t7) - q2phevap

R(evap+6) = e2p(u2phevap*a2phevap,caevap) - e2phevap

Call UsEvap(1,w,(t7+t71)/2.,(t71+t9)/2.,xi,Devap,ertmult,tma,
&   w*4/(pi()*Devap**2),q2phevap,a2phevap/alphaevap,Vdotevap,AAFE,
&   alphaevap,NSECTE,Usupevapc,U2phevapc)
R(evap+7) = u2phevapc - u2phevap

mdotaevap = vdotevap*60/va(patm,taevapout)
R(evap+8) = mdotaevap*cpa(taevapout) - caevap
```

This group of equations calculates the heat transfer rate in the two-phase zone by using an effectiveness rate equation. The effectiveness, overall heat transfer coefficient, and the heat capacity of the evaporator inlet air are also calculated.

```
R(evap+9) = caevap*(ta2ph - taevapout) - q2phevap
```

This equation calculates the heat transfer in the two-phase zone using an air-side energy balance.

D.2.4.3 Superheated Zone

```
IF (Evap2phX) THEN
   R(evap+10) = 0 - qsupevap
ELSE
   R(evap+10) = w*(h9 - h71) - qsupevap
END IF
```

This equation calculates the heat transfer rate in the superheated zone by using a refrigerant-side energy balance.

```
R(evap+11) = esupevap*cminsupevap*(tma - t71) - qsupevap

R(evap+12) = ec(usupevap*asupevap,cminsupevap,cmaxsupevap)
&               - esupevap

Call UsEvap(2,w,(t7+t71)/2.,(t71+t9)/2.,xi,Devap,ertmult,tma,
&  w*4/(pi()*Devap**2),q2phevap,a2phevap/alphaevap,Vdotevap,AAFE,
&  alphaevap,NSECTE,Usupevapc,U2phevapc)
R(evap+13) = usupevapc - usupevap

IF (Evap2phX) THEN
   R(evap+14) = 0.9 - cminsupevap
ELSE
   R(evap+14) = qsupevap/(t9 - t71) - cminsupevap
END IF

IF (Evap2phX) THEN
   R(evap+15) = 1 - cmaxsupevap
ELSE
   R(evap+15) = caevap - cmaxsupevap
END IF
```

This group of equations calculates the heat transfer rate in the superheated zone by using an effectiveness rate equation. Once again, the effectiveness and overall heat transfer coefficient, and minimum and maximum heat capacities for the refrigerant and air flow streams are calculated. Notice once again that in the last two equations, dummy values are assigned if the exit of the evaporator is two-phase, to assure non-zero values (for explanation see subcooled zone in section D.2.1).

```
R(evap+16) = caevap*(tma - ta2ph) - qsupevap
```

This final equation calculates the heat transfer in the superheated zone using an air-side energy balance.

D.3 System Equations

D.3.1 Thermodynamic Property and State Equations

In addition to the component models, described in the previous section, there are several equations which define the thermodynamic states in the system. These equations are entirely independent of the component equations. They mainly consist of property function calls from the NIST REFPROP subroutines, for such variables as enthalpy, density, and saturation temperature. These properties are needed by the component models for the energy and mass equations. This is also where the pressures around the system are interrelated to one another by pressure drop equations. This part of the model is divided up into sections according to the component in which the property is used. A typical example of property equations from the desuperheating zone of the condenser is shown below exactly as it appears in the code. The governing equations in this section are marked with the counter variable `prop`.

```
      fdesup = asupcond/acond
      R(prop+8) = DpSupCond - dpspHX(Dcond,STC,NSECTC,w,RTBCND*fdesup,
     &    1./rho1,1./rho21,t1,t21,DZC*fdesup,rough,0)

      R(prop+9) = p1 - DpSupCond - p21

      R(prop+10) = TsatP(p21) - t21

      R(prop+11) = htx(t21,1.0D0) - h21

      R(prop+12) = 1.0/vtx(t21,1.0D0) - rho21
```

First the pressure drop in zone was calculated by the subroutine dpspHX, which is for single-phase heat exchanger tubing. This value then relates the pressure at the entrance of the condenser to the saturated vapor pressure at the exit of the two-phase zone. Then it was possible to calculate the saturation temperature, enthalpy, and density at that point. This procedure is followed around the entire system refrigerant loop until all the state points are determined.

D.3.2 Simple Cabinet Model

The cabinet equations relate the heat load of the cabinets to the cooling capacity which the evaporator is providing. It is a simple model based on the UA's of each compartment determined from reverse heat leak tests (Rubas, 1993). The heat load for each compartment is the sum of the energy conduction through the walls plus the internal load supplied by heaters. The heaters were used for experimental purposes to maintain steady-state operation. The air steams from the two compartments mix prior to flowing across the evaporator and then separate after exiting the evaporator fan. The model also allows stratification effects in the compartments to be examined. If the parameter TzTfrez is set to zero then the average compartment temperatures, Tfrez and Tfrig, are different from their respective air streams entering the evaporator, Tz and Tf. If it is set to one, the average temperature and the entering temperature for each compartment are set equal. A schematic of the air flow pattern in the cabinet is shown in Figure D.4.

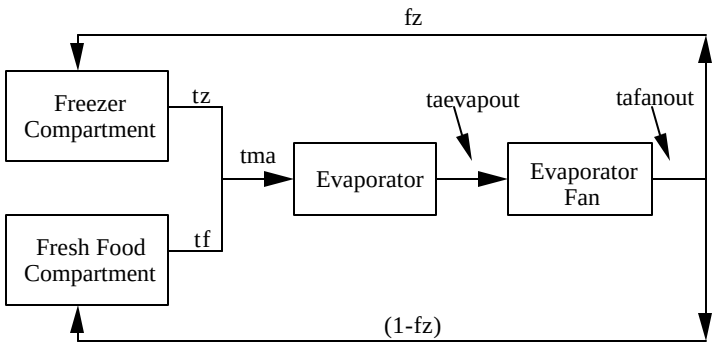

Figure D.4 Schematic of cabinet model

The governing equations in this section are marked with the counter variable `cab`.

```
R(cab+0) = BTU(UAz)*(tamb - tfrez) + BTU(Qfrez)  - Qz

R(cab+1) = BTU(UAf)*(tamb - tfrig)  + BTU(Qfresh)  - Qf
```

These equations calculate the total heat loads in each of the compartments. It is calculated as the sum of the energy which is conducted through the wall, that is calculated with user-defined UA values, and the load provided by the heaters, Qfrez and Qfrez.

```
mdotaevap = vdotevap*60/va(patm,taevapout)
R(cab+2) = mdotaevap*(ha(tafanout)-ha(taevapout)) - BTU(pevap)
```

This equation calculates the amount that the fan power increases the energy of the air stream after the exit of the evaporator and prior to reentering the cabinets.

```
  mdotaevap = vdotevap*60/va(patm,taevapout)
  R(cab+3) = mdotaevap*fz*(ha(tafanout) - ha(tz)) + Qz/RunTime
  If (NonZeroFlag) R(cab+3) = Qz + RunTime + fz + tafanout
&     + taevapout

  mdotaevap = vdotevap*60/va(patm,taevapout)
  R(cab+4) = (1-fz)*mdotaevap*(ha(tafanout) - ha(tf)) + Qf/RunTime
  If (NonZeroFlag) R(cab+4) = Qf + RunTime + fz + tafanout
&     + taevapout
```

These two equations relate the heat load in each cabinet to the rate that the evaporator is removing energy from each cabinet. The fraction of the air flow through the evaporator which goes through the freezer cabinet, fz, and the RunTime are calculated. The variable RunTime is used when the cooling capacity exceeds the heat load, in which case the temperature in the cabinets decreases until the compressor shuts off when the temperature reaches the desired setting. It is defined as the fraction of time that the system is running. In cases where the model is being used to simulate a experimental data point, in which the cabinets were maintained at a temperature by the heaters, the RunTime should be one.

```
R(cab+5) = fz*ha(tz) + (1 - fz)*ha(tf) - ha(tma)
```

This equation determines the temperature of the air entering the evaporator. It is calculated using an mass-weighted enthalpy balance.

```
R(cab+6) = (qevap - BTU(pevap))/BTU(pcond+pevap+pcomp) - COP

R(cab+7) = (pcond + pevap + pcomp)*RunTime*365*24/1000 - E
```

These two equations calculate the performance of the system, COP, and the annual energy usage, E.

D.3.3 Total Charge Equation

The total charge conservation equation allows the model to simulate off-design conditions. It accounts for the charge in each component of the system as well as the amount dissolved in the oil. The model uses an empirical model developed by (Grebner and Crawford, 1992). These governing equations are included with the cabinet model are also marked with the counter variable `cab`.

D.3.3.1 Refrigerant/Oil Mixture Equilibrium Equations

```
R(cab+8) = Mref/(Mref + Moil) - Woil

Aoil = K1oil + (K2oil/woil**(1.0/2.0))
Boil = K3oil + (K4oil/woil**(1.0/2.0)) + (K5oil/woil) +
&            (K6oil/woil**(3.0/2.0)) + (K7oil/woil**2.0)
R(cab+9) = (1 - Woil)*(Aoil + Boil*p11) - Tstar

R(cab+10) = ((t0+460) - (Tsat11+460))/(Tsat11+460) - Tstar
```

This group of equations calculates the amount of refrigerant, Mref, dissolved in the oil in the system, Moil.

D.3.3.2 Charge Conservation Equation

```
R(cab+11) = MCond + MEvap + MDisLine + MLiqLine + MAccum
&             + MSuctLine + MComp + MCapTube + Mref - mtotal
```

This is simply the total charge conservation equation.

D.4 Auxiliary Subroutines

This group of three subroutines, IC, BC, and FC, are located in the file named CHECKMOD.f. They are subroutines that are used by the ACRC equation solver (Mullen, 1994) and are separate from the file containing the list of governing equations. Each subroutine is described in the sections which follow.

D.4.1 IC

The IC, or initial check, subroutine is called by the equation solver prior to calling any of the governing equations for the first time. Therefore, it is perhaps better described as a pre-processing routine. It is needed to tell the equation solver at each iteration whether the superheating or subcooled zones are present in the evaporator and condenser, respectively. The routine determines which group of equations to use in each operation mode (refer to section D.1.3 on equation switching). In the simulation mode, the initial guesses in the XK file which are provided by the user, most commonly from a previous solution, determine how to set the equation flags. In design mode, the flags are set by the parameters subcool and superheat. These parameters are necessary because the parameters

setsub and setsup can be used as either temperature differences (to set degrees subcooling or superheat) or qualities(to set xoc or xoe). This does not mean to imply that the IC routine is limited in use for this sole purpose. It is simply the only function which is needed for RFSIM.

In simulation mode, the routine begins by initially assuming that the equation flags Evap2phX and Cond2phX are false (i.e. a superheated evaporator and a subcooled condenser). It then checks the variables xoc and xoe to determine what the quality is at the exit of the condenser and evaporator, respectively. If xoe is found to be equal to 1, then the equation flag Evap2phX is changed to true, and the set of superheated evaporator equations is used. Similarly, if xoc is found equal to zero, the set of subcooled condenser equations is used.

D.4.2 BC

As the equation solver marches toward the solution, the heat exchanger exits may change frequently. Therefore the BC, or boundary check, subroutine is called by the equation solver following each iteration. It checks certain user-specified variables to see if they are exceeding a prescribed set of limits after the last iteration step. If a variable is discovered to have escaped its limits, the most common result is a switch of the equations which reflects the direction in which the solution is trying to head. For example, if the condenser exit is being modeled as two-phase and the quality at the exit of the condenser, after an iteration, goes negative, then the equations require a subcooled zone in the solution, and the equation flag Cond2phX is changed to false.

There are two sets of boundary checks in the BC subroutine: one for simulation mode and one for design mode. The simulation mode will be discussed first. The logical check statements that are currently in use are a reflection of the most common signals for equation switching.

D.4.2.1 Simulation Mode

```
IF ((.not.Cond2phX).and.(t3.gt.t20)) THEN
      Cond2phX = .true.
      Switch = .true.
      t3 = t20
      xoc = 0.01d0
      asubcond = 0.0d0
      qsub = 0.0d0
      cminsub = 0.9d0
      cmaxsub = 1.0d0
      esubcond = 0.0d0
      fsubcond = 0.0d0
      DPin = (2.0/3.0)*DPin
```

This statement is checking to see if the exit temperature of the condenser, t3, is higher than the condensing temperature, t20, during a subcooled case, which is clearly impossible. If this condition is found to exist then the list of variable assignments is executed. Notice that they all involve variables which are related to the subcooled equations. The last equation is necessary because the inlet region of the capillary tube is modeled using three two-phase segments for a two-phase inlet and two two-phase segments for a subcooled inlet.

```
ELSE IF ((Cond2phX).and.(xoc.lt.0.)) THEN
      Cond2phX = .false.
      Switch = .true.
      t3 = t20 - 4.
```

```
        xoc = 0.0d0
        asubcond = 0.4d0
        qsub = 10.0d0
```

Conversely, the opposite trends must also be checked. If the current state of the solution is two-phase and the quality at the exit goes below zero, then the subcooed equations are used. This time hardwired initial guesses for the variables t3, asubcond, and qsub are set to reflect a possible subcooled condition.

```
IF ((Evap2phX).and.(xoe.gt.1.)) THEN
      Evap2phX = .false.
      Switch = .true.
      t9 = t71 + 1.0d0
      xoe = 1.0d0
      asupevap = 1.0d0
      qsupevap = 10d0
      cmaxsupevap = caevap
      cminsupevap = qsupevap/(t9-t71)
      a2phevap = aevap - asupevap
```

This statement checks to see if the quality at the outlet of the evaporator is greater than one, while using the two-phase equations.

```
ELSE IF ((.not.Evap2phX).and.(t9.lt.t71)) THEN
      Evap2phX = .true.
      Switch = .true.
      t9 = t71
      xoe = 0.97d0
      asupevap = 0.0d0
      qsupevap = 0.0d0
      cmaxsupevap = 1.0d0
      cminsupevap = 0.9d0
```

This statement checks to see if the exit evaporating temperature is lower than the evaporating temperature, while using the superheated equations.

```
ELSE IF ((.not.Evap2phX).and.(a2phevap.gt.Aevap)) THEN
      Evap2phX = .true.
      Switch = .true.
      t9 = t71
      xoe = 0.97d0
      asupevap = 0.0d0
      qsupevap = 0.0d0
      cmaxsupevap = 1.0d0
      cminsupevap = 0.9d0
```

Lastly, this statement checks to see if the calculated two-phase area in the evaporator is greater than the total evaporator area, in which case it defines a plausible two-phase exit condition.

D.4.2.2 Design Mode

This set of boundary checks is used in design mode. Since the user specifies the exit conditions of the heat exchangers (by definition), this code ensures that those conditions remain fixed.

```
            IF ((.not.Cond2phX).and.(t3.gt.t21)) then
                  t3 = t20 - setsub
                  xoc = 0.0d0
                  asubcond = 0.4d0
                  qsub = 10.0d0
            ELSE IF ((Cond2phX).and.(xoc.lt.0.)) then
                  t3 = t21
                  xoc = setsub
                  asubcond = 0.0d0
                  qsub = 0.0d0
            END IF

CCC         (EVAPORATOR)
            IF ((Evap2phX).and.(xoe.gt.1.)) then
                  t9 = t71
                  xoe = setsup
                  asupevap = 0.0d0
                  qsupevap = 0.0d0
            ELSE IF ((.not.Evap2phX).and.(t9.lt.t71)) then
                  t9 = t71 + setsup
                  xoe = 1.0d0
                  asupevap = 0.01d0
                  qsupevap = 0.5d0
                  cmaxsupevap = caevap
                  cminsupevap = qsupevap/(t9 - t71)
                  a2phevap = Aevap - asupevap
            ELSE IF ((.not.Evap2phX).and.(a2phevap.gt.Aevap)) then
                  t9 = t71 + setsup
                  xoe = 1.0d0
                  asupevap = .01d0
                  qsupevap = 0.5d0
                  cmaxsupevap = caevap
                  cminsupevap = qsupevap/(t9 - t71)
                  a2phevap = Aevap - asupevap
            END IF
```

The last group of checks here keeps the area variables correct, regardless of the mode of operation.

```
CCC     (EVAPORATOR)
        IF (Evap2phX) then
           a2phevap = Aevap
           asupevap = 0.0d0
        END IF

CCC     (CONDENSER)
        IF (Cond2phX) then
           asubcond = 0.0d0
        END IF
```

D.4.3 FC

The FC, or final check, subroutine is a post-processor. Its only function in RFSIM is to: (1) check that the saturation temperatures used in the compressor maps are within the curve fit limits, and (2) calculate the irreversiblity in various components. The latter is accomplished by calling the subroutine Irrev found in the EQNSUBS.f file.

D.5 Model-Specific Functions and Subroutines

This group of functions and subroutines is located in the EQNSUBS.f file. By no means is this section meant as a complete explanation of the theory behind each one. For more information on the capillary tube-suction line heat exchanger please refer to Appendix C. Otherwise, please reference the sources cited in the individual sections, since parts of this file were adapted from other simulation programs. In each group of routines, there is a brief explanation of the solution algorithm and argument variables used.

D.5.1 Component Curve Fits

These are the two compressor maps which were mentioned in section D.2.1. They are both biquadratic curve fits which are functions of the saturation temperatures at the inlet and outlet of the compressor. The function declarations are shown below.

```
DOUBLE PRECISION FUNCTION wf(Tcond, Tevap)
DOUBLE PRECISION FUNCTION Pcompf(Tcond, Tevap)
```

The first function, wf, determines the compressor mass flow rate in (lbm/hr), and the second function, Pcompf, determines the compressor power in (Watts). Tcond is the saturation temperature at the outlet of the compressor, which in this instance is state 1. Likewise, Tevap is the saturation temperature at the inlet of the compressor, state 11. Both functions are also dependent upon the refrigerant which is being used in the model. Thus, if the particular refrigerant being modeled in not among the several curve fits which are present in each function, a new curve fit must be made. The common block REFRGRNT.INC is included in both functions and chooses the correct equation.

D.5.2 Charge Inventory Functions

The charge inventory functions are used to calculate the amount of refrigerant mass in each component. The governing equations for mass were shown in the component models in section D.2. The function Mass, which is shown below, only calculates the mass in (lbm) of the component which is specified by the component flag variable, compflag. A key to the component flags can be found in the function itself.

```
DOUBLE PRECISION FUNCTION Mass(compflag,Acond,asubcond,a2ph1,
&  a2ph2,asupcond,Aevap,a2phevap,asupevap,Dcond,Devap,dpsuction,
&  w,xoc,xi,xoe,t20,t21,t3,p3,t7,t71,t9,p9,t11,rho1,rho20,rho21,
&  rho70,rho71,rho11,voldisline,Volcond,volbcap,volliqline,volfltr,
&  volcap,Volevap,volaccum,volsuctline,volcomp)
```

While all of the parameters and variables that are necessary to calculate all the components charge are included in the argument list, only the ones which are needed for the specified component are used. For a complete explanation of the arguments, please refer to the variable and parameter definitions in Appendix E.

The functions GLIntegrate and KH are used by the function Mass to calculate the charge in the two-phase components of the system (the condenser and evaporator). GLIntegrate performs numerical integration of the Hughmark void fraction correlation over a given quality range using Gaussian-Legandre quadrature to determine the refrigerant gas density weighting factor. For a more complete explanation of the equations which were used to calculate the refrigerant mass, please refer to Appendix B.

D.5.3 Irreversibility Calculations

This subroutine is called in the FC subroutine, after a solution has been reached. It calculates the irreversibility (Btu/hr) which is generated in the compressor, condenser, evaporator, and tubing (discharge line, capillary tube, and suction line) as well as that due to the refrigeration effect. All of these values, along with the total, are written to the output file in the parameter list.

D.5.4 Capillary Tube-Suction Line Heat Exchanger

The subroutine ctslhx, contains most of the capillary tube-suction line heat exchanger (ct-sl hx) equations in a sequential form. The governing equations are located here instead of in the EQNS.f file along with all of the other component models to keep the number of equations in the system model to a manageable size and to eliminate numerous initial guesses. A complete explanation of the model and solution theory can be found in Appendix C, and a description of the code can be found in section D.2.3. It must be called any time that the 6 ct-sl hx variables used in the system governing equations, described in section D.2.3, need to be evaluated.

In summary, when the subroutine is given pcrit, xcrit, DPout, DTsl, DPin, Dct, Dsl, t9, p9, and p20, it calculates Lin, Lhx, Lout, xoc or xflash, DTsub, and w. The variables DL and Lsub return information about the relative sizes of the subcooled (Lsub) and two-phase (DL) lengths in the inlet region.

D.6 General Functions and Subroutines

The functions and subroutines which are found in the FUNCTION.f file are general routines which are not model-specific. Therefore, they may be used with other applications without any modifications. They are grouped into five categories and described in the following sections.

D.6.1 Utility Functions

This category consists of a relatively small group which includes the following functions:

```
DOUBLE PRECISION FUNCTION BTU(Watts)
DOUBLE PRECISION FUNCTION pi()
```

BTU converts from units of BTU to Watts while pi returns the value of p.

D.6.2 Effectiveness Functions

This group contains functions which calculate the effectivenesses of the heat exchangers.

```
DOUBLE PRECISION FUNCTION epc(UA, cmin, cmax)
DOUBLE PRECISION FUNCTION ec(UA, cmin, cmax)
DOUBLE PRECISION FUNCTION e2p(UA, cmin)
```

The functions epc and ec calculate the effectiveness of a parallel counterflow and a counterflow heat exchanger, respectively, while the function e2p is for a two-phase heat exchanger.

D.6.3 Property Functions

These functions calculate various properties and dimensionless numbers for air, saturated liquid refrigerant, and saturated vapor refrigerant. For a complete listing of all the functions and a brief description, please refer to Appendix E.

D.6.4 Pressure Drop Functions

The functions which are in this section calculate the pressure drop in various types of tubes. These include pressure drop in a single-phase flow heat exchanger, a two-phase flow heat exchanger, and a suction line.

```
      DOUBLE PRECISION FUNCTION dpspHX(D,ST,NSECT,w,RTB,vin,vout,tin,
     &                     tout,DZ,rough,liquid)
      DOUBLE PRECISION FUNCTION dp2phACRC(w, PF, EqCircuit, D,
     &    TubeLen, NumRtb, Drtrnbnd, f2ph, tin, tout, xin, xout, volv,
     &    voll, Nintegration)
      DOUBLE PRECISION FUNCTION dptpHX(D,ST,NSECT,w,RTB,tout,tin,vvtp,
     &                     vltp,DZ,xout,xin)
      DOUBLE PRECISION FUNCTION dpsuct(D,ST,NSECT,w,RTB,vin,vout,
     &                        tin,tout,DZ,rough,suprht)
      DOUBLE PRECISION FUNCTION fdeSouza(T,G,D,X,Vf,Vg,V)
      DOUBLE PRECISION FUNCTION fColebrook(T,G,D,epsD,X)
      DOUBLE PRECISION FUNCTION fBlasius(T,G,D)
```

The definitions of the variables and parameters in the argument lists of each function can be found in the functions themselves in Appendix G. The pressure drop correlations which are taken from the ORNL heat pump model (Fischer and Rice, 1983), account for pressure drop due to momentum, friction (based on the Moody friction factor) , and return bends. The two-phase pressure drop in the ACRC correlation accounts for pressure drop due to friction, acceleration, and return bends. The final three functions calculate friction factors and are used in the capillary tube-suction line heat exchanger model.

D.6.5 Overall Heat Transfer Coefficient Subroutines

The final group of subroutines in the FUNCTION.f file calculates the overall heat transfer coefficient (U) in the heat exchangers.

```
      Subroutine UsCond(zone,w,t1avg,t2avg,t3avg,Dcond,crtmult,NSECTC,
     &  Gcond,vdotcond,AAF,alphacond,Usubcond,U2phcond,Usupcond)

      Subroutine USEvap(zone,w,t7avg,t9avg,xi,Devap,ertmult,tma,Gevap,
     &   mdotaevap,q2phevap,a2phevapIN,Rairevap,alphaevap,NSECTE,
     &   Usupevapc,U2phevapc)
```

UsCond is obviously for the condenser and UsEvap for the evaporator, but they both have the same form. First, only one zone of the heat exchanger is calculated at a time. This is controlled by the variable "zone" in the argument list. Once the zone is chosen, the subroutines calculate U in the following manner (Admiraal, 1993). The equation for U is in the form

$$\frac{1}{U_t} = \frac{1}{h_{air}} + \frac{\alpha}{h_i} \qquad \text{(D.3)}$$

where U_t is the total U, h_{air} is the air-side heat transfer coefficient (tube resistance is neglected), α is the ratio of the outside area of the heat exchanger to the inside area, and h_i is the refrigerant-side heat transfer coefficient. The subroutine calculates the air-side heat transfer coefficient using an empirical correlation (Cavallaro, 1994), and then calculates h_i. There are several correlations to calculate h_i depending upon which zone is being calculated. In the single-phase zones, the Gnielinski correlation is used in the functions hvap2 and hliq2. However, there are also functions in this file that are not currently in use that use the Dittus-Boelter correlation (hvap and hliq). In the two-phase zones, the correlations developed by Chato and Dobson (Dobson et. al., 1993) and Chato and Wattelet (Wattelet, 1994) are used in the condenser and evaporator, respectively. Definitions for all the arguments can be found in each of the individual functions.

D.7 Procedure to Change Refrigerants

TheACRC Refrigerator/Freezer model is capable of running with refrigerants other than R12. Currently, three different refrigerants can be modeled: R12, R134a , and R290 (propane). If any refrigerants other than these are desired then there are four steps to take.

1. Change the refrigerant flag (reflag) in the REFRGRNT.INC file. (This parameter selects the refrigerant in the NIST property routines and in the refrigerant dependent functions)
2. Create new curve fits of properties in FUNCTION.f file. (These include: Cpl, Cpv, kl, kv, mul, muv). Add new critical pressure to Pcritical function.
3. Create new compressor maps.
4. Obtain new empirical coefficients for refrigerant-oil solubility correlation (Grebner and Crawford, 1992).

D.8 Operating Modes

The ACRC Refrigerator/Freezer model can operate in one of two modes: design mode or simulation mode. It is controlled by the parameter, design. If set equal to one, the model operates in design mode, otherwise, it operates in simulation mode. In design mode, the user specifies the state of the refrigerant at the exit of both the condenser and the evaporator, by setting the parameters subcool, setsub, superheat, and setsup. The parameters subcool and superheat are necessary to indicate the type of exit in the heat exchangers as well as whether the parameters setsub and setsup are temperature differences or qualities. Additionally, the total amount of charge, mtotal, is set as a variable (X), since the variable for degrees of subcooling, setsub, was changed to an parameter (K). Finally, the capillary tube-suction line heat exchanger is removed from the model and the ct-sl hx effectiveness, ectslhx, must be specified by the user rather than calculated (ectslhx always remains a parameter). This forces the model to assume that the system total charge and the capillary tube are optimized to achieve these specified conditions. Therefore the design model can not predict the performance of the refrigerator over broad operating ranges.

The model may be changed into simulation mode by specifying the total charge as a parameter, and setsub as a variable, as well as including the capillary tube-suction line heat exchanger model, which calculates a mass flow rate through the capillary tube. Now the system model is capable of predicting the performance at off-design conditions by iterating to determine the state of the refrigerant at the exit of the evaporator and condenser.

D.9 Setting Parameters and Initial Guesses for Variables

The parameters and variables are found in the XK file (the name of this file can be changed in the solver settings file, SLVERSET, by the user). The excerpts below have been taken from this file as an example.

```
** XK initialization file: initializes variable guesses and parameter values.
**   Parameters are flagged with "K" and variables are flagged with "X."
**   The units are delimited with '[ ]'.
**   The last number signifies the number of decimal places (0-10).
** The ORDER of the input lines CANNOT CHANGE without program modification.
Flag  Name          XK#              Value  Units          # of digits
***********   DO NOT DELETE THESE FIRST SEVEN LINES!    ***************
X  asupcond     = XK(  1) =         0.8873 [ft^2]                    4
X  a2ph2        = XK(  2) =         1.1077 [ft^2]                    4
X  a2ph1        = XK(  3) =         4.6550 [ft^2]                    4
     .               .                .     .                        .
     .               .                .     .                        .
K  NSECTE       = XK(173) =           1.0 [ ]                        1
K  patm         = XK(174) =         14.40 [psia]                     2
K  pcond        = XK(175) =         25.73 [Watts]                    2
K  pevap        = XK(176) =         16.36 [Watts]                    2
K  Qfresh       = XK(177) =          43.1 [Watts]                    1
```

The first seven lines state the purpose and briefly explain the format of the file. Do not delete these first seven lines. They are not read by the solver and are for the user's benefit only, but must remain in the file so that the parameters and variables are read correctly. The remaining lines list the parameters and variables that are used in the model with each line providing the following six pieces of information.

1. A flag in the very first space that indicates whether the value is a parameter (marked by a K) or a variable (marked by an X). Note that there must be two spaces following the letter before the name.
2. The name of the parameter/variable, as it is used in the governing equations file, EQNS.f, and defined in the EQUIVLNT.INC file.
3. The corresponding element in the array XK for that parameter/variable. The name for this element must agree with the name in the EQUIVLNT.INC file.
4. The initial guess for the variable (if marked with an X) or the parameter value (if marked with a K).
5. The units of the parameter/variable. This information is restated in the output file.
6. The number of digits after the decimal point which will be shown in the output file (0-10), with -1 signifying to print the unformatted value (16 significant digits).

The variables are listed first in the order that they appear in the EQUIVLNT.INC file, and are followed by the parameters. If the user wishes to exchanger variables and parameters, all that is required is to switch the flag letter. Then when the equation solver asks you if any parameters and variables were switched, reply with a y and a new nonzerolist will be created for the new list of X's and K's. Simply changing the values of the parameters does not elicit a new nonzerolist. For more information please refer to Mullen (1994)

D.10 ACRC Equation Solver

This user's reference was written to provide all the information that would be necessary to use RFSIM. However, the solver has many additional capabilities, such as being able to do uncertainty analyses and multiple runs, which are not described in this manual. For any further details or questions concerning the ACRC equation solver, please refer to Mullen (1994).

References

Admiraal, D.M. and C.W. Bullard, "Heat Transfer in Refrigerator Condensers and Evaporators," University of Illinois at Urbana-Champaign, ACRC TR-48, 1993.

Cavallaro, A.R., "Effects of Varying Fan Speed on a Refrigerator/Freezer System," University of Illinois at Urbana-Champaign, ACRC TR-63, 1994.

Dobson, M.K., J.C. Chato, D.K. Hinde and S.P. Wang, "Experimental Evaluation of Internal Condensation of Refrigerants R-134a and R-12," University of Illinois at Urbana-Champaign, ACRC TR-38, 1993.

Fischer, S.K. and C.K. Rice, The Oak Ridge Heat Pump Models , Oak Ridge National Laboratory, ORNL/CON-80/R1, 1983.

Grebner, J.J. and R.R. Crawford, "The Effects of Oil on the Thermodynamic Properties of Dichlorodifluoromethane (R-12) and Tetrafluoroethane (R-134a)," University of Illinois at Urbana-Champaign, ACRC TR-13, 1992.

Mullen, C. E. and C. W. Bullard, "Room Air Conditioner System Modeling," University of Illinois at Urbana-Champaign, ACRC TR-60, 1994.

Porter, K.J. and C.W. Bullard, "Modeling and Sensitivity Analysis of a Refrigerator/Freezer System," University of Illinois at Urbana-Champaign, ACRC TR-31, 1992.

Rubas, P.J. and C.W. Bullard, "Assesment of Factors Contributing to Refrigerator Cycling Losses," University of Illinois at Urbana-Champaign, ACRC TR-45, 1993.

Wattelet, J.P., "Heat Transfer Flow Regimes of Refrigerants in a Horizontal-Tube Evaporator," University of Illinois at Urbana-Champaign, ACRC TR-55, 1994.

Appendix E: Definition of Parameters, Variables, Functions, and Subroutines

E.1 Parameters

The following section lists all the parameters which are typically specified to run the refrigerator model in simulation mode. They are grouped alphabetically, but within each group, they are listed arbitrarily. For example, looking at the length parameters, the first listed is the discharge line length followed by the condenser length and so on around the system until the beginning is reached. First, the name of the parameter is given, which in most instances is an abbreviation of the real name. For those parameters which aren't self-explanatory, a description is provided. Following the description are a typical value for the parameter, its units, and the component in which it is used. The typical values are only meant to show the parameter's order of magnitude, not to describe a specific configuration.

Table E.1 Description of parameters used in refrigeration model

Parameter Name	Description	Typical Values	Units	Component
AAF1C	Frontal air-flow area in inlet section of condenser	0.5075	ft^2	cond
AAF2C	Frontal air-flow area in outlet section of condenser	0.4172	ft^2	cond
AAFE	Frontal air-flow area in evaporator	0.3854	ft^2	evap
alphacond	Ratio of external area to internal area of condenser	2.58	-	cond
alphaevap	Ratio of external area to internal area of evaporator	5.0	-	evap
Cooling	Available energy associated with the refrigerating effect	140.0	Btu/hr	cab
crtmult	Multiplier for the refrigerant-side heat transfer correlations in the condenser to simulate microfinned tubing	1.0	-	cond
design	set = 1 for design mode set = 0 for simulation mode	0	-	flag
Ddisc	Inside diameter of the discharge line	0.0214	ft	disln
Dcond	Inside diameter of the condenser	0.017	ft	cond
Dliq	Inside diameter of the liquid line	0.0214	ft	liqln
Dct	Inside diameter of the capillary tube	0.00275	ft	captube
Devap	Inside diameter of the evaporator	0.0266	ft	evap
Dsuct	Inside diameter of the suction line	0.0214	ft	suctln
DfanC	Inside diameter of the condenser fan housing	0.5	ft	cond
DZC	Total length of straight tubes in the condenser	43.5	ft	cond
DZE	Total length of straight tubes in theevaporator	35.9	ft	evap
ertmult	Multiplier for the refrigerant-side heat transfer correlations in the evaporator to simulate microfinned tubing	1.0	-	evap
ectslhx	effectiveness of ct-sl hx	0.8	-	captube
fanc	Condenser fan speed multiplier	1.0	-	cond
fane	Evaporator fan speed multiplier	1.0	-	evap
fleak	Percentage of air which leaks out after condenser fan	0.0	-	cond
frecirc	Fraction of exit air recirculating into the condenser	0.0	-	cond
fupstream	Fraction of condenser area upstream of compressor	0.7	-	cond
hbarcomp	Average heat transfer coefficient of compressor shell	4.172	Btu/hr/°F	comp
Itot	Total amount of irreversibilites generated	775.0	Btu/hr	all
Icomp	Irreversibilities generated in the compressor	462.0	Btu/hr	comp

Parameter Name	Description	Typical Values	Units	Component
Icond	Irreversibilities generated in the condenser	142.0	Btu/hr	cond
Ievap	Irreversibilities generated in the evaporator	126.0	Btu/hr	evap
Ipipes	Irreversibilities generated in the tubing	45.0	Btu/hr	all
K1oil	Coefficient for refrigerant-oil mixture solubility	-0.6e-2	-	oil
K2oil	Coefficient for refrigerant-oil mixture solubility	0.42e-1	-	oil
K3oil	Coefficient for refrigerant-oil mixture solubility	0.2e-2	-	oil
K4oil	Coefficient for refrigerant-oil mixture solubility	-0.33e-2	-	oil
K5oil	Coefficient for refrigerant-oil mixture solubility	0.17e-2	-	oil
K6oil	Coefficient for refrigerant-oil mixture solubility	-0.29e-3	-	oil
K7oil	Coefficient for refrigerant-oil mixture solubility	0.164-4	-	oil
Ldisline	Length of discharge line	1.33	ft	disln
Lcond	Length of condenser (including return bends)	49.2	ft	cond
Lliqline	Length of liquid line	1.5	ft	liqln
Lin	Length of inlet region of capillary tube	3.36	ft	captube
Lsub	Length of subcooled region in inlet section of capillary tube	0.49	ft	captube
DL	Length of two-phase region in inlet section of capillary tube	2.87	ft	captube
Lhx	Length of heat exchanger region of capillary tube	4.3	ft	captube
Lout	Length of outlet region of capillary tube	1.18	ft	captube
Levap	Length of evaporator (including return bends)	39.0	ft	evap
Lsuctline	Length of suction line	7.0	ft	suctln
moil	Mass of oil in system	0.7	lbm	oil
NSECTC	Number of equivalent circuits in the condenser	1.0	-	cond
NSECTE	Number of equivalent circuits in the evaporator	1.0	-	evap
patm	Atmospheric pressure	14.4	psia	cond/evap
pcond	Condenser fan power	25.7	Watts	cond
pevap	Evaporator fan power	16.6	Watts	evap
Qfresh	Heat added to fresh food compartment from heater	0.0	Watts	cab
Qfrez	Heat added to freezer compartment from heater	0.0	Watts	cab
rough	Surface roughness inside tubing	0.5e-5	ft	all
RTBCND	Number of return bends in condenser	35.0	-	cond
RTBEVP	Number of return bends in evaporator	17.0	-	evap
subcool	Indicates type of condenser outlet in design mode 0 = two-phase exit, 1 = subcooled exit	1	-	flag
superheat	Indicates type of evaporator outlet in design mode 0 = two-phase exit, 1 = superheated exit	1	-	flag
setsub	Degrees of subcooling or quality at condenser outlet (determined by subcool)	1.8	°F	cond
setsup	Degrees of superheating or quality at evaporator outlet (determined by superheat)	0.0	°F	evap
STC	Spacing between tubes in the condenser	0.104	ft	cond
STE	Spacing between tubes in the evaporator	0.083	ft	evap
tamb	Ambient room temperature	90.0	°F	cab
tf	Air temp. entering evaporator from fresh food compartment	37.0	°F	cab
tfrig	Average air temperature in the fresh food compartment	37.0	°F	cab
tz	Air temp. entering evaporator from freezer compartment	5.3	°F	cab
tfrez	Average air temperature in the freezer compartment	5.3	°F	cab

Parameter Name	Description	Typical Values	Units	Component
TzTfrez	= 0, then avg. compartment temp ? inlet temp. to evaporator = 1, then avg. compartment temp = inlet temp. to evaporator	1.0	-	flag
UAf	Overall heat transfer coefficient for fresh food compartment	0.898	W/°F	cab
UAz	Overall heat transfer coefficient for freezer compartment	0.53	W/°F	cab
vdotcond	Volumetric air flow rate in condenser	156.0	ft^3/min	cond
vdotevap	Volumetric air flow rate in evaporator	65.3	ft^3/min	evap
voldisline	Volume of discharge line	0.48e-3	ft^3	disln
volbcap	Volume of bell cap connectors on mass flow meter	0.96e-4	ft^3	liqln
volfltr	Volume of filter-dryer	0.48e-3	ft^3	liqln
volliqline	Volume of liquid line	0.54e-3	ft^3	liqln
volcap	Volume of capillary tube	0.62e-4	ft^3	captube
volaccum	Volume of accumulator	0.34e-2	ft^3	evap
volsuctline	Volume of suction line	0.2e-2	ft^3	suctln
volcomp	Volume of compressor	0.95e-1	ft^3	comp

E.2 Variables

This section defines all of the Newton-Raphson variables which are used in the refrigerator model. The format is identical to that for the parameters just listed. The typical values show the order of magnitude of the variable and can be used as rough estimates for initial guesses. However, the values shown are very dependent upon operating conditions, such as the ambient and cabinet temperatures. In practice, initial guesses are obtained from an earlier solution, and then the parameters are changed incrementally to obtain new initial guesses from successive solutions.

Table E.2 Description of variables used in refrigerator model

Variable Name	Description	Typical Values	Units	Component
asupcond	Area of desuperheating zone of condenser	0.78	ft^2	cond
a2ph2	Area of second two-phase zone of condenser	1.2142	ft^2	cond
a2ph1	Area of first two-phase zone of condenser	4.58	ft^2	cond
asubcond	Area of subcooled zone of condenser	0.075	ft^2	cond
a2phevap	Area of two-phase zone of evaporator	7.15	ft^2	evap
asupevap	Area of superheated zone of evaporator	9.132	ft^2	evap
Aoil	Variable used in oil solubility equation	0.177	-	oil
Boil	Variable used in oil solubility equation	0.00296	-	oil
cacondin	Heat capacity of condenser inlet air	159.0	Btu/hr-°F	cond
cacond2ph1	Heat capacity of air in first two-phase zone of condenser	156.0	Btu/hr-°F	cond
cacond2ph2	Heat capacity of air in second two-phase zone of condenser	97.0	Btu/hr-°F	cond
caevap	Heat capacity of evaporator inlet air	80.0	Btu/hr-°F	evap
cminsupcond	Minimum heat capacity of desuperheating zone of condenser	2.0	Btu/hr-°F	cond
cmaxsupcond	Maximum heat capacity of desuperheating zone of condenser	62.0	Btu/hr-°F	cond

Variable Name	Description	Typical Values	Units	Component
cminsub	Minimum heat capacity of subcooled zone of condenser	2.6	Btu/hr-°F	cond
cmaxsub	Maximum heat capacity of subcooled zone of condenser	2.8	Btu/hr-°F	cond
cminsupevap	Minimum heat capacity of superheating zone of evaporator	1.6	Btu/hr-°F	evap
cmaxsupevap	Maximum heat capacity of superheating zone of evaporator	79.0	Btu/hr-°F	evap
COP	Coefficient of performance	0.9	-	-
DPin	Pressure steps in inlet region of capillary tube	12.0	psia	captube
DPout	Pressure steps in outlet region of capillary tube	13.0	psia	captube
Dpdischarge	Pressure drop in discharge line	0.005	psia	disln
DpSupCond	Pressure drop in desuperheating zone of condenser	0.07	psia	cond
Dp2phCond	Pressure drop in two-phase zone of condenser	0.43	psia	cond
DpSubCond	Pressure drop in subcooled zone of condenser	0.0006	psia	cond
DpLiquid	Pressure drop in liquid line	0.0	psia	cond
Dp2phEvap	Pressure drop in two-phase zone of evaporator	0.15	psia	evap
DpSupEvap	Pressure drop in superheated zone of evaporator	0.22	psia	evap
DpSuction	Pressure drop in suction line	0.4	psia	suctln
DTsl	Temperature steps in suction line of interchanger	22.0	°F	suctln
E	Total yearly system energy consumption	2400.0	kW-hr/yr	-
esupcond	Effectiveness of desuperheating zone of condenser	0.83	-	cond
e2ph1	Effectiveness of first two-phase zone of condenser	0.18	-	cond
e2ph2	Effectiveness of second two-phase zone of condenser	0.09	-	cond
esubcond	Effectiveness of subcooled zone of condenser	0.1	-	cond
e2phevap	Effectiveness of two-phase zone of evaporator	0.3	-	evap
esupevap	Effectiveness of superheated zone of evaporator	0.99	-	evap
fsubcond	Ratio of subcooled area in inlet section of condenser	0.016	-	cond
fsupcond	Ratio of superheated area in outlet section of condenser	0.4	-	cond
fz	Fraction of evaporator air flow into freezer	0.9	-	cab
h0	Refrigerant enthalpy at compressor outlet	95.0	Btu/lbm	comp
h1	Refrigerant enthalpy at condenser inlet	95.0	Btu/lbm	cond
h21	Refrigerant enthalpy at x=1 of condenser	85.0	Btu/lbm	cond
h20	Refrigerant enthalpy at x=0 of condenser	30.0	Btu/lbm	cond
h3	Refrigerant enthalpy at outlet of condenser	29.0	Btu/lbm	cond
h4	Refrigerant enthalpy at inlet of capillary tube	29.0	Btu/lbm	captube
h5	Refrigerant enthalpy at outlet of capillary tube	18.0	Btu/lbm	captube
h71	Refrigerant enthalpy at x=1 of evaporator	72.0	Btu/lbm	evap
h9	Refrigerant enthalpy at outlet of evaporator	75.0	Btu/lbm	evap
h11	Refrigerant enthalpy at inlet of compressor	85.0	Btu/lbm	comp
mtotal	Total mass of refrigerant in system	0.5	lbm	-
MDisLine	Mass of refrigerant in discharge line	0.0015	lbm	disln
MCond	Mass of refrigerant in condenser	0.25	lbm	cond
MLiqLine	Mass of refrigerant in liquid line	0.09	lbm	liqln
MCapTube	Mass of refrigerant in capillary tube	0.003	lbm	captube
MEvap	Mass of refrigerant in evaporator	0.09	lbm	evap
MAccum	Mass of refrigerant in accumulator	0.0014	lbm	evap
MSuctLine	Mass of refrigerant in suction line	0.0007	lbm	suctln
MComp	Mass of refrigerant in compressor	0.032	lbm	comp

Variable Name	Description	Typical Values	Units	Component
Mref	Mass of refrigerant dissolved in oil	0.037	lbm	oil
p0	Pressure at compressor outlet	150.0	psia	comp
p1	Pressure at condenser inlet	150.0	psia	cond
p21	Pressure at x=1 of condenser	150.0	psia	cond
p20	Pressure at x=0 of condenser	149.0	psia	cond
p3	Pressure at outlet of condenser	149.0	psia	cond
p4	Pressure at inlet of capillary tube	149.0	psia	captube
p7	Pressure at inlet of evaporator	16.0	psia	evap
p71	Pressure at x=1 of evaporator	16.0	psia	evap
p9	Pressure at outlet of evaporator	15.0	psia	evap
p11	Pressure at inlet of compressor	14.0	psia	comp
pcomp	Compressor power	180.0	Watts	comp
pcrit	Critical pressure at capillary tube outlet (choked flow)	27.0	psia	captube
qcond	Heat transfer of entire condenser	760.0	Btu/hr	cond
qsupcond	Heat transfer of desuperheating zone of condenser	120.0	Btu/hr	cond
q2ph2	Heat transfer of second two-phase zone of condenser	100.0	Btu/hr	cond
q2ph1	Heat transfer of first two-phase zone of condenser	535.0	Btu/hr	cond
qsub	Heat transfer of subcooled zone of condenser	5.0	Btu/hr	cond
qevap	Heat transfer of entire evaporator	660.0	Btu/hr	evap
q2phevap	Heat transfer of two-phase zone of evaporator	620.0	Btu/hr	evap
qsupevap	Heat transfer of superheated zone of evaporator	40.2	Btu/hr	evap
qcomp	Heat transfer of compressor shell	500.0	Btu/hr	comp
Qf	Total fresh food cabinet load	300.0	Btu/hr	cab
Qz	Total freezer cabinet load	425.0	Btu/hr	cab
rho1	Density of refrigerant at inlet of condenser	3.0	ft^3/lbm	cond
rho21	Density of refrigerant at x=1 of condenser	3.7	ft^3/lbm	cond
rho20	Density of refrigerant at x=0 of condenser	77.5	ft^3/lbm	cond
rho70	Density of refrigerant at x=0 of evaporator	92.0	ft^3/lbm	evap
rho71	Density of refrigerant at x=1 of evaporator	0.4	ft^3/lbm	evap
rho11	Density of refrigerant at inlet of compressor	0.34	ft^3/lbm	comp
RunTime	Fraction of time compressor runs	1.2	-	-
t0	Temperature at compressor outlet	170.0	°F	comp
t1	Temperature at inlet of condenser	170.0	°F	cond
t21	Temperature at x=1 of condenser	110.0	°F	cond
t20	Temperature at x=0 of condenser	109.0	°F	cond
t3	Temperature at outlet of condenser	108.0	°F	cond
t4	Temperature at inlet of capillary tube	108.0	°F	captube
t7	Temperature at inlet of evaporator	-17.0	°F	evap
t71	Temperature at x=1 of evaporator	-18.0	°F	evap
t9	Temperature at outlet of evaporator	8.0	°F	evap
t11	Temperature at inlet to compressor	75.0	°F	comp
Tsat1	Saturation temperature at p1 (for compressor map)	109.0	°F	comp
Tsat11	Saturation temperature at p11 (for compressor map)	-19.0	°F	comp
tacondin	Air temperature at inlet of condenser	90.0	°F	cond

Variable Name	Description	Typical Values	Units	Component
ta2ph1	Air temperature at inlet of first two-phase zone of condenser	90.0	°F	cond
ta2phmid	Air temperature between the first and second two-phase zones of condenser, before condenser fan	94.0	°F	cond
tacomp	Air temperature after condenser fan that passes over compressor shell	95.0	°F	cond
ta2ph2	Air temperature at inlet of second two-phase zone of condenser	97.0	°F	cond
tasup	Air temperature at inlet of desuperheating zone of condenser	97.0	°F	cond
tacondout	Air temperature at outlet of condenser	98.0	°F	cond
tma	Air temperature at inlet to evaporator	8.0	°F	evap
ta2ph	Air temperature at inlet to two-phase zone of evaporator	7.5	°F	evap
taevapout	Air temperature at outlet of evaporator	-1.0	°F	evap
tafanout	Air temperature after evaporator fan	2.0	°F	evap
Tstar	Non-dimensional degree of superheat for refrigerant/oil mixture	0.2	-	oil
usupcond	Overall heat transfer coefficient for desuperheating zone of cond.	4.8	Btu/hr-ft^2-°F	cond
u2ph1cond	Overall heat transfer coefficient for 1st two-phase zone of cond.	6.7	Btu/hr-ft^2-°F	cond
u2ph2cond	Overall heat transfer coefficient for 2nd two-phase zone of cond.	7.3	Btu/hr-ft^2-°F	cond
usubcond	Overall heat transfer coefficient for subcooled zone of cond.	4.2	Btu/hr-ft^2-°F	cond
u2phevap	Overall heat transfer coefficient for two-phase zone of evap.	4.2	Btu/hr-ft^2-°F	evap
usupevap	Overall heat transfer coefficient for superheated zone of evap.	1.4	Btu/hr-ft^2-°F	evap
w	Refrigerant mass flow rate	12.0	lbm/hr	all
Woil	Fraction of liquid refrigerant in oil/refrigerant mixture	0.052	-	oil
xcrit	Critical quality at outlet of capillary tube (choked flow)	0.18	-	captube
xoc	Quality at outlet of condenser	0.0	-	cond
xi	Quality at inlet of evaporator	0.25	-	evap
xoe	Quality at outlet of evaporator	1.0	-	evap

E.3 Non-Residual Variables

Along with the parameters and variables just defined, there are several other variables throughout the model that are called non-residual variables. Some of these can be classified as intermediate parameters such as the condenser area, acond, which is strictly a function of other parameters, while others, such as fdesup, are combinations of parameters and variables and are therefore not included in the variable list. Finally, there are variables acting as flags that enhance the speed of the model, such as CTdone, which indicates whether the capillary tube-suction line heat exhchange subroutine has been called already during a call to CalcR. A complete list of these variables follows.

Table E.3 Description of non-residual variables

Variable Name	Description	Units	Component
Acond	Total air-side area in the condenser	ft^2	cond
Aevap	Total air-side area in the evaporator	ft^2	evap
AlreadyAsked	Logical flag which indicates if the user has already answered whether the equations or XK files have changed, warrenting a new non-zero list.	-	solver
Aoil	Variable used in oil solubility equations	-	oil
Boil	Variable used in oil solubility equations	-	oil
cab	Counter variable for cabinet equations	-	solver
comp	Counter variable for compressor equations	-	solver
cond	Counter variable for condenser equations	-	solver
Cond2phX	Logical flag specifying outlet condition of condenser	-	solver
ctsldone	Logical flag which indicates if captube-suction line heat exchanger subroutine has been called	-	solver
DTsubg	Degrees of subcooling at inlet of capillary tube calculated by ctslhx subroutine	°F	captube
ELEMENT	Row number of non-zero list	-	solver
EQNUM	Governing equation number for partial derivative calculations	-	solver
evap	Counter variable for evaporator equations	-	solver
Evap2phX	Logical flag specifying outlet condition of evaporator	-	solver
f2phcond	Fraction of condenser which is two-phase		cond
f2phevap	Fraction of evaporator which is two-phase		evap
fdesup	Fraction of condenser which is superheatied		cond
fsubarea	Fraction of condenser which is subcooled		cond
int	Counter variable for ct-sl hx equations	-	solver
Ling	Length of inlet region of ctsl hx calculated by ctslhx subroutine	ft	captube
Lhxg	Length of heat exchanger region of ctsl hx calculated by ctslhx subroutine	ft	captube
Loutg	Length of outlet region of ctsl hx calculated by ctslhx subroutine	ft	captube
mdotacond	Mass flow rate of air through the condenser	lbm/hr	cond
mdotaevap	Mass flow rate of air through the evaporator	lbm/hr	evap
NonZeroFlag	Logical flag that is set true if partial derivitive matrix is being calculated	-	solver
NonZeroList	Binary array indicating non-zero elements of partial derivative matrix	-	solver
printnzl	Logical flag that prints the numbers of non-zero residuals for each variable on the screen if set to true (used for debugging)	-	solver
prop	Counter variable for state property variables equations	-	solver
R	Array of residual values	-	solver
ts	Temperature of compressor shell (function of compressor discharge temp)	°F	comp
Usupcondc	Overall heat transfer coefficient for desuperheating zone of condenser calculated by UsCond subroutine	Btu/hr-ft^2-°F	cond
U2phcondc	Overall heat transfer coefficient for two-phase zone of condenser calculated by UsCond subroutine	Btu/hr-ft^2-°F	cond
Usubcondc	Overall heat transfer coefficient for subcooled zone of condenser calculated by UsCond subroutine	Btu/hr-ft^2-°F	cond

Variable Name	Description	Units	Component
U2phevapc	Overall heat transfer coefficient for two-phase zone of evaporator calculated by UsEvap subroutine	Btu/hr-ft^2-°F	evap
Usupevapc	Overall heat transfer coefficient for superheated zone of evaporator calculated by UsEvap subroutine	Btu/hr-ft^2-°F	evap
v0	Specific volume of refrigerant at outlet of compressor	ft^3/lbm	comp
v3	Specific volume of refrigerant at outlet of condenser	ft^3/lbm	vond
v9	Specific volume of refrigerant at outlet of evaporator	ft^3/lbm	evap
vaircomp	Velocity of air over the compressor shell	ft/sec	cond
VariableNum	Variable number corresponding to X array	-	solver
Volcond	Total volume in condenser	ft^3	cond
Volevap	Total volume in evaporator	ft^3	evap
wcap	Mass flow rate calculated by ctslhx subroutine	lbm/hr	captube
xflashg	Quality of refrigerant at flash point in capillary tube calculated by ctslhx subroutine	-	captube
xocg	Inlet quality to capillary tube calculated by ctslhx subroutine	-	captube

E.4 Model-Specific Functions and Subroutines

The following table gives a brief description of the model specific functions and subroutines which are used to solve RFSIM. These procedures are considered model-specific because they are only valid for a particular system model. In other words, these procedures have the configuration or specifications of a particular system embedded in them and are not interchangeable between different models. For example, the first two functions, wf and pcompf, are only valid for the compressor in the Amana TC18MBL experimental refrigerator and none other. These functions would have to be modified for use with any other system. For a more detailed description, see the code listing in Appendix G.

Table E.4 Description of model-specific functions and subroutines

Name	Brief Description
wf	Returns the refrigerant mass flow rate predicted by map equations as a funciton of (Tsat1, Tsat11)
pcompf	Returns the compressor power predicted by map equations as a function of (Tsat1, Tsat111)
GLIntegrate	Returns the refrigerant gas density weighting factor (Wg) using Hughmark void fraction correlation and Gaussian-Legendre quadrature integration
KH	Returns parameter used by Hughmark void fraction correlation in GLIntegrate
Mass	Returns the amount of refrigerant in each component of the refrigerator/freezer system
Irrev	This subroutine calculates the irreversibilities produced in various components in the system
ctslhx	This subroutine models the capillary tube-suction line heat exchanger
hxsolver	This subroutine solves the simultaneous equations in the heat exchanger region of the ct-sl hx
hxresid	This subroutine calculates the residuals which are used in the hxsolver subroutine when the suction line outlet temperature is given and the capillary tube inlet temperature and quality are found
hxresid2	This subroutine calculates the residuals which are used in the hxsolver subroutine when the capillary tube inlet quality is zero and the temperatures at the capillary tube inlet and suction line outlet are found
tpact	This subroutine solves a two-phase segment in an adiabatic region of the capillary tube

ract	This subroutine solves the two-phase portion of a segment in the adiabatic outlet region of the capillary tube where flashing has occured as a result of recondensation
spact	This subroutine solves a single-phase (liquid) segment in an adiabatic region of the capillary tube
slprops	This subroutine calculates all properties needed for the suction line at a segment boundary

E.5 General Functions and Subroutines

The following table gives a brief description of the general functions and subroutines which are used to solve RFSIM. Unlike the previously listed model-specific procedures, these procedures can be used interchangeably with any model without any modifications. For a more detailed description, see the code listing in Appendix G.

Table E.5 Description of general functions and subroutines

Name	Brief Description
BTU	Converts Watts to Btu/hr
pi	Returns the value for p
epc	Returns the effectiveness of a parallel counterflow heat exchanger
ec	Returns the effectiveness of a counterflow heat exchanger
e2p	Returns the effectiveness of a two-phase heat exchanger
cpa	Returns the specific heat of air given the temperature
Cpl	Returns the specific heat of saturated liquid refrigerant given the temperature
Cpv	Returns the specific heat of saturated vapor refrigerant given the temperature
Cpsup	Returns the specific heat of superheated vapor refrigerant given the temperature and pressure
ha	Returns the enthalpy of air given the temperature
ka	Returns the thermal conductivity of air given the temperature
kl	Returns the thermal conductivity of saturated liquid refrigerant given the temperature
kv	Returns the thermal conductivity of saturated vapor refrigerant given the temperature
mua	Returns the viscosity of air given the temperature
mul	Returns the viscosity of saturated liquid refrigerant given the temperature
muv	Returns the viscosity of saturated vapor refrigerant given the temperature
PrAir	Returns the Prandtl number of air given the temperature given the temperature
Prl	Returns the Prandtl number of saturated liquid refrigerant given the temperature given the temperature
Prv	Returns the Prandtl number of saturated vapor refrigerant given the temperature given the temperature
Pcritical	Returns the critical pressure of the refrigerant
ReAir	Returns the Reynolds number of air given the temperature, mass flux, and diameter
Rel	Returns the Reynolds number of saturated liquid refrigerant given the temperature, mass flux, and diameter
Rev	Returns the Reynolds number of saturated vapor refrigerant given the temperature, mass flux, and diameter
va	Returns the specific volume of air given the temperature and pressure
dpspHX	Returns the pressure drop for a single-phase zone of a heat exchanger (taken from ORNL code)
dp2phACRC	Returns the pressure drop for a two-phase zone of a heat exchanger (developed by ACRC)
dptpHX	Returns the pressure drop for a two-phase zone of a heat exchanger (taken from ORNL code)
dpsuct	Returns the pressure drop for the suction line (taken from ORNL code)
Moody	Returns the Moody friction factor (explicit form of correlation taken from ORNL code)
Xtt	Returns the Lockhart-Martinelli parameter

Z	Returns the frictional multiplier for calculating pressure drop (based on data taken from ORNL code)
ZZ	Returns the accelerational multiplier for calculating pressure drop (based on data taken from ORNL code)
fdeSouza	Returns the friction factor for two-phase flow in smooth pipes (using Souza correlation)
fColebrook	Returns the mass weighted average friction factor for two-phase flow (using Colebrook correlation)
fBlasius	Returns the friction factor for single-phase fully developed turbulent flow in smooth tubes (using Blasius correlation)
UsCond	This subroutine calculates the superheated, two-phase, and subcooled overall heat transfer coefficients for the condenser, based on geometric parameters specified in the input file
UsEvap	This subroutine calculates the superheated and two-phase overall heat transfer coefficients for the evaporator, based on geometric parameters specified in the input file
haircnd	Returns the air side heat transfer coefficient in condenser (using curve fit by Cavallaro)
hairevp	Returns the air side heat transfer coefficient in evaporator (using curve fit by Cavallaro)
hliq	Returns the refrigerant side liquid heat transfer coefficient (using Dittus Boelter correlation)
hvap	Returns the refrigerant side vapor heat transfer coefficient (using Dittus Boelter correlation)
hliq2	Returns the refrigerant side liquid heat transfer coefficient (using Gnielinski correlation)
hvap2	Returns the refrigerant side vapor heat transfer coefficient (using Gnielinski correlation)
h2phcondACRC	Returns the two-phase heat transfer coefficient for the condenser (using Dobson correlation)
h2phevapACRC	Returns the two-phase heat transfer coefficient for the evaporator (using Wattelet correlation)

Appendix F: Comparison of Predicted and Experimental Results

F.1 Design Model

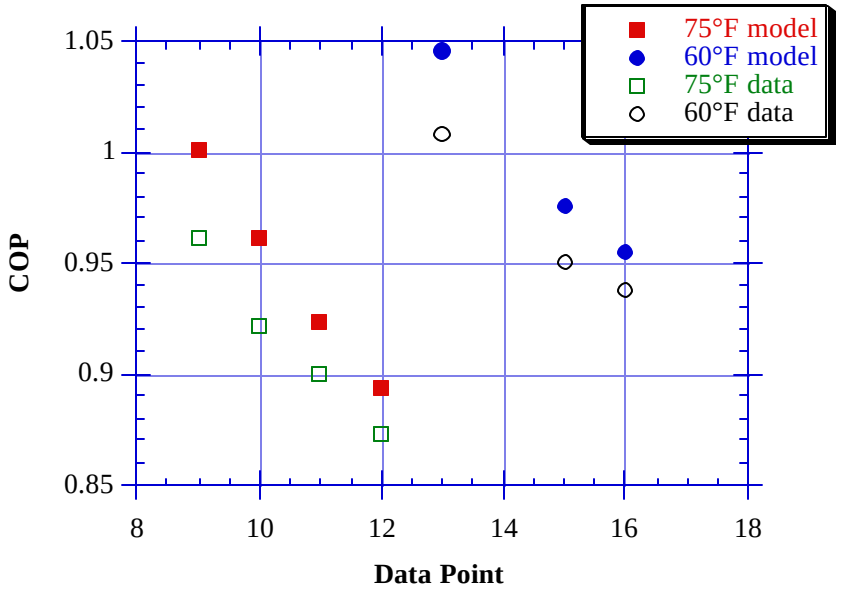

Figure F.1 COP comparison

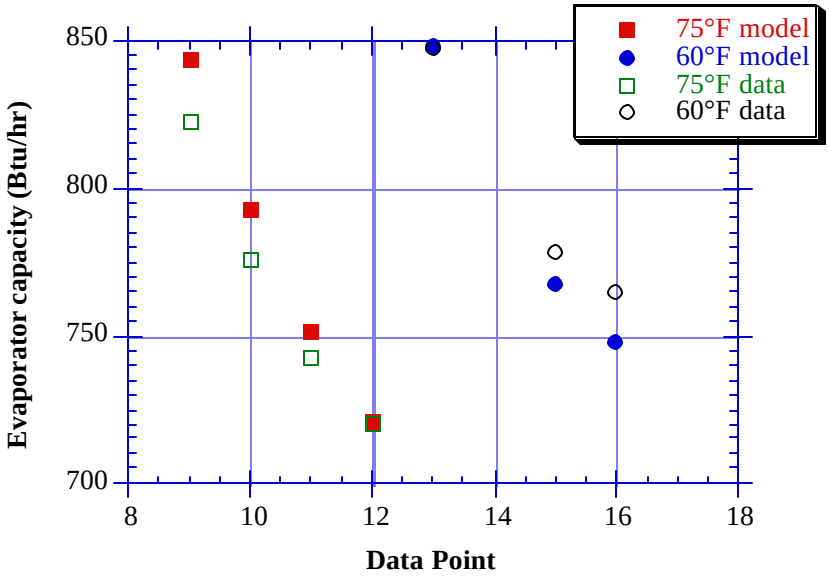

Figure F.2 Qevap comparison

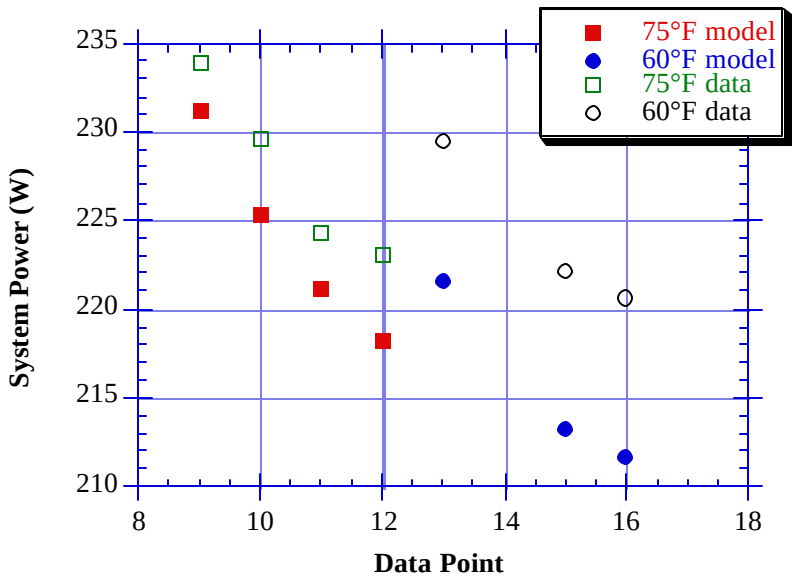

Figure F.3 System power comparison

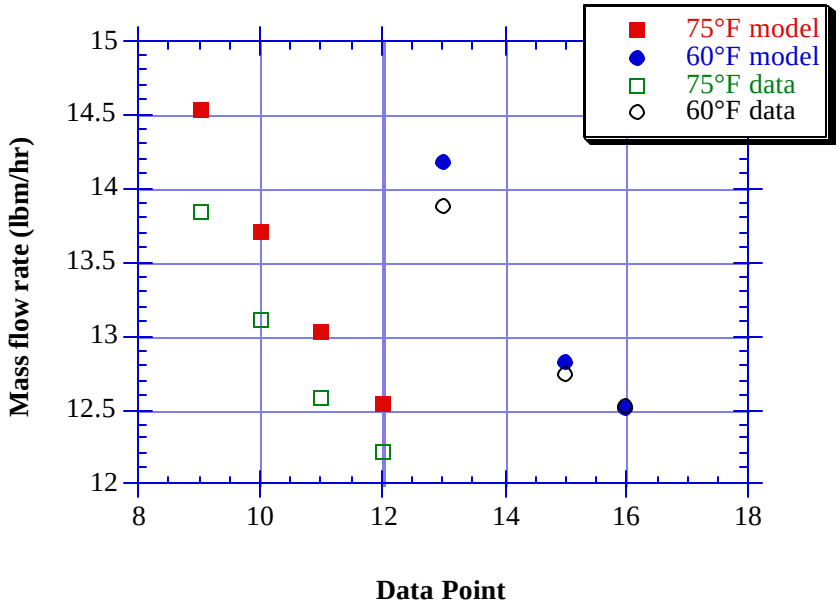

Figure F.4 Mass flow rate comparison

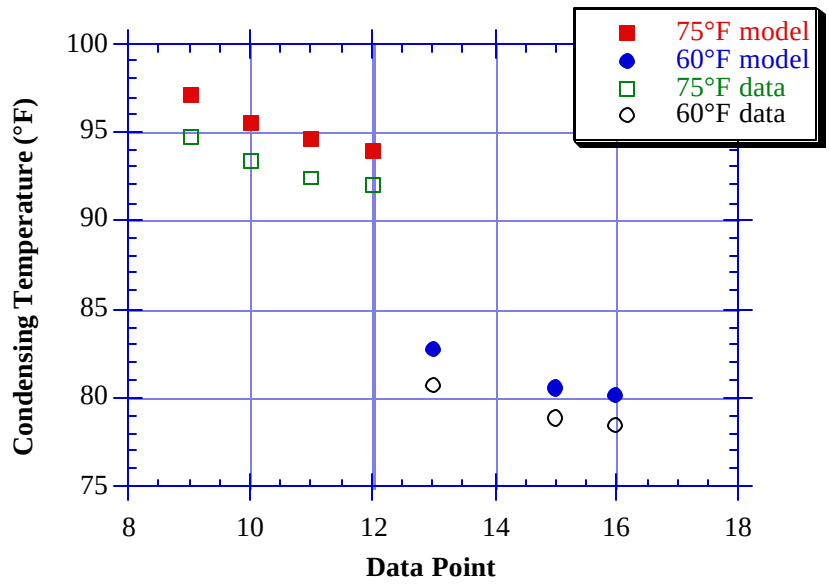

Figure F.5 Condensing temperature comparison

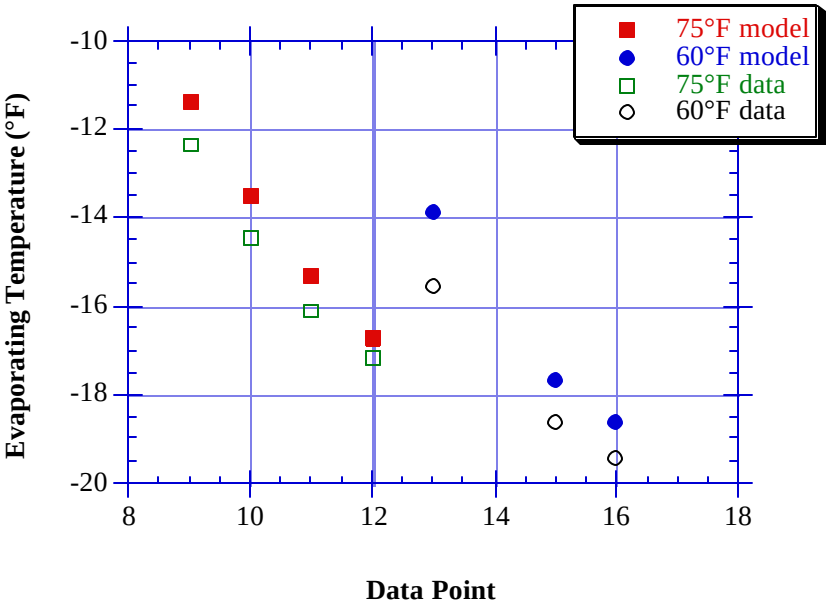

Figure F.6 Evaporating temperature comparison

F.2 Simulation Model

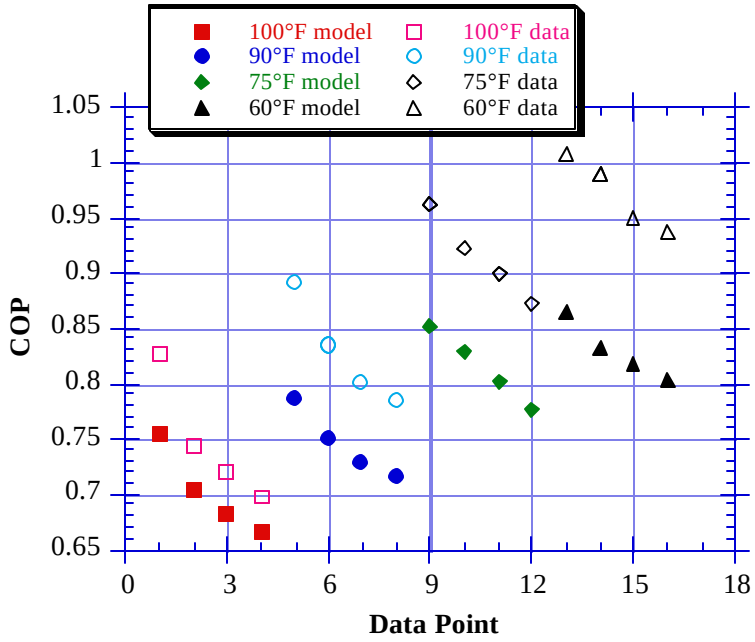

Figure F.7 COP comparison

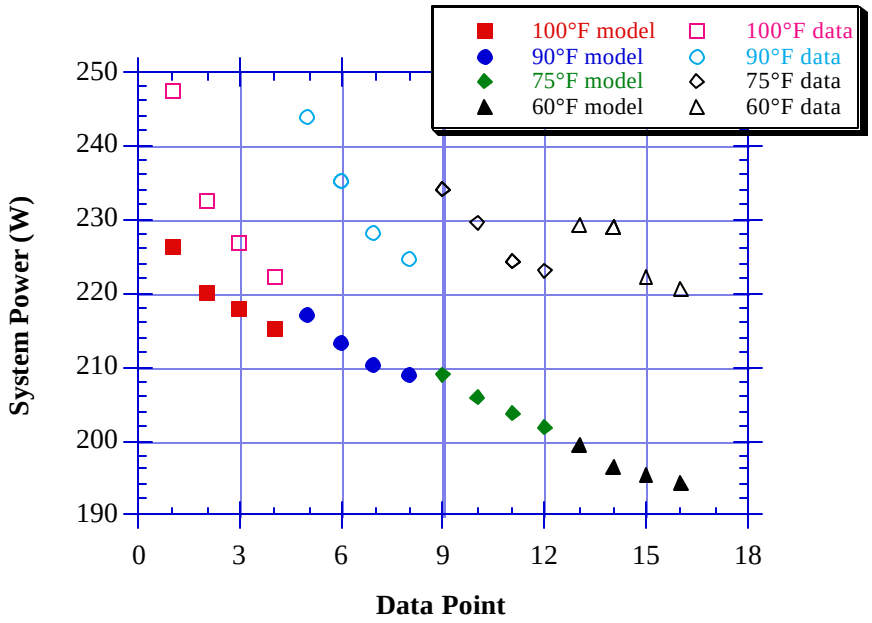

Figure F.8 System power comparison

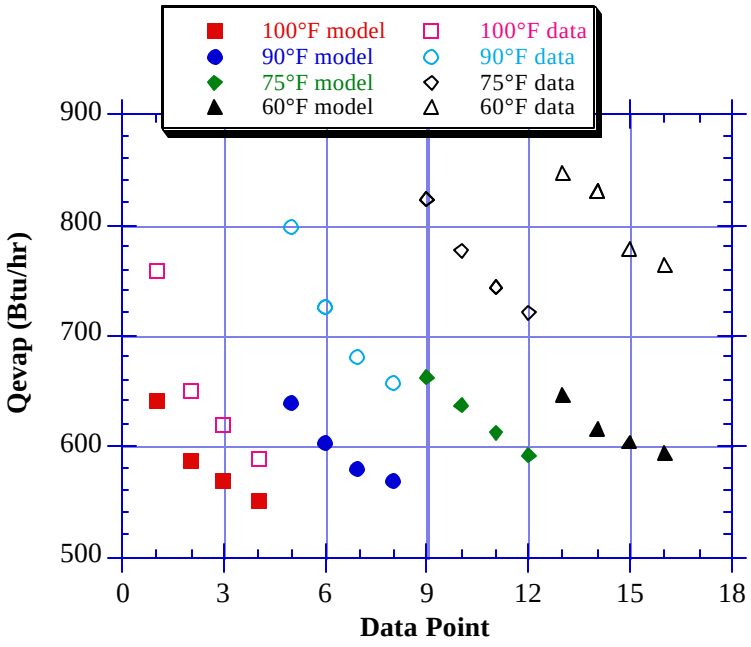

Figure F.9 Qevap comparison

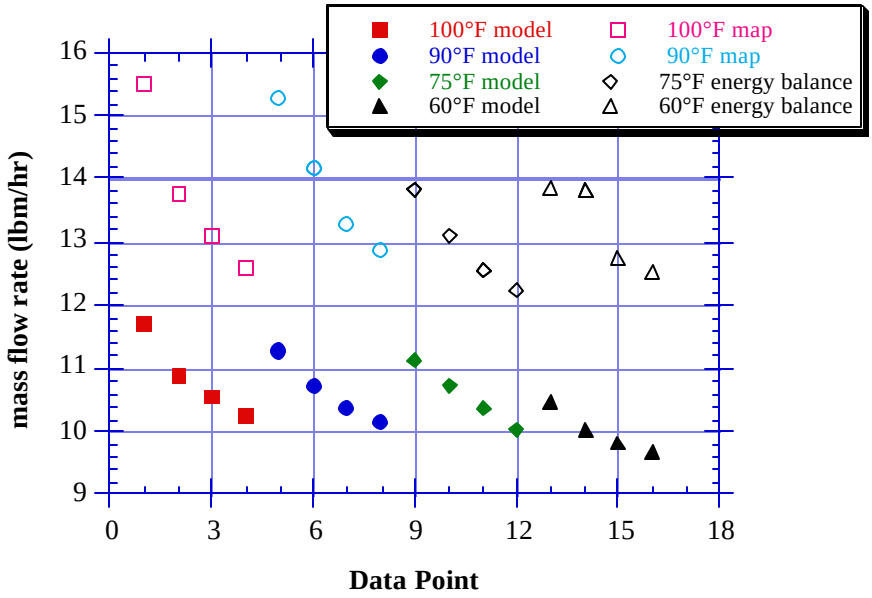

Figure F.10 Mass flow rate comparison

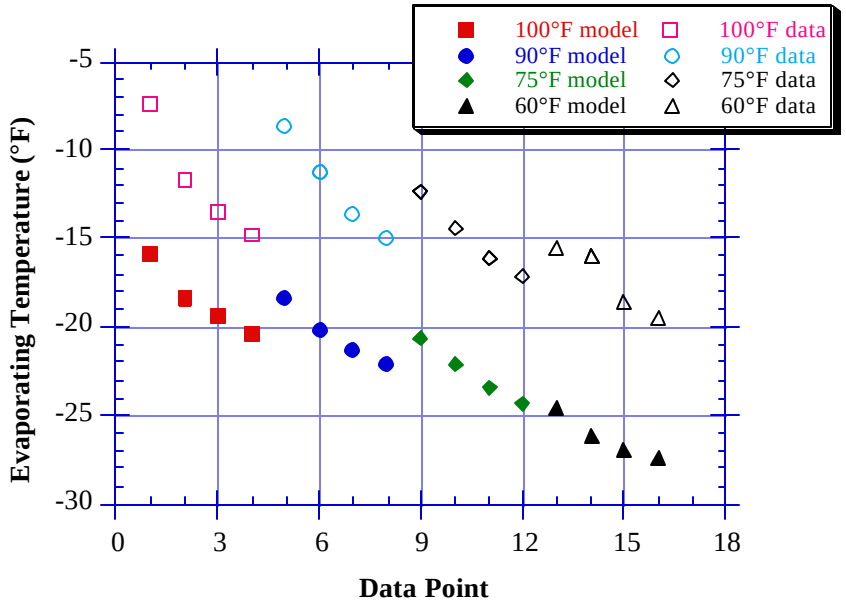

Figure F.11 Evaporating temperature comparison

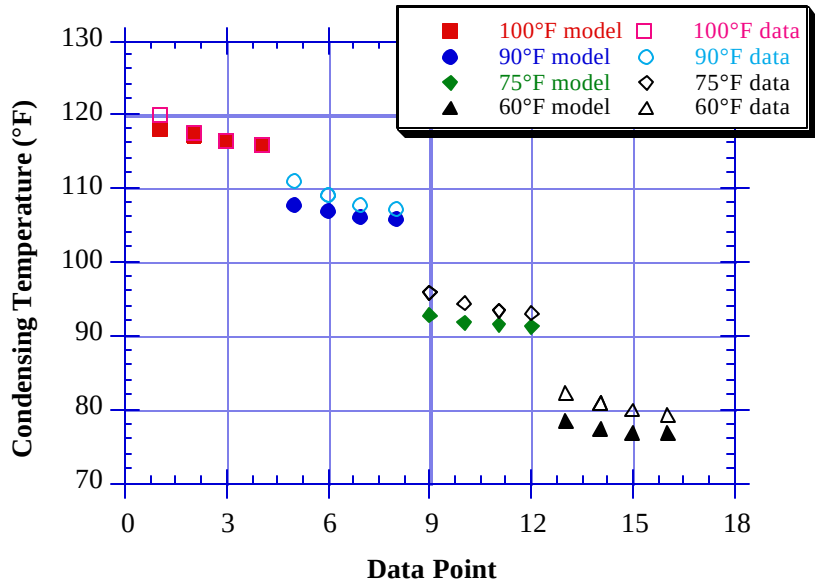

Figure F.12 Condensing temperature comparison

F.3 Simulation Model with Propane

All of the model solutions converged to the specified tolerance except for the lowest evaporator inlet temperatures in each ambient temperature group. Therefore, these points are not compared in the following graphs.

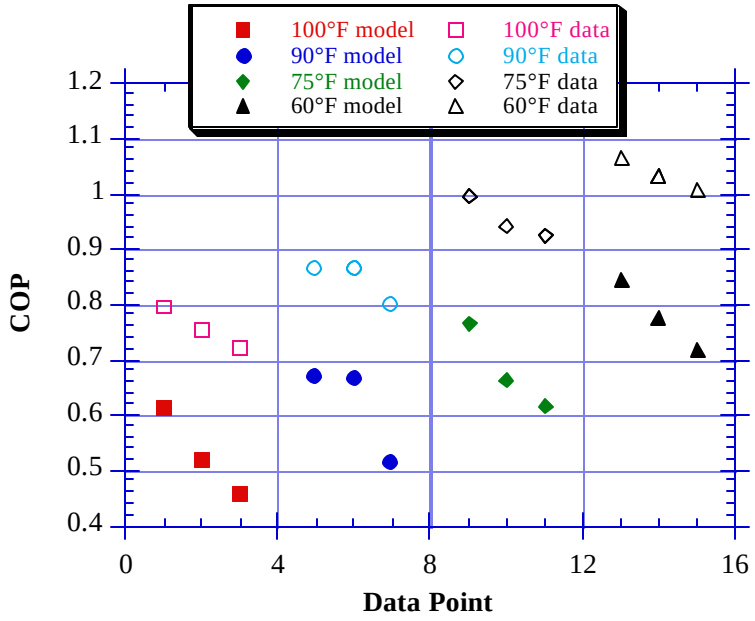

Figure F.13 COP comparison

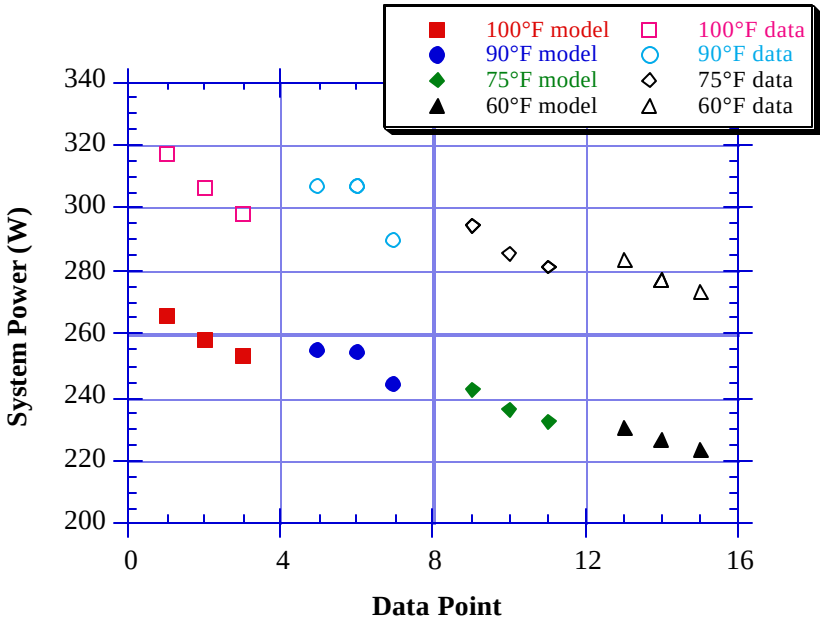

Figure F.14 System power comparison

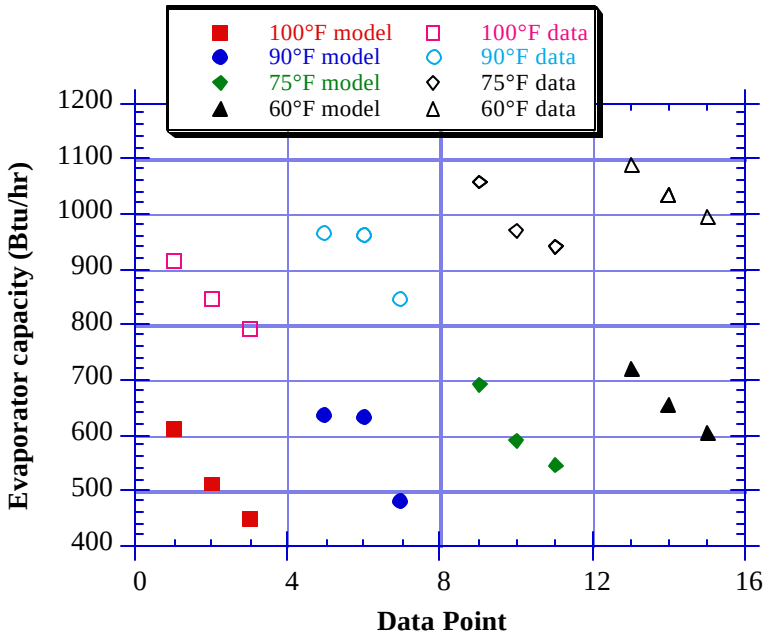

Figure F.15 Qevap comparison

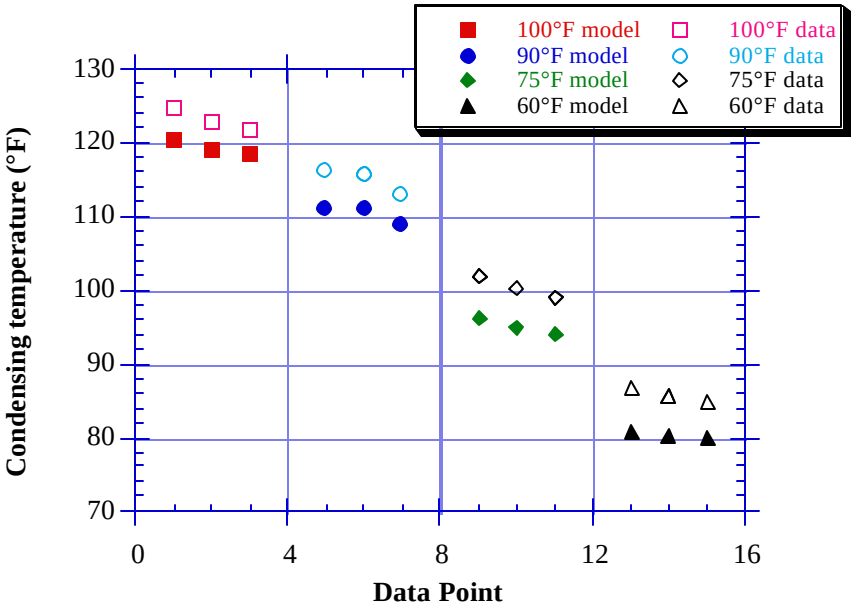

Figure F.16 Condensing temperature comparison

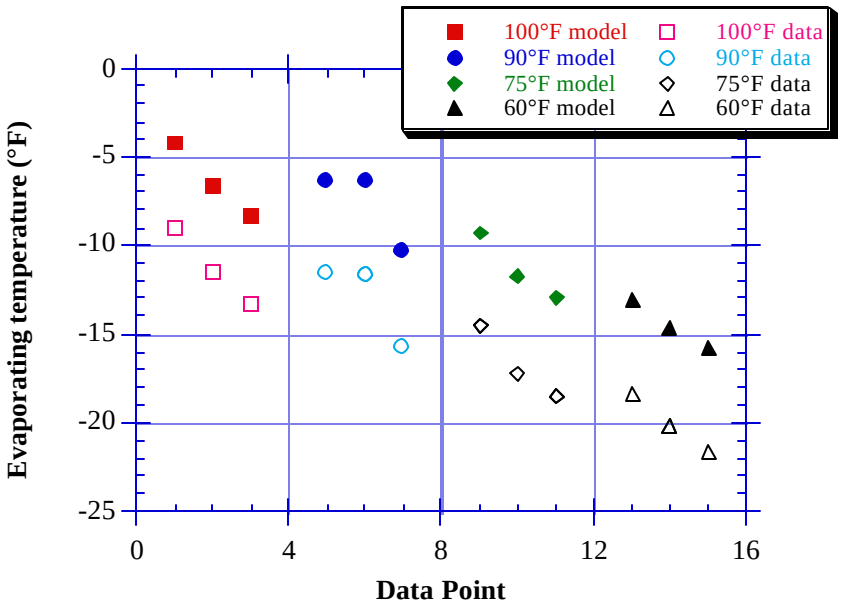

Figure F.17 Evaporating temperature comparison